AD-A159 049 PI CONTROL OF A SINGLE-DUCT VAV (VARIABLE AIR VOLUME) 1/2
HVAC (HEATING VENTI (U) CONSTRUCTION ENGINEERING
RESEARCH LAB (ARMY) CHAMPAIGN IL G PERCIVALL JUN 85
UNCLASSIFIED CERL-TM-E-85/05 F/G 13/1 NL

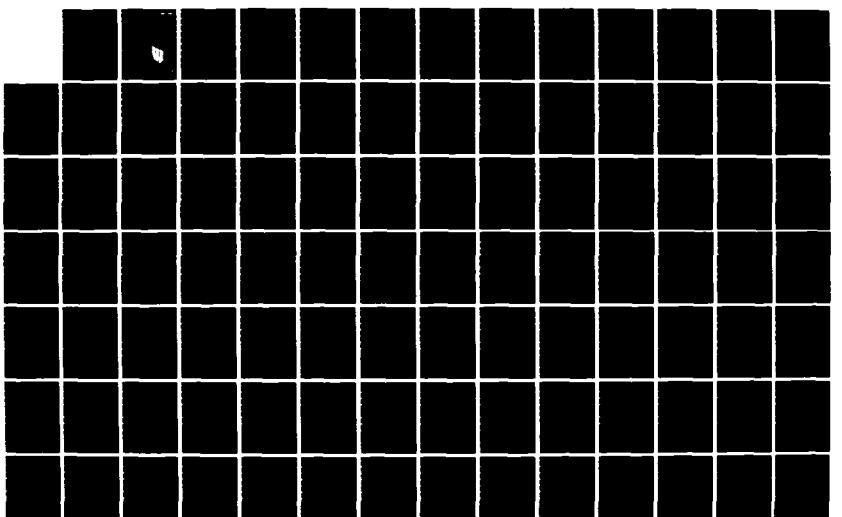

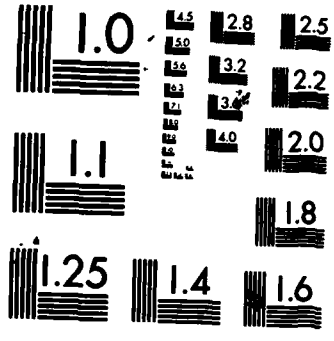

US Army Corps
of Engineers
Construction Engineering
Research Laboratory

USA-CERL

TECHNICAL MANUSCRIPT E-85/05
June 1985

PI CONTROL OF A SINGLE-DUCT VAV HVAC SYSTEM

by
George Percivall

This manuscript documents an investigation of the feedback control of a variable air volume heating and air-conditioning system for a moderately sized multiroom building. The primary objective of the study was to determine if commonly applied single-loop control system design principles are adequate for designing air-conditioning control systems. The research established that the sensitivity of the single-input single-output conventional design to the presence of the multi-input multi-output interconnection was insignificant. Also, the Ziegler-Nicholas control parameter tuning technique produced highly oscillatory control systems when applied to an air-conditioning system. Modified tuning formulas are presented.

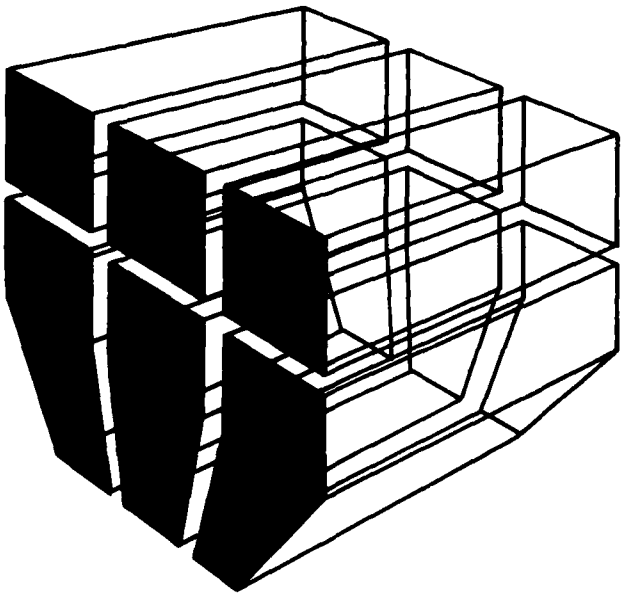

This manuscript is the result of work done in partial fulfillment of the requirements for an M.S. degree in Electrical Engineering from the University of Illinois at Urbana-Champaign.

Approved for public release; distribution unlimited.

The contents of this report are not to be used for advertising, publication, or promotional purposes. Citation of trade names does not constitute an official indorsement or approval of the use of such commercial products. The findings of this report are not to be construed as an official Department of the Army position, unless so designated by other authorized documents.

DESTROY THIS REPORT WHEN IT IS NO LONGER NEEDED
DO NOT RETURN IT TO THE ORIGINATOR

UNCLASSIFIED

SECURITY CLASSIFICATION OF THIS PAGE (When Data Entered)

REPORT DOCUMENTATION PAGE		READ INSTRUCTIONS BEFORE COMPLETING FORM
1. REPORT NUMBER CERL-TM-E-85/05	2. GOVT ACCESSION NO. AD-A159 044	3. RECIPIENT'S CATALOG NUMBER
4. TITLE (and Subtitle) PI CONTROL OF A SINGLE-DUCT VAV HVAC SYSTEM		5. TYPE OF REPORT & PERIOD COVERED FINAL 6. PERFORMING ORG. REPORT NUMBER
7. AUTHOR(s) George Percivall		8. CONTRACT OR GRANT NUMBER(s)
9. PERFORMING ORGANIZATION NAME AND ADDRESS U.S. Army Construction Engineering Research Laboratory P.O. Box 4005 Champaign, IL 61820-1305		10. PROGRAM ELEMENT, PROJECT, TASK AREA & WORK UNIT NUMBERS 4A162781AT45-B-008
11. CONTROLLING OFFICE NAME AND ADDRESS		12. REPORT DATE June 1985 13. NUMBER OF PAGES 110
14. MONITORING AGENCY NAME & ADDRESS(if different from Controlling Office)		15. SECURITY CLASS. (of this report) UNCLASSIFIED 15a. DECLASSIFICATION/DOWNGRADING SCHEDULE

16. DISTRIBUTION STATEMENT (of this Report)

Approved for public release; distribution unlimited.

17. DISTRIBUTION STATEMENT (of the abstract entered in Block 20, if different from Report)

18. SUPPLEMENTARY NOTES

Copies are available from the National Technical Information Service, Springfield, VA 22161

19. KEY WORDS (Continue on reverse side if necessary and identify by block number)

HVAC systems
heating
air conditioning equipment
ventilation
control systems

20. ABSTRACT (Continue on reverse side if necessary and identify by block number)

This manuscript documents an investigation of the feedback control of a variable air volume heating and air-conditioning system for a moderately sized multiroom building. The primary objective of the study was to determine if commonly applied single-loop control system design principles are adequate for designing air-conditioning control systems. The research established that the sensitivity of the single-input single-output conventional design to the presence of the multi-input multi-output interconnection was insignificant.

DD FORM 1 JAN 73 1473 EDITION OF 1 NOV 65 IS OBSOLETE

UNCLASSIFIED

SECURITY CLASSIFICATION OF THIS PAGE (When Data Entered)

BLOCK 20. (Continued)

Also, the Ziegler-Nichols control parameter tuning technique produced highly oscillatory control systems when applied to an air-conditioning system. Modified tuning formulas are presented.

This manuscript is the result of work done in partial fulfillment of the requirements for an M.S. degree in Electrical Engineering from the University of Illinois at Urbana-Champaign.

FOREWORD

This research was conducted for the Office of the Assistant Chief of Engineers (OACE) under Project 4A162781AT45, "Energy and Energy Conservation"; Technical Area B, "Installation Energy Conservation"; Work Unit 008, "Control of Existing Buildings." The work was conducted by the Energy Systems Division (ES), U.S. Army Construction Engineering Research Laboratory (USA-CERL). The OACE Technical Monitor was Mr. Bernard Wasserman, DAEN-ZCF-U.

COL Paul J. Theuer is Commander and Director of USA-CERL, and Dr. L. R. Shaffer is Technical Director.

This report is also partial fulfillment of a thesis requirement for the Masters of Science degree from the Electrical Engineering Department of the University of Illinois at Urbana-Champaign. The advisor for this thesis was Professor Jose B. Cruz.

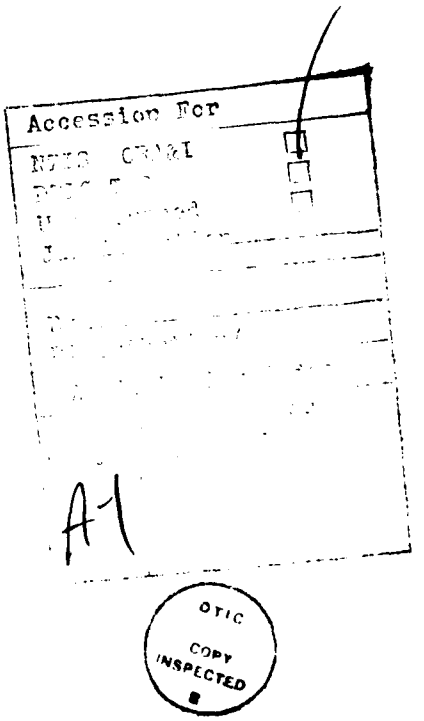

TABLE OF CONTENTS

LIST OF TABLES

LIST OF FIGURES

LIST OF FIGURES (Cont'd)

LIST OF FIGURES (Cont'd)

LIST OF FIGURES (Cont'd)

I. INTRODUCTION

This is a report of an investigation of the feedback control of a variable air volume (VAV) heating, ventilating, and air conditioning (HVAC) system for a moderate size multiroom building. The primary objective is to maintain the room temperature within a given band. This report looks at one method of achieving this goal. This method utilizes proportional control of the room temperatures and proportional-integral control of three other quantities. Each of these controllers is isolated from the others and attempts to control its own quantity without concern of the effect upon the other quantities--hence the name decentralized control. Of course, these local loops are expected to benefit each other by maintaining their quantity in control. The purpose of this investigation is to discern how well these expectations are met; that is, given a good design of the local loop controllers, what is the resulting control when these isolated subsystems are interconnected into the complete system?

II. THE SISO DESIGN OF CONTROL

The HVAC system to be studied is shown in Figure 1. It is called single duct because there is one main duct providing cool supply air to all the zones. (A zone is a room or a group of rooms for which a single temperature measurement is considered to reflect the temperature of the entire space.) The main duct contains a cooling coil which in warmer months chills the supply air to a desired setpoint. The zones in turn have valves to decrease the volume of cool supply air entering the zone. In the winter months, the cooling coil is shut off; the zone valves are at a minimum flow setting and the zone air temperature is controlled by a heating coil which reheats the supply air. Each zone has its own reheat coil and air valve.

The VAV description means that the air flow into the zones can be varied by the air valves, or more commonly, the VAV boxes. In order to avoid overpressure in the ducts and also to allow energy savings, the speed of the fan in the supply duct can be modulated, resulting in variable air volume flow.

The remaining active ingredient of the system is the mixing box which mixes return air from the zones and outdoor air. This air is then routed to the face of the cooling coil in the supply duct. The amounts of outdoor and return air which are mixed depend upon the desired mixed air temperature.

All of the controlled quantities and the means of effecting changes have been mentioned; along with the symbols which will be used, they are now summarized. The mixed air temperature, T_{am}, is effected by changing the fractions of return air, f_{ret}, (at temperature T_{ret}), and of outdoor air, $1-f_{ret}$ (at temperature T_{out}), which comprise the mixed air. The cool air temperature in the supply duct, T_{cool}, is affected by the mass flow of water through the cooling coil, $\dot{m}_{wc}$. The gage pressure in the supply duct, P_c, is affected by the fan motor speed or frequency, f_{in}. The temperature of air in a zone, T_{zi} (where i=1,2,3,4, i.e., there will be four zones), is affected by: the mass flow of supply air into the zone, $\dot{m}_{azi}$, in the summer; and the mass flow of hot water in the reheat coil, $\dot{m}_{wzi}$, in the winter. Again, these quantities are, first, the quantities which should be controlled or regulated in a prescribed manner and, second, the quantities which can be commanded to change in an attempt to achieve control of the first quantitites; e.g., control of T_{cool} is achieved by commands to $\dot{m}_{wc}$.

These input-output pairs are the basis for the local-loop subsystems. Of course they are not the only inputs affecting the controlled quantities; there are also the interconnections. Although it will be helpful when designing the controllers to think of the system as local-loop subsystems, ultimately the interconnections must be considered. Figure 2 shows a block diagram of the

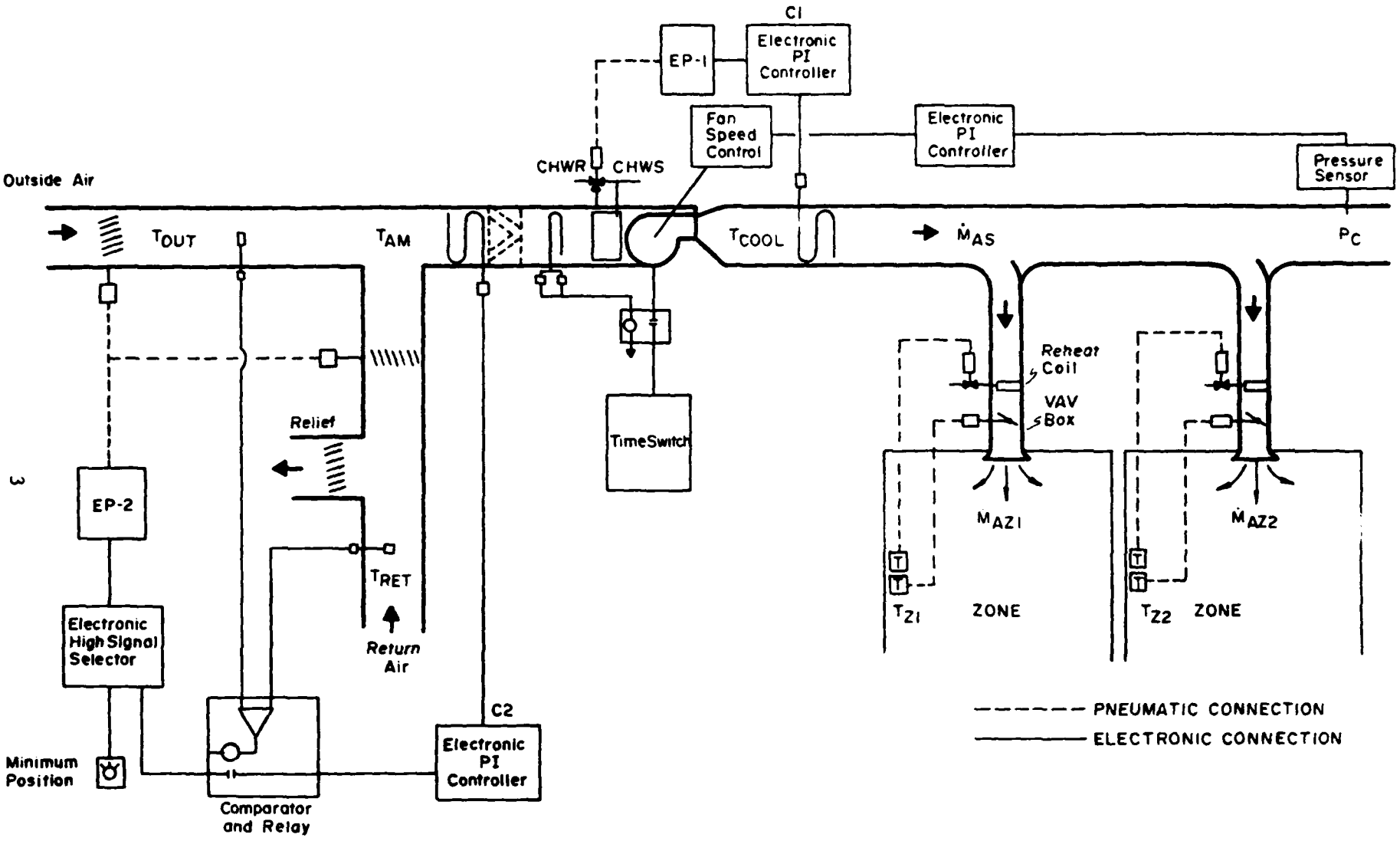

Figure 1. Single-duct VAV HVAC system.

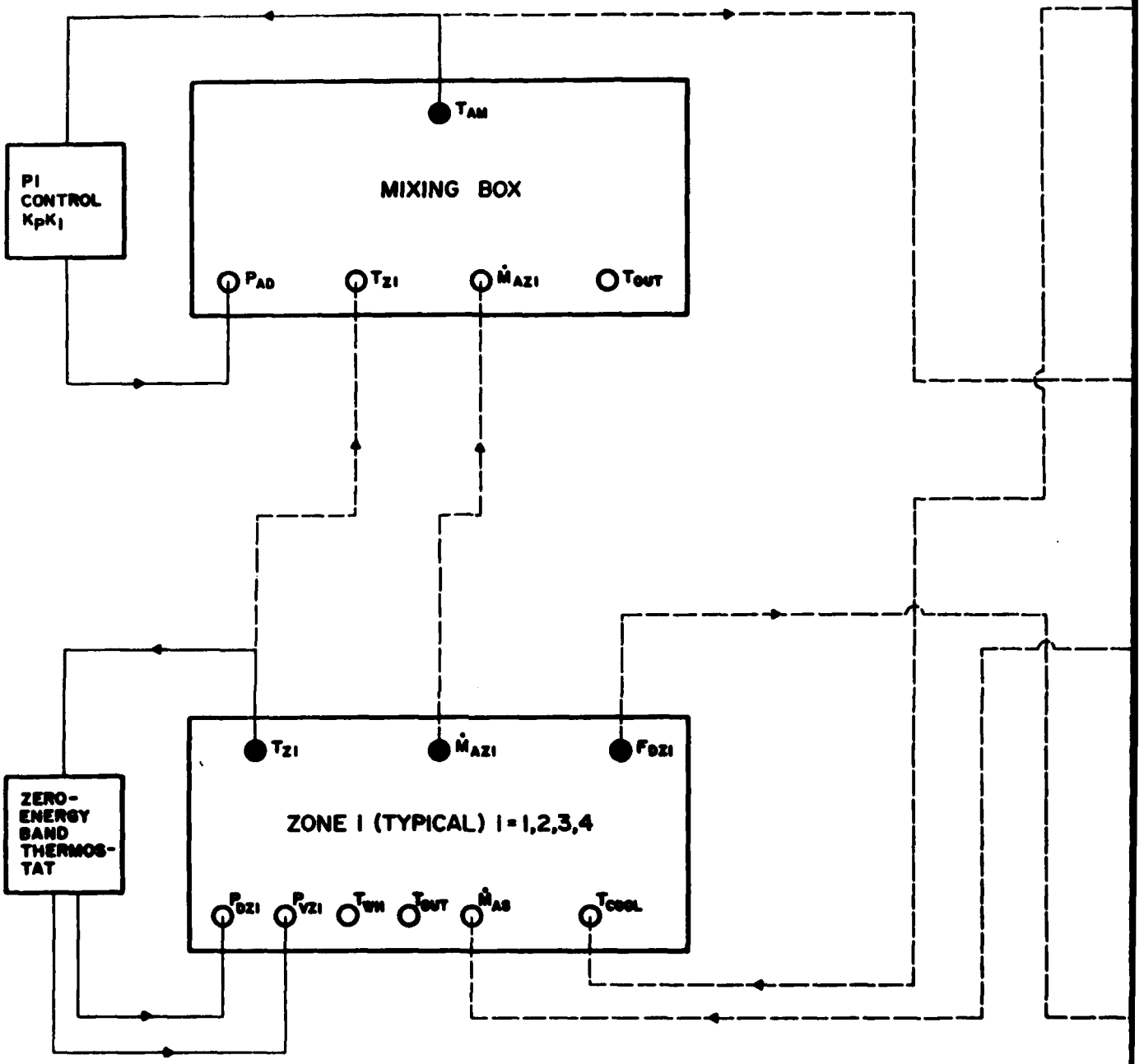

Figure 2. HVAC system decomposition.

10 of 2

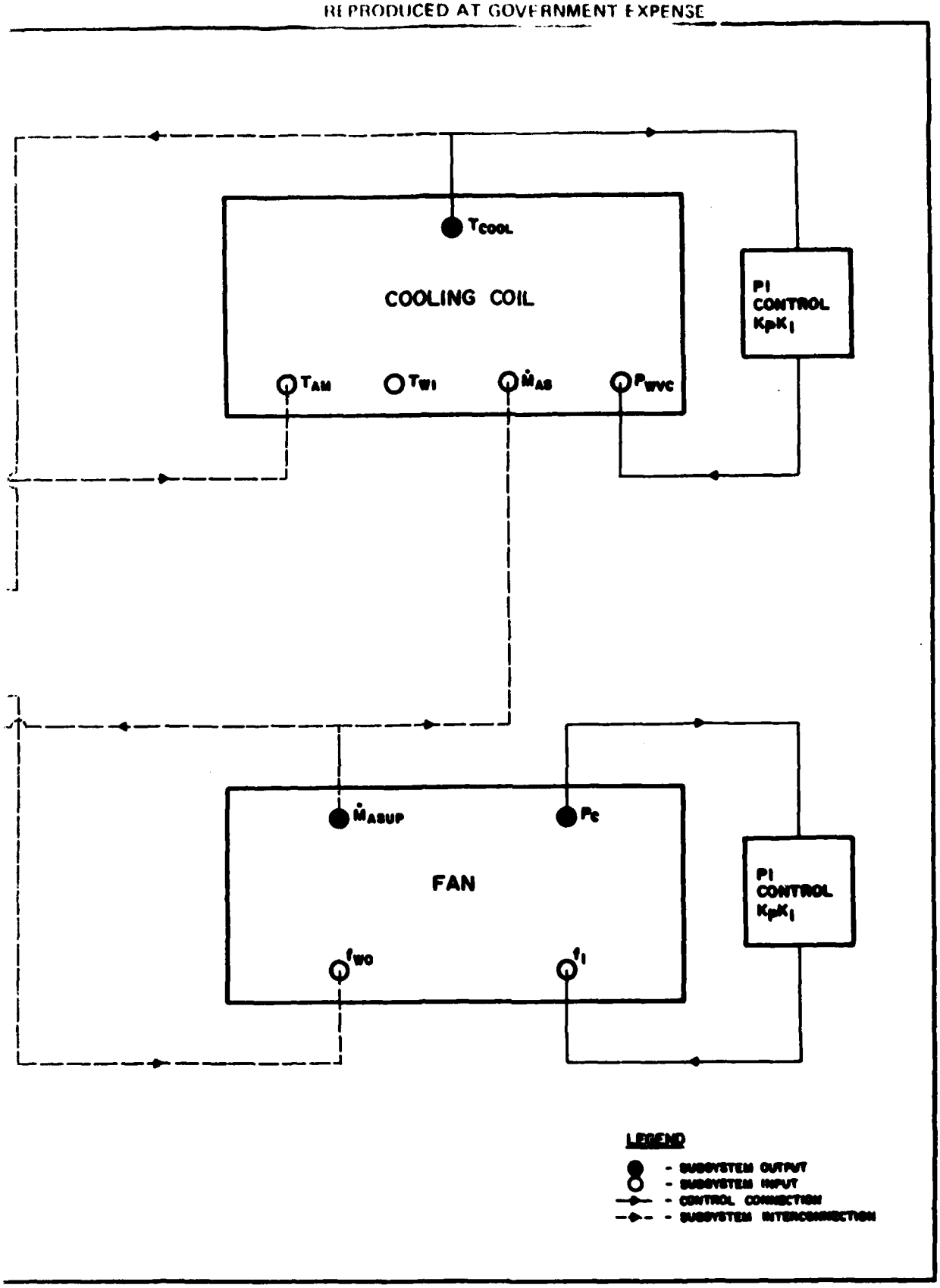

entire system decomposed as independent subsystems. (In this figure the actuators have been included in the subsystem blocks, so in place of $\dot{m}_{wc}$ is P_{wv}, the pneumatic pressure to the valve controlling $\dot{m}_{wc}$ into the cooling coil. f_{ret} is replaced by P_{ad}, the pneumatic pressure to the actuator which sets f_{ret}. $\dot{m}_{azi}$ and $\dot{m}_{wzi}$ are replaced, respectively, by P_{dzi} and P_{vzi}, the pneumatic pressures to the VAV box and water valve actuators which control $\dot{m}_{azi}$ and $\dot{m}_{wzi}$.)

It is now possible to point out the difference between the single-variable local-loop subsystems and the multivariable system. All the local loops are single-input single-output (SISO) systems with the inputs and outputs being scalars; e.g., for the cooling coil, the input is P_{wv} and the output is T_{cool}; further, the input-output relation can be described by a single transfer function. Note that there are seven SISO local loop subsystems. Alternatively, the subsystems can be unified into a multi-input multi-output (MIMO) system with the input and output being vectors; the input, U, in summer is

$$U = (P_{ad}\ P_{vc}\ f_1\ P_{dz1}\ P_{dz2}\ P_{dz3}\ P_{dz4})^T \qquad \text{(II-1)}$$

and in winter,

$$U = (P_{ad}\ P_{vc}\ f_1\ P_{vz1}\ P_{vz2}\ P_{vz3}\ P_{vz4})^T \qquad \text{(II-2)}$$

The output is Y,

$$Y = (T_{am}\ T_{cool}\ P_c\ T_{z1}\ T_{z2}\ T_{z3}\ T_{z4})^T \qquad \text{(II-3)}$$

Further, the input-output relation is now described by a 7 by 7 matrix, whose elements are transfer functions. This matrix will be called the system plant transfer function matrix. Note that the seven on-diagonal elements of this matrix are identically the seven local loop SISO transfer functions, and the 42 off-diagonal elements describe the interconnections between the subsystems. For example, the second row first column element of the system plant transfer function matrix describes the change in T_{cool} due to a change in P_{ad}.

It is obvious that the MIMO approach is a more complete description of the entire system than a description by seven SISO subsystems without interconnections. Of course with this increase in complexity of description come more questions when this MIMO approach is used for design purposes. For instance, in a typical SISO feedback control system there are four elements: the plant, whose output is the control variable; a feedback compensator; a summation device, which compares the feedback signal to a reference or setpoints; and a feedforward compensator which provides the input to the plant. To achieve the desired control, the design of two elements is necessary: the feedback and feedforward compensators. Alternatively, for the MIMO description , the feedback and feedforward compensators contain 49 elements each. So, although the MIMO design may be able to provide better control of the seven outputs, the difficulty of design is increased over the SISO approach by 7 to 1.

In order to achieve a workable design, this investigation will use a SISO approach to designing the controllers. Moreover, the feedback compensator will include no elements beyond what is necessary for sensing the plant output, resulting in the need for seven feedforward compensator designs.

The system under consideration is a common HVAC system, and it is desired that the design be implemented with commonly available components. For this reason the industrial grade proportional-integral (PI) process controller was selected as the feedforward compensators. The only remaining facet of the design is the selection of the two PI controller gain values: the proportional control gain K_p and the integral control gain K_I. These values will be obtained once the PI controller is attached to the plant by using the procedure devised by J. G. Ziegler and N. B. Nichols[1] for selecting optimum settings for automatic controllers.

Before proceeding to evaluate the controller design just described, it may be fruitful to describe what other types of design are possible. Given the system plant transfer function matrix description, it is feasible to provide precompensation, which amounts to counteracting the interconnection effect, resulting in a new system plant with all off-diagonal elements being zero. At that point the simpler SISO approach to controller design would be optimal. Precompensation would entail selecting on- and off-diagonal elements of the feedback and feedforward compensator matrices. This approach, or any centralized controller approach where all seven plant outputs can be used to select appropriate plant inputs, would increase in complexity at a quick rate; however, given the improvement in components--e.g., electronic-to-pneumatic transducers--allowing more accurate modeling and the power of Direct Digital Control for sensing and computation, the results might be worth the work.

At present the controller design is SISO and our task is to insure that this design provides good control. The next step is to develop our system description by modeling the plant and associated components.

III. MATHEMATICAL MODELING OF THE SISO SUBSYSTEMS

A preliminary description (Chapter II) and sketch (Figure 1) of the system have already been given. It is now necessary to detail the system description to allow for the use of computer simulation and frequency analysis techniques. The approach of the next two chapters will utilize the SISO-MIMO distinction made in the previous chapter; first, the SISO subsystem dynamics will be mathematically described; then in the next chapter the MIMO system will be described by filling in the interconnections in the system plant transfer function matrix and associated feedback and feedforward compensator matrices.

There are seven SISO subsystems: the mixing box, the cooling coil, the fan and associated ducts, and the four zones. Because these four types of subsystems have many components in common and utilize the same feedback control design, a standard form for all the subsystems will be adopted. This form is shown in the block diagram of Figure 3. The description will now proceed by selecting a block in this diagram, describing the block for each subsystem, and then selecting another block.

A. The Plants

The first plant to be considered is the mixing box (see Figures 4 and 5). The mixing box plant is the damper and ducts which mix the return and outdoor airstreams to produce the mixed airstream. The mixing box will be used in one of two ways, depending upon the return and outdoor air temperatures. If the outdoor air is hotter than the return air, the damper is set for a maximum return air fraction, f_{ret}^{max}, and no control of the return air fraction of the mixed air, f_{ret}, is allowed. (For ventilation purposes a minimum of 15% outdoor air is required in the mixed air, so, $f_{ret}^{max} = 0.85$.) Secondly, if the outdoor air is colder than the return air, dynamic control of the air damper or f_{ret} is allowed. The relation between the mixed air temperature, T_{am}, and the return air fraction, f_{ret}, is given by,

$$t_m \dot{T}_{am} = -T_{am} + f_{ret}T_{ret} + (1-f_{ret})\, T_{out} \qquad \text{(III-1)}$$

where:

T_{out} = the outdoor air temperature
T_{ret} = the return air temperature
t_m = 0.1 sec, is the mixing box time constant

Note that even during this mode, the return air fraction is constrained to be between zero and 85 percent.

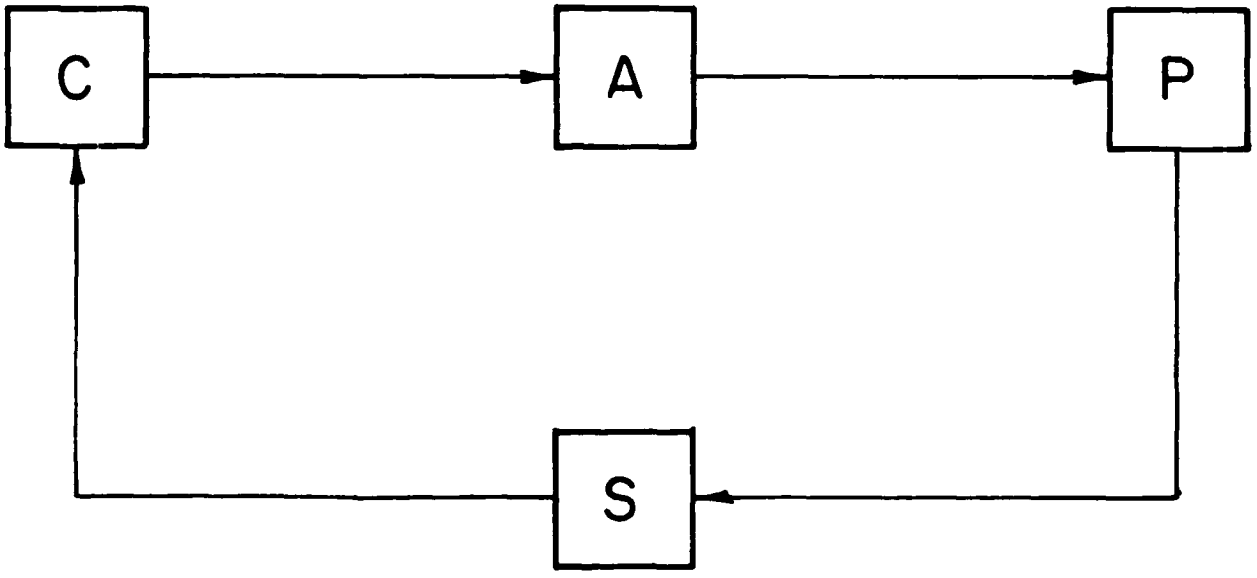

C: Controller

A: Actuator

S: Sensor

P: Plant

Figure 3. SISO standard form.

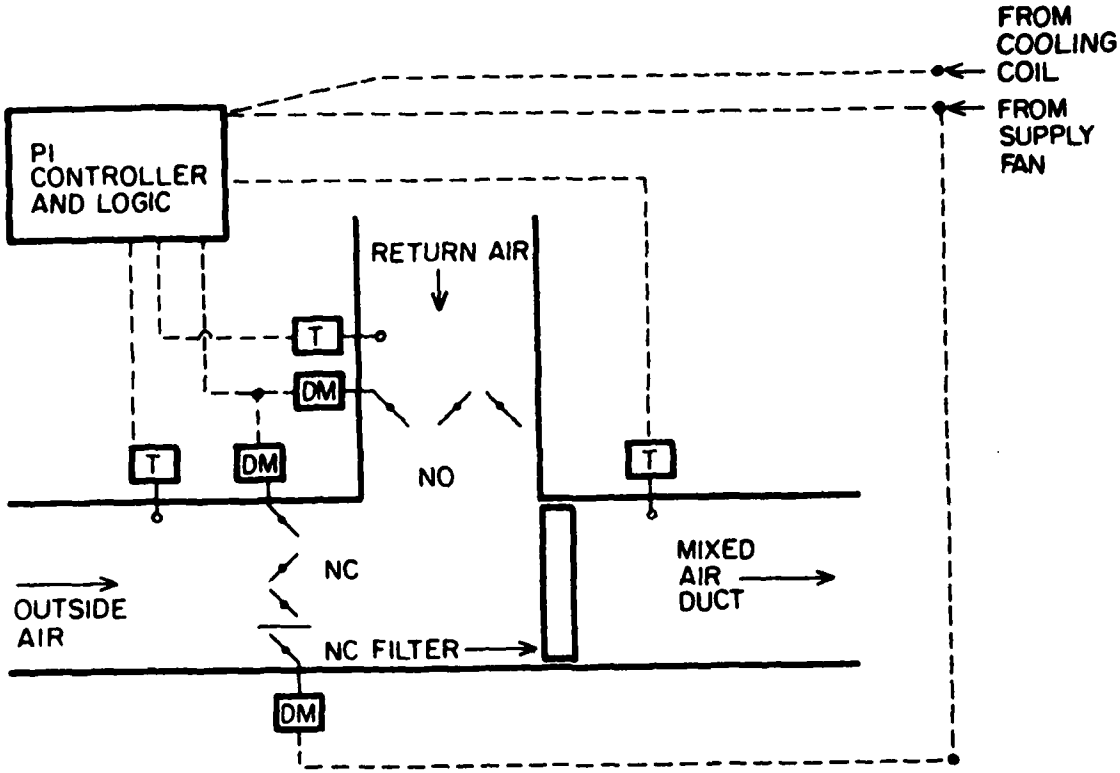

Figure 4. Mixing box HVAC diagram.

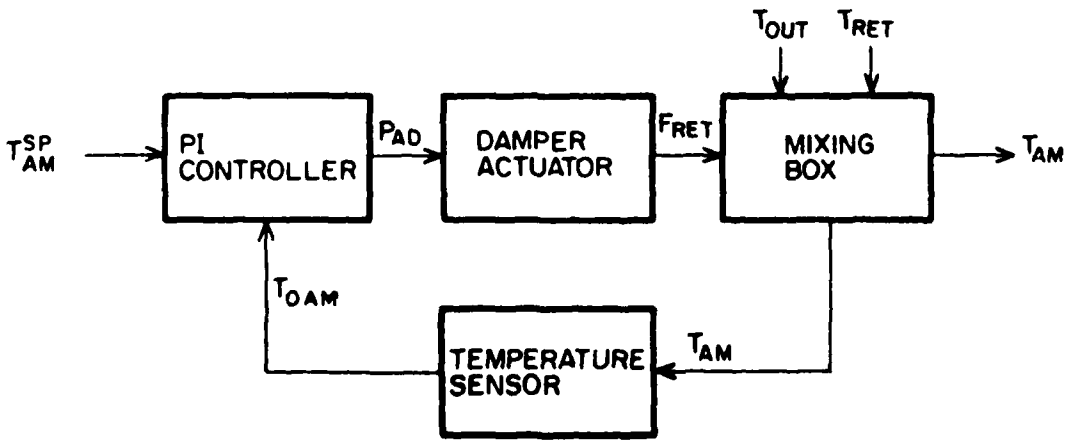

Figure 5. Mixing box block diagram.

The cooling coil plant is considered to have three inputs: the mass flow of chilled water through the coil, $\dot{m}_{wc}$; the mass flow of air across the coil, $\dot{m}_{asup}$; and the temperature of the incoming air, T_{am}, the mixed air temperature (see Figures 6 and 7). The output is the leaving air temperature which becomes the cool supply air temperature, T_{cool}. The description of the dynamics is taken in part from a paper by J. R. Gartner and H. L. Harrison[2] which was further developed by I. Gondal[3] and also in part from experiments performed at the U.S. Army Construction Engineering Research Laboratory (USA-CERL). The Gartner and Harrison derivation begins with an infinitesimal cross-section of the tube which is in crossflow; develops differential equations for the primary fluid (the chilled water), the tube, and the secondary fluid (the cool air); and transforms these equations into transfer functions. For the subsystem, the important equation relates changes in $\dot{m}_{wc}$ to changes in T_{cool}, given by

$$\alpha_2 \ddot{T}_{cool} + \alpha_1 \dot{T}_{cool} + \alpha_o T_{cool} = \beta_o \dot{m}_{wc} + \beta_1 \ddot{m}_{wc} \qquad \text{(III-2)}$$

where the α's and β's depend in a complicated manner upon the steady-state inlet water, inlet air, and outlet air temperatures; the steady-state air and water mass flows; and the dimensions and materials of the coil. The effect of changes in T_{cool} due to changes in T_{am} and $\dot{m}_{as}$ will be given when the interconnections are detailed.

The second plant to be considered, the fan subsystem plant, includes the fan motor, the fan cabinet, and the duct system. (See Figures 8 and 9.) The motor is a two pole-pair, squirrel-cage induction motor, the pulley set has a one-to-one ratio, and the fan cabinet is of the centrifugal forward-curved blade type. The input to the motor is the frequency of the electric power supply, and the output is the rotational speed of the fan shaft, $\dot{\theta}_f$, in RPM's. As derived from a model including damping and the moment of inertia of the fan and from experimental observations, the input-output relation is,

$$\frac{\dot{\theta}_f(s)}{F_{in}(s)} = \frac{29.17}{1 + s \cdot t_m} \qquad \text{(III-3)}$$

where $t_m = 0.361$ sec. is the fan motor time constant and s is the frequency domain variable. To relate the $\dot{\theta}_f$ to $\dot{m}_{as}$ and P_c, the fan curves must be used. When operating as a subsystem, the fan is riding a "system" curve which is determined by the fraction of wide-open-cfm, f_{wo}, determined by the ducts and zone damper positions. This relation will be given as an interconnection, and for now, f_{wo} will be assumed constant. By taking points from the fan curve and using least-squares curve fits, the following lines were obtained:

$$P_f\ [p_a] = A + B \cdot \dot{\theta}_f\ [\text{RPM}] \qquad \text{(III-4)}$$

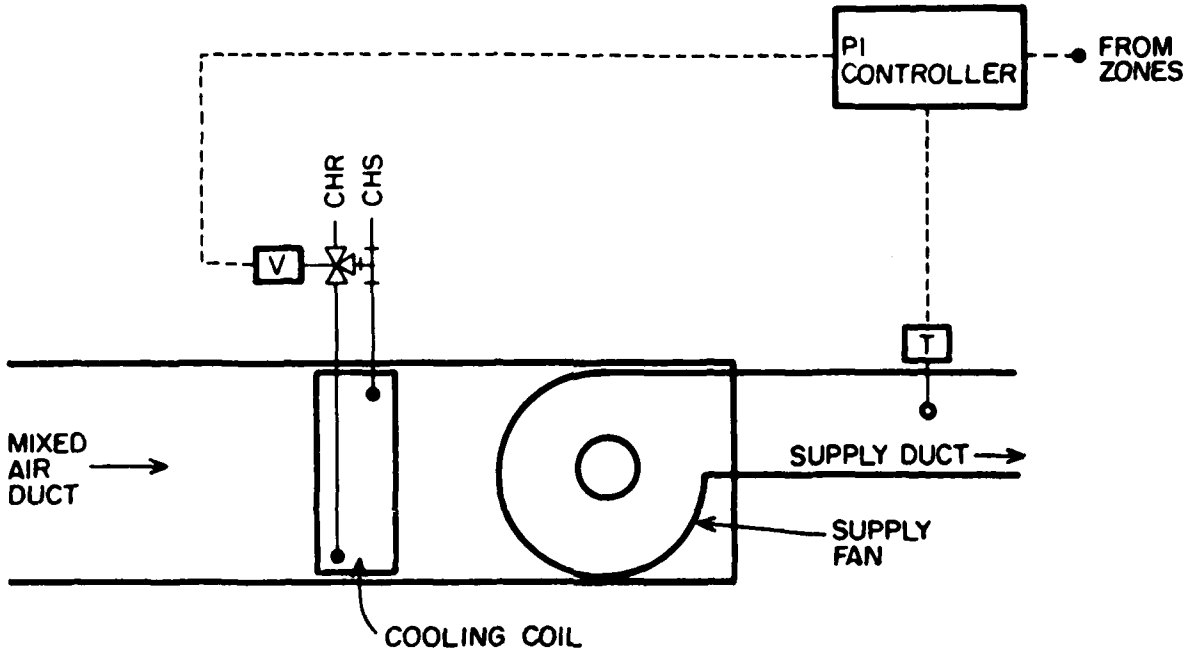

Figure 6. Cooling coil HVAC diagram.

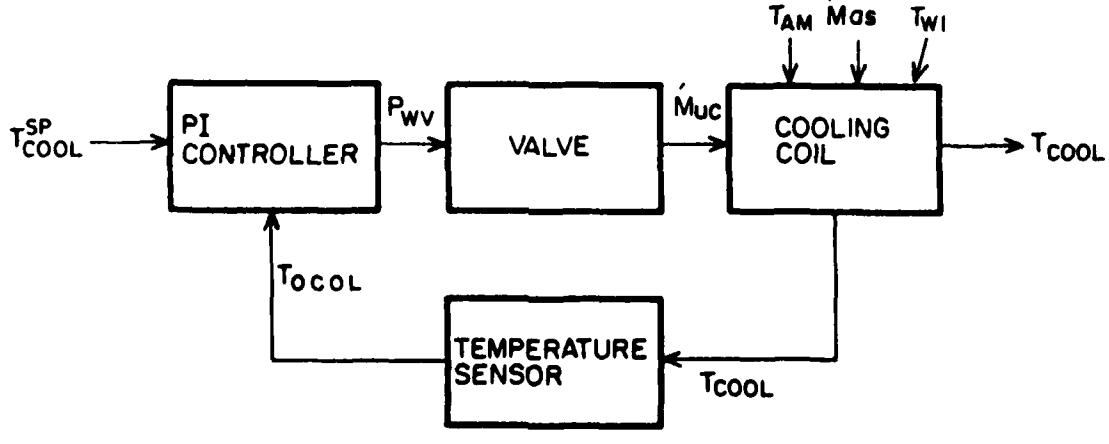

Figure 7. Cooling coil block diagram.

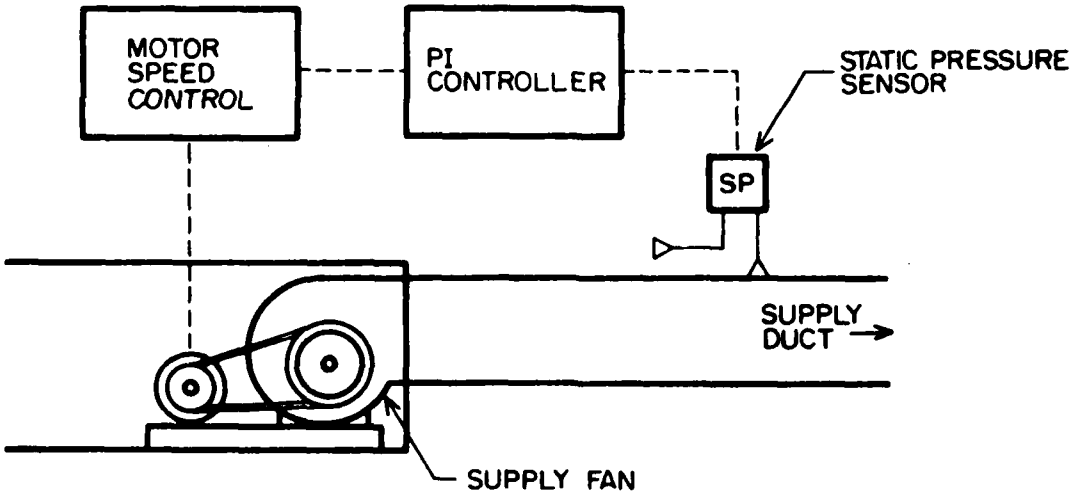

Figure 8. Fan HVAC diagram.

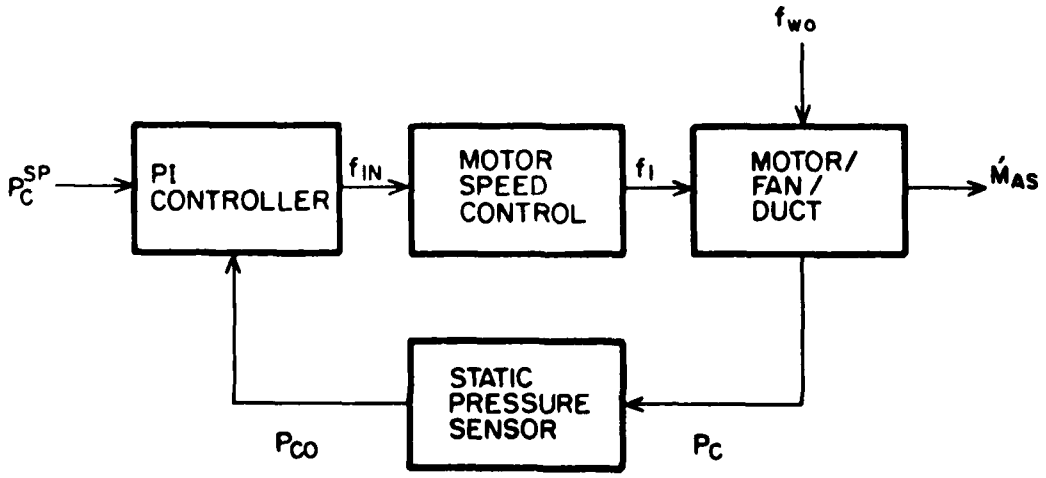

Figure 9. Fan block diagram.

where:

$$A = -1466 + 1349 \cdot f_{wo}$$

$$B = 2.356 - 2.169 \cdot f_{wo}$$

and

$$\dot{m}_{as} \left[\frac{kg}{sec}\right] = A + B \cdot \dot{\theta}_f [RPM] \qquad \text{(III-5)}$$

where:

$$A = -0.1252 + 0.661 \cdot f_{wo} - 0.6684 \cdot f_{wo}^2$$

$$B = -1.417 \cdot 10^{-4} + 5.224 \cdot 10^{-3} \cdot f_{wo}$$

So, for changes in motor speed, $\delta\dot{\theta}_f$, the resulting changes in mass flow, $\delta\dot{m}_{as}$,[1] and pressure across the fan, δP_f, for constant f_{wo} are given by the constants

$$F_1 = \frac{\delta P_f}{\delta \dot{\theta}_f}\Big|_{\delta f_{wo}=0} = 2.356 - 2.169 \cdot f_{wo} \qquad \text{(III-6)}$$

$$F_2 = \frac{\delta \dot{m}_{as}}{\delta \dot{\theta}_f}\Big|_{\delta f_{wo}=0} = -1.417 \cdot 10^{-3} + 5.224 \cdot 10^{-3} \cdot f_{wo} \qquad \text{(III-7)}$$

Here it should be noted that the duct friction losses from the fan to the pressure sensor are assumed to be appreciable. It was assumed that for a pressure gain of 698 pa across the fan, the pressure in the duct was 125 pa or

$$\frac{\delta p_c}{\delta p_f} = 0.1786 \qquad \text{(III-8)}$$

The last subsystem plant is that of the zones (see Figures 10 and 11). This includes the zone air and walls, and the reheat coil, which is used only in the winter. The zone walls and contained air can be described in the heat flux equation,

$$C_{zi} \dot{T}_{zi} = Q_w + Q_D + Q_J + L_i \qquad \text{(III-9)}$$

[1] The units of $\dot{m}_{as}$ are kg/sec. For an air density of 1.229 kg/m^3, 1 kg/sec corresponds to 1724 CFM.

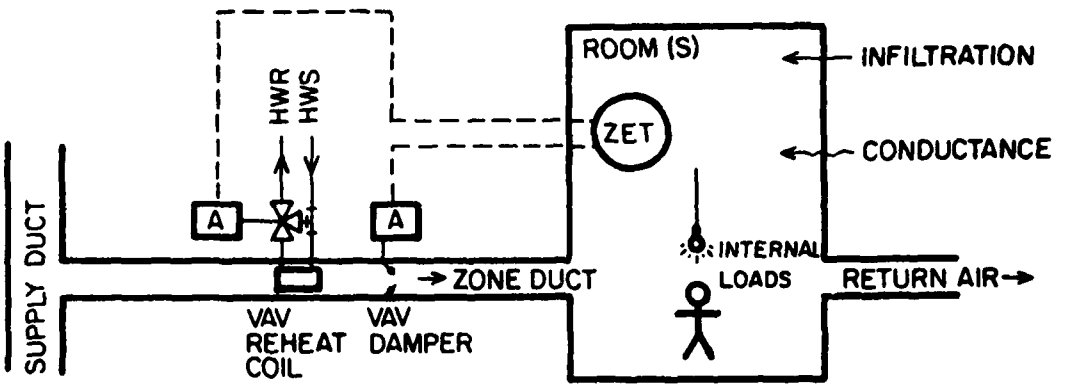

Figure 10. Zone HVAC diagram.

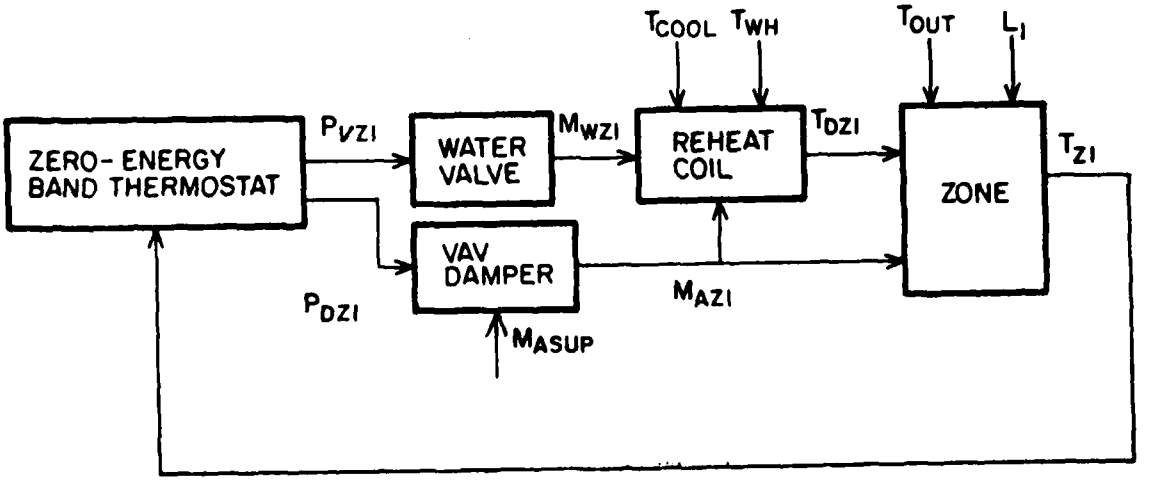

Figure 11. Zone block diagram.

where:

C_{zi} = the heat capacity of the air in the zone (700. kJ/°C)
Q_w = the heat flux through the walls to the outdoors
Q_D = the heat flux from the duct containing the reheat coil and the VAV damper
Q_J = the heat flux due to infiltration
L_i = the constant internal load in the zone due to lights, equipment, and people.

The load in zone i, L_i, is considered to be a constant parameter but later its value will be chosen to obtain a desired steady-state zone temperature. Q_J and Q_W are described by

$$Q_J + Q_W = \mu (T_{out} - T_{zi}) + C_{zi} F_I (T_{out} - T_{zi}) \qquad \text{(III-10)}$$

where:

T_{out} = is the outside temperature
μ = is the conductance through the zone walls (0.0644 kw/°C)
F_I = is the infiltration rate (1/3600 sec-1)

The flux Q_D is given by

$$Q_D = \dot{m}_{azi} (T_{dzi} - T_{zi}) \qquad \text{(III-11)}$$

where:

$\dot{m}_{azi}$ = mass flow of air into the room through the duct (in the summer this is varied by the VAV damper, and set to a minimum flow position in the winter)
T_{dzi} = temperature of the duct air as it enters the zone

In the summer when the reheat coil is not operating, $T_{dzi} = T_{cool}$; in winter the coil has a hot water mass flow, $\dot{m}_{wzi}$, and the duct temperature is described by an equation derived in the same manner as the cooling coil (see Equation III-2), so,

$$\alpha_{2zi} \ddot{T}_{dzi} + \alpha_{1zi} \dot{T}_{dzi} + \alpha_{ozi} T_{dzi} = \beta_1 \ddot{m}_{wzi} + \beta_o \dot{m}_{wzi} \qquad \text{(III-12)}$$

where the α's and β's are constants which depend upon the steady-state temperatures and mass flows, and upon the coil dimensions and materials.

B. The Controllers

Two types of controllers are used in this system. The first is an electronic PI controller which is assumed to react so fast that any dynamics are neglected and the output is instantaneous. As a function of the error, e,

between a temperature T and a setpoint temperature T^{sp}, i.e., $e = T^{sp}-T$, the controller output is C_{out},

$$C_{out}(t) = K_p \cdot e(t) + K_I \cdot \int e(t)dt \qquad \text{(III-13)}$$

In industrial applications this is sometimes written

$$C_{out}(t) = K_p \left[e(t) + \frac{1}{T_I} \int e(t)dt\right] \qquad \text{(III-14)}$$

where:

K_p = the proportional gain
K_I = the integral gain
$T_I = K_p/K_I$, is the integral time constant

This controller is used in the mixing box, cooling coil, and fan subsystems.

The setpoints which are necessary to determine the error term in the controllers are determined in various ways. The setpoint temperature for the cooling coil, T^{sp}_{cool}, is determined by the highest zone temperature, $T_{high} = \max_i [T_{zi}]$, as

$$T_{cool} = \begin{cases} 18.3^oC \text{ if } T_{high} < 24.2^oC \\ 113.4-3.93 \cdot T_{high} \text{ if } 24.2 < T_{high} < 25.6^oC \\ 12.8^oC \text{ if } T_{high} > 25.6^oC \end{cases} \qquad \text{(III-15)}$$

This variable setpoint was used to obtain the steady-state values but was not used in the step tests of Chapters V and VII. The setpoint for the mixing box, T^{sp}_{am}, is set in coordination with T^{sp}_{cool}, as,

$$T^{sp}_{am} = T^{sp}_{cool} - 1.1^oC \qquad \text{(III-16)}$$

Finally, the setpoint for the fan subsystem controller, P^{sp}_c, is a constant throughout the study,

$$P^{sp}_c = 622 \text{ pa} \qquad \text{(III-17)}$$

The zone subsystem uses a different controller. Recall that the zone controls its temperature in two ways: 1) by modulating the mass flow of air down the zone duct with the VAV box and 2) by letting hot water flow in the reheat coil, warming the supply air before it enters the zone. This scheme of control is performed by the zero energy band thermostat (ZET) (see Figure 12). This name is given because there is a band of temperatures (68 to 75°F) between which it is said that no energy is consumed. Actually, when in this

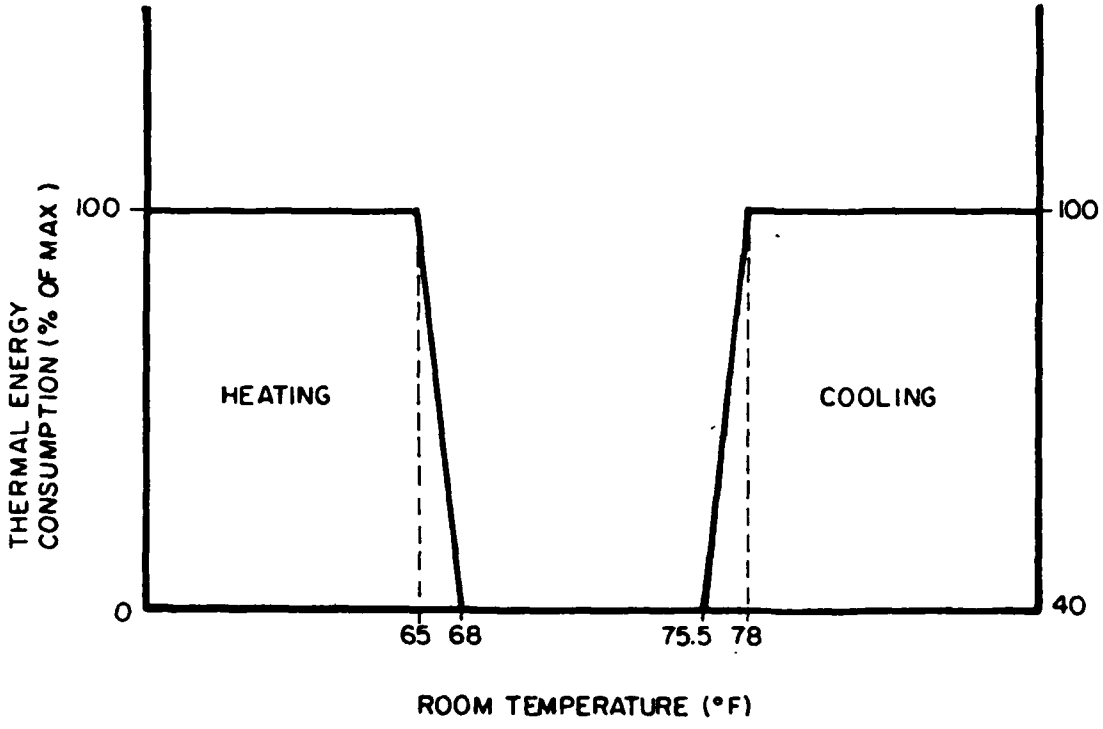

Figure 12. Zero energy band thermostat.

band the air flow is set to a minimum which does comprise a heat flux, but the name is descriptive and common so it will be used. Note that because this device is pneumatic, its dynamics are not negligible. The device has one input, T_{zi}, and two outputs: the pneumatic pressure to the reheat coil water valve, P_{vzi}, and the pneumatic pressure to the VAV box actuator, P_{dzi}. The ZET has five modes of operation:

1) for $T_{zi} < 18.3°C$ (65°F)

$$P_{dzi} = P_{ad}^{min}, \quad P_{vzi} = P_{wv}^{max} \tag{III-18}$$

where $P_{wv}^{max} = 89.6$ kpa, $P_{ad}^{min} = 56.2$ kpa

2) for $18.3°C < T_{zi} < 20.0$

$$P_{dzi} = P_{ad}^{min}$$

$$t_{cz} \cdot \dot{P}_{vzi} = -P_{vzi} + P_{wv}^{min} + (P_{wv}^{max} - P_{wv}^{min}) * \frac{(T_{zi} - 20.0)}{(18.3 - 20.0)}$$

where $t_{cz} = 1.0$ sec, is the time constant of the ZET and, $P_{wv}^{min} = 62.1$ kpa

3) for $20.0 < T_{zi} < 24.2$

$$P_{dzi} = P_{ad}^{min} \qquad P_{vzi} = P_{wv}^{min}$$

4) for $24.2 < T_{zi} < 25.6$

$$t_{cz} \cdot \dot{P}_{dzi} = -P_{dzi} + P_{ad}^{min} + (P_{ad}^{max} - P_{ad}^{min}) \cdot \frac{(T_{zi} - 24.2)}{(25.6 - 24.2)}$$

$$P_{vzi} = P_{wv}^{min}$$

and 5) for $T_{zi} > 25.6$

$$P_{dzi} = P_{ad}^{max}, \quad P_{vzi} = P_{wv}^{min}$$

This controller performs only proportional control. The gain is set by the difference in the temperatures between which the ZET modulates the output

pressure and also by difference of the extreme pressures.[ii] This is different than with the PI controllers where the selection of the gain settings is a necessary and crucial procedure, which will be the topic of the next chapter.

C. The Sensors

In order that the PI controller can calculate the error, it must have an electronic representation of the control variable. This voltage is provided by a sensing device having a non-negligible dynamic response. The transfer function of all the measurement operations has the form

$$\frac{Y^0(s)}{Y(s)} = \frac{1}{1 + t_j s} \qquad \text{(III-19)}$$

where Y^0 is the Laplace transform of the measured variable, Y is the transform of the variable which is measured, and t_j is the sensor time constant. Here Y can be T_{am}, T_{cool}, or P_c; Y^0 can be T_{oam}, T_{ocol}, or P_{oc}, and t_j can be t_{sm}, t_{sc}, or t_{sf} for the mixing box, cooling coil, and fan subsystems, respectively. This defines the observed mixed air temperature, T_{oam}, where the mixing box sensor time constant t_{sm} = 10.0 secs; the observed cold deck temperature, T_{ocol}, where the cold deck sensor time constant, t_{sc} = 10.0 secs; and the observed duct static pressure P_{oc}, where the static pressure sensor time constant t_{sf} = 0.1 sec. Actually, the static pressure sensor dynamics arise from the sensor and a 30.5-m (100-ft) tube necessary to reach the duct. This length of tube also introduces a transport lag or pure time delay into the fan subsystem feedback due to the finite speed of the propagation of this pressure signal. This pure time delay has a transfer function of $\exp(-s \cdot t_{bdl})$ where t_{bdl}=0.1 sec is the tube delay time.

The ZET is placed directly in the zone so that there is not a separate measuring device for the zone subsystem.

D. The Actuators

The actuators are the final link in the subsystem, translating the electronic signal of the controller into an action in the plant. For the mixing box and cooling coil, this is a two-component operation: the electronic to pneumatic (E/P) transducer produces a pressure signal from the electronic controller output, and the pneumatic actuator uses this pressure signal to move an air damper or water valve. These two components are described independently. The E/P is described by

[ii] The gains associated with the ZET were fixed throughout the course of this study.

$$\frac{P(s)}{C(s)} = \frac{(P^{max} - P^{min})}{1 + t_{ep} \cdot s} \qquad \text{(III-20)}$$

where:

P(s) = the transform of the output pressure: P_{ad} for the mixing box; P_{wv} for the cooling coil

C(s) = the transform of the respective controller output

t_{ep} = 2.4 secs, the E/P time constant

The E/P time constant was obtained from a frequency plot of peak-to-peak pressure output vs. peak-to-peak sine wave voltage input. The break frequency of this corner plot was found by extrapolating a line with -20 dB/decade slope, curve-fit to the highest frequency data points up to the zero-frequency gain level. The inverse of the frequency at this intersection is the time constant of the single-pole transfer function model, Eqn. III-20.

Further confirmation of this model was obtained by applying a step-input in the voltage and observing the output with a strip chart recorder. This procedure produced a value of $t_{ep} = 2.0 \pm 0.5$ secs which includes the value obtained by the frequency plot method.

The pressure output of the E/P in the mixing box subsystem is connected to the actuator and damper combination in the duct or mixing chamber. The relation between the damper position and the pneumatic pressure is described by

$$\frac{F_{ret(s)}}{P_{ep}(s)} = \frac{f_{ret}^{max}}{(P_{ad}^{max} - P_{ad}^{min})} \cdot \frac{1}{1 + t_{am} \cdot s} \qquad \text{(III-21)}$$

where:

t_{am} = 3.2 secs, the mixing box actuator time constant

$F_{ret}(s)$ = the transform of f_{ret}, the return air fraction

$P_{ep}(s)$ = the transform of P_{ep}

The constant t_{am} was obtained by the same frequency plot procedure as t_{ep}.

The pressure output of the E/P in the cooling coil is connected to the chilled water valve actuator. The valve and actuator dynamics are described by

$$\frac{M_{wc}(s)}{P_{ep}(s)} = \frac{1}{1 + t_{ac}s}, \frac{\dot{m}_{wc}^{max}}{(P_{wv}^{max} - P_{wv}^{min})} \qquad \text{(III-22)}$$

where:

$\dot{m}_{wc}^{max}$ = 3.15 kg/sec (50 GPM),[iii] the maximum mass flow of water through the coil

$M_{wc}(s)$ = the transform of $\dot{m}_{wc}$

t_{ac} = 3.2 secs, the water valve and actuator time constant.

Here it has been assumed that the dynamics of the valve/actuator combination are the same as the damper/actuator combination, i.e., $t_{ac} = t_{am}$.

The E/P and actuator models have been presented here as separate and isolated components. This is how the frequency plot experiments were performed. However, when performing the step input tests to obtain further confirmation, a slight overshoot of the final damper position was observed when the E/P was given a step input in voltage. Again the overshoot was small, but perhaps a better model might combine the E/P and actuator into a single model. At present, the transfer function between f_{ret} and c_{out} is given by

$$\frac{F_{ret}(s)}{C(s)} = \frac{f_{ret}^{max}}{(1 + t_{ep}s)(1 + t_{am}s)} \qquad \text{(III-23)}$$

and perhaps a better model would be

$$\frac{F_{ret}(s)}{C(s)} = \frac{f_{ret}^{max}}{1 + as + bs^2} \qquad \text{(III-24)}$$

where the polynomial in the denominator may have complex roots indicating oscillatory behavior. For this report, the first model was used.

Both the E/P and the actuators suffer from the nonlinear effect of hysteresis. This cannot be accounted for by transfer functions so it cannot be included in the frequency analysis, but it can be included in the simulation via a subroutine named "BACKLASH." The hysteresis problem was made evident by Dolan[4] (see Figures 13 and 14) for dampers and valves, and by the present author for E/P's. For the valve and damper the hysteresis is characterized by having a backlash of 0.5% of full span; for the E/P's this number is 1%. A plot to demonstrate this is shown in Figure 15, which shows $\dot{m}_{wc}$ with hysteresis (MDWC) vs. $\dot{m}_{wc}$ without hysteresis (PMOWC) during a simulation with standing oscillations. Note the difference between the paths as PMDWC increases and as PMODWC decreases.

[iii] This conversion assumes a water density of 998. kg/m^3.

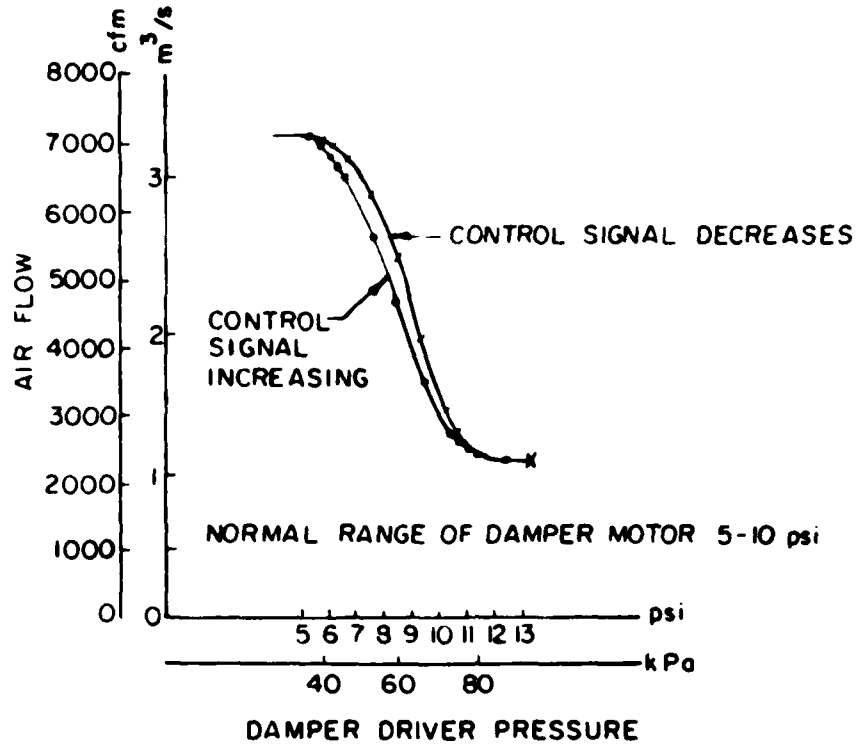

Figure 13. Hysteresis - air damper.

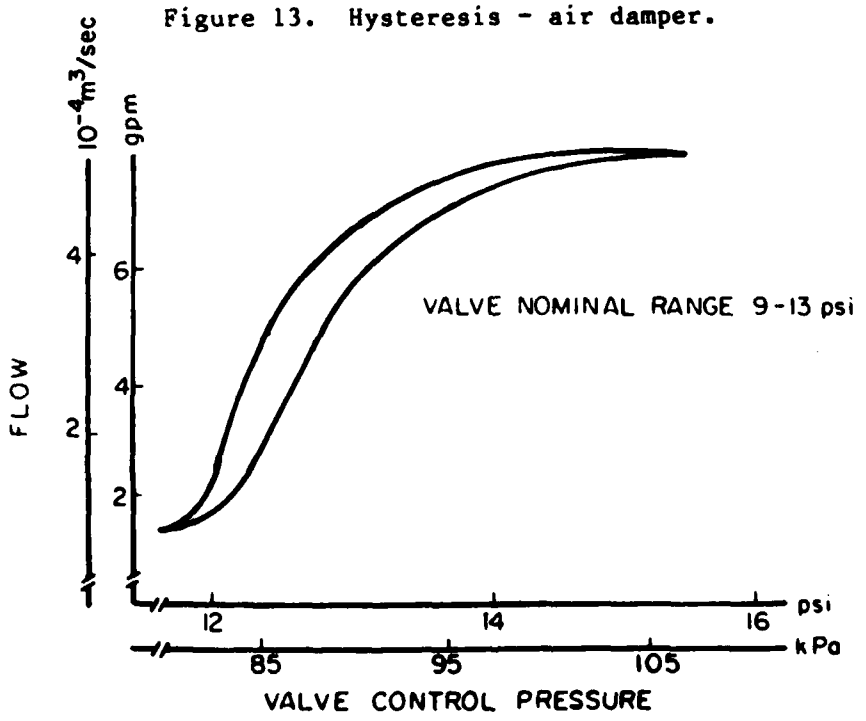

Figure 14. Hysteresis - water valve.

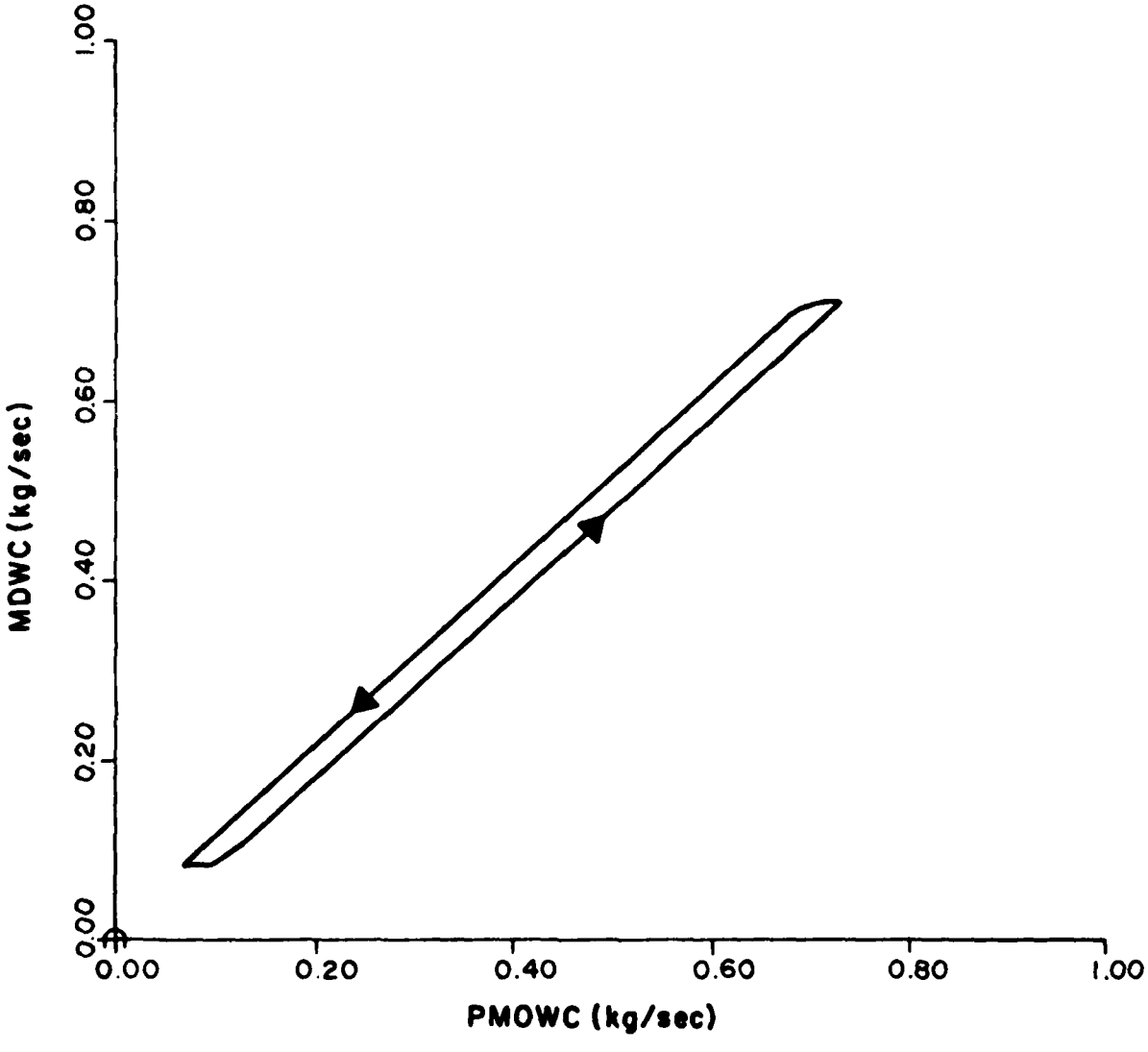

Figure 15. Hysteresis simulation.

The zones, because they use the pneumatic ZET, do not require an E/P transducer. They still require actuators. The transfer function between the reheat coil water mass flow ($\dot{m}_{wzi}$) and the pneumatic pressure (P_{vzi}) is given by

$$\frac{M_{wzi}(s)}{P_{vzi}(s)} = \frac{\dot{m}^{max}_{wzi}}{(P^{max}_{wv} - P^{min}_{wv})} \cdot \frac{1}{1 + t_{az}s} \qquad \text{(III-25)}$$

where:

$\dot{m}^{max}_{wzi}$ = 0.126 kg/sec (corresponding to 2 GPM), the maximum water mass flow in zone reheat coil

t_{az} = 3.2 secs, the zone actuator time constant with (t_{az}=t_{am}).

The relation between the mass flow of air into the zone and the pneumatic pressure applied to the actuator can be described in two steps: the first is dynamic, the second is numerical. The transfer function between the ZET output damper pressure, P_{dzi}, and the zone damper fraction of full open, f_{dzi}, is

$$\frac{F_{dzi}(s)}{P_{dzi}(s)} = \frac{1 - f^{min}_{dz}}{(p^{max}_{ad} - P^{min}_{ad})} \cdot \frac{1}{1 + t_{az}s} \qquad \text{(III-26)}$$

where f^{min}_{dz} is the minimum zone air damper fraction (=0.4). The relation between the damper fraction and zone air mass flow is given by

$$\dot{m}_{az} = \dot{m}^{max}_{az} \cdot f_{dzi} \qquad \text{(III-27)}$$

where $\dot{m}^{max}_{az}$ is the maximum air mass flow into the zone. This maximum is a constant for the subsystem alone but varies when the interconnections are introduced.

The actuator block of the fan subsystem is the motor speed controller. This electronic unit converts a D.C. voltage signal from the PI controller into a frequency signal. As the input voltage is varied from 0 to 10 volts D.C. the three-phase frequency varies from 0 to 60 Hz while the output voltage is varied to maintain constant volts-per-Hz ratio. The manufacturer describes the motor speed controller by stating that given a step input in voltage, the output frequency will ramp to the new value. The immediate temptation is to model this as a simple integrator with transfer function, s^{-1}. This does describe the output until it reaches the new value where the ramp is shut off, indicating a transfer function, $s^{-1}(1 - e^{-st_1})$ where t_1 is the time necessary to reach the new value given the preset ramp slope. For a single known step input, this is useful; but for a simulation where the inputs are not simple or known prior to modeling, this transfer function is not suitable.

For the simulation, the manufacturer's description was used on the discrete time level. The simulation uses a Runge-Kutta integration technique, which, instead of producing a continuous line vs. time, results in a staircase output. The output is constant over a length of time called the calculation interval, Δt, after which the output jumps to a new value. The motor speed controller is described by limiting the change in output frequency, Δf_1, requested by the input voltage, Δf_1^o. If Δf_1^o is less than $m/\Delta t$, it is allowed, i.e.,

$$\Delta f_1 = \begin{cases} \min\,(\Delta f_1^o,\ m/\Delta t) \text{ if } \Delta f_1^o \geq 0 \\ \max(\Delta f_1^o,\ -m/\Delta t) \text{ if } \Delta f_1^o < 0 \end{cases} \qquad \text{(III-28)}$$

Because this strategy is implemented on the smallest time-scale level, it can accommodate any input voltage variations as well as any other model. Also, it does produce a ramp output which stops discontinuously at the new value selected by a step input.

For the analysis techniques, this model, (III-28), is also of no use and a less accurate model must be used. For analysis, the relation between the input voltage, C_{out}, from the controller and the output frequency, f_1, is given by

$$\frac{F_1(s)}{C_{out}(s)} = \frac{60 \text{ Hz}}{10 \text{ volts}} \cdot \frac{1}{1 + t_{msc}s} \qquad \text{(III-29)}$$

where

$F_1(s)$ = the transform of F_1
$C_{out}(s)$ = the transform of C_{out}
t_{msc} = 3.0 secs, the motor speed controller time constant

The motor speed controller time constant value was selected to be appropriate to the slope used which was m = 4 Hz/sec.

This concludes the SISO description of the four subsystem types. Next, the MIMO approach will be used to combine the subsystems into a whole system, making many subsystem constant parameters into the time-varying inputs by describing the interconnections.

IV. MATHEMATICAL MODELING OF THE MIMO SYSTEM

Having described the SISO local loops, it is now possible to put all seven subsystems together and form the whole system. This will be done in two steps: first, the interconnections between the subsystems will be presented, primarily from a simulation point of view; second, the necessary transfer functions will be obtained from the system plant signal flow graph in order to fill in the elements of the plant transfer function matrix.

A. Subsystem Interconnections

It is now necessary to obtain descriptions of how the subsystems affect each other. Quantities which were assumed to be constant in the isolated subsystems will not be made variable as they are affected by changes in the other subsystems. The interconnections will be presented by how they affect each subsystem.

The mixing box subsystem is affected by changes in the zone air temperatures through the return air temperature. This is shown by considering T_{ret},

$$T_{ret} = \left(\sum_{i=1}^{4} \dot{m}_{azi} \cdot T_{zi}\right) / \left(\sum_{i=1}^{4} \dot{m}_{azi}\right) \qquad \text{(IV-1)}$$

Changes in both T_{zi} and $\dot{m}_{azi}$ can affect T_{ret}. Also there is a transport lag time between the time at which T_{zi} or $\dot{m}_{azi}$ changes and the time at which T_{ret} at the mixing box changes. This is due to finite mass flow rate and duct lengths between the zone and mixing box. This return duct delay time is $t_{dlr} = 61.0/\dot{m}_{as}$), where $\dot{m}_{as}$ is the mass flow rate of air in the return duct in kg/sec. This is based on a return air duct length of 27.4 m (90 ft).

The cooling coil output, T_{cool}, is affected by two other variables, T_{am} and $\dot{m}_{as}$. The derivation by Gartner and Harrison of the transfer functions of a tube in crossflow mentioned earlier also includes the relations between the output (exiting secondary fluid temperature T_{cool}), and the inputs (entering secondary fluid temperature, T_{am}, and secondary fluid mass flow, $\dot{m}_{as}$). The first of these transfer functions was found to be unusable because it gave an erroneous initial reaction (although the final values are thought to be correct). The second relation was used and is given by the transfer function

$$\frac{T_{cool}(s)}{\dot{m}_{as}(s)} = \frac{\delta_o + \delta_1 s + \delta_2 s^2}{\alpha_2 s^2 + \alpha_1 s + \alpha_o} \qquad \text{(IV-2)}$$

where the α's are the same as in III-2 and the δ's depend upon the same quantities as the α's and β's.

Instead of using the results derived by Gartner and Harrison for correlating changes in T_{cool} with changes in T_{am}, the relationship was derived experimentally. Using the full-scale HVAC laboratory at USA-CERL under the direction of Richard Rundus, an input of T_{am} described by

$$T_{am}(t) = T^{o}_{am} \cdot [1 - EXP\ (t/a)] \qquad \text{(IV-3)}$$

was imposed on the cooling coil operating at various steady-state flow conditions. By recording the T_{cool} output data and assuming a model of

$$\frac{T_{cool}(s)}{T_{am}(s)} = \frac{G}{1 + s/b} \qquad \text{(IV-4)}$$

a least squares curve-fit was made to the predicted T_{cool} response of

$$T_{cool}(t) = T^{o}_{cool} + G \cdot \Delta T_{am} \cdot \left(1 - \frac{ae^{-bt} - be^{-at}}{a-b}\right) \qquad \text{(IV-5)}$$

This procedure resulted in the values of G = 0.4 and b = 0.25 sec^{-1} which indicate a time constant of the cooling coil for changes in incoming air of 4.0 secs.

It should also be mentioned that the temperature of the mixed air at the face of the cooling coil is 1.1°C (2°F), warmer than at the mixing box due to the heat generated by the fan which is located in the intervening duct. There is also a time delay associated with this ductwork which is $t_{dlm} = 20.0/\dot{m}_{as}$ which is based on a 5.5-m (18-ft.) length of duct.

The next subsystem to be considered is the fan. That there is a connection between the fan "system" curve and the zone damper positions via the fraction of wide-open-cfm, f_{wo}, was mentioned earlier (see Chapter III--The Plants). This connection will now be correlated with experimental data. Previous experiments on the USA-CERL HVAC lab have produced an envelope on the fan curve corresponding to various damper positions. For the particular HVAC system under study--a single duct system, a corresponding f_{wo} of 67% was observed when four dampers were wide open (f_{dzi}=1.0, i=1,2,3,4); when all four zone dampers were in the minimum position (f_{dzi} = 0.4, i=1,2,3,4), the f_{wo} was seen to be 50%. So, assuming that the f_{wo} moves linearly with f_{dzi}, the relation becomes

$$f_{wo} = 0.387 + 0.071 \cdot \sum_{i=1}^{4} f_{dzi} \qquad \text{(IV-6)}$$

The other points on the fan curve envelope tend to lend credibility to this model. The delay between the change in damper position and change in fan "system" curve is assumed to be negligible (<0.1 sec), because the signal is pressure wave propagated at the speed of sound.

Having given the relation between f_{wo} and f_{dzi}, it is now necessary to relate changes in f_{wo} to changes in $\dot{m}_{as}$ and P_c. This will be done by the same procedure which led to equations III-6 and III-7. From the fan curve the following two relations were obtained.

$$P_f[P_a] = A + B \cdot f_{wo} \tag{IV-7}$$

where:

$$A = 261.8 - 0.429 \cdot \dot{\theta}_f \text{ [RPM]}$$

$$B = 240.9 - 0.393 \cdot \dot{\theta}_f \text{ [RPM]}$$

and

$$\dot{m}_{as}[\text{kg/sec}] = A + B \cdot f_{wo} \tag{IV-8}$$

where:

$$A = 0.1889 - 1.392 \quad 10^{-4} \cdot \dot{\theta}_f[\text{RPM}]$$

$$B = -0.2747 + 5.224 \cdot 10^{-4} \cdot \dot{\theta}_f \text{ [RPM]}$$

So, for a small change in f_{wo}, δf_{wo}, the changes in $\dot{m}_{as}$ and P_c can be found by using the constants:

$$F_3 = \frac{\delta P_c}{\delta f_{wo}} \Big|_{\delta\dot{\theta}_f=0} = 240.9 - 0.3929 \cdot \dot{\theta}_f^o \tag{IV-9}$$

$$F_4 = \frac{\delta \dot{m}_{as}}{\delta f_{wo}} \Big|_{\delta\dot{\theta}_{f=0}} = -0.2747 + 5.224 \cdot 10^{-4} \cdot \dot{\theta}_f^o \tag{IV-10}$$

where $\dot{\theta}_f^o$ is the steady-state operating point of the motor. So using the linearized fan model about the steady-state operating point, determined by $\dot{\theta}_f^o$ and f_{wo}^o,

$$\delta P_c = F_1 (f_{wo}^o) \cdot \delta\dot{\theta}_f + F_3(\dot{\theta}_f^o) \cdot \delta f_{wo} \tag{IV-11}$$

$$\delta \dot{m}_{as} = F_2(f_{wo}^o) \cdot \delta\dot{\theta}_f + F_4(\dot{\theta}_f^o) \cdot \delta f_{wo} \tag{IV-12}$$

where δP_c and $\delta \dot{m}_{as}$ are changes in P_c and $\dot{m}_{as}$ from their respective steady-state values, and F_1 and F_2 are given by III-6 and III-7.

The last subsystem is the zone. Here there are two interconnections affecting the zone air mass flow $\dot{m}_{azi}$ and the zone duct temperature T_{zdi}. Recall from the SISO subsystem zone actuators description (Chapter III, Section D) the equation III-27,

$$\dot{m}_{azi} = \dot{m}_{az}^{max} \cdot f_{dzi} \qquad \text{(IV-13)}$$

It is now necessary to give meaning to the maximum zone air mass flow, $\dot{m}_{az}^{max}$. This is the maximum $\dot{m}_{azi}$ a zone would be allowed to receive if its damper were moved to the wide-open position, $f_{dzi}=1.0$. If the supply air mass flow, $\dot{m}_{as}$, were for a moment considered independent of damper position, then $\dot{m}_{az}^{max}$ would depend upon $\dot{m}_{as}$ and all the zone damper positions as

$$\dot{m}_{az}^{max} = \dot{m}_{as} / \left(\sum_{i=1}^{4} f_{dzi}\right) \qquad \text{(IV-14)}$$

This insures that when an individual zone requests more air by changing its damper position, the change in mass flow into that zone is achieved by reducing the air mass flow into the other zones and not by changing the total supply air mass flow; note,

$$\dot{m}_{as} = \sum_{i=1}^{4} \dot{m}_{azi}$$

$$= \sum_{i=1}^{4} f_{dzi}\, \dot{m}_{az}^{max}$$

$$= \sum_{i=1}^{4} f_{dzi} \cdot \dot{m}_{as} / \left(\sum_{i=1}^{4} f_{dzi}\right) = \dot{m}_{as}$$

Of course, $\dot{m}_{as}$ does change when the zone damper positions change, but this is due to the fan "system" curve change and not the manner in which $\dot{m}_{as}$ is split into the $\dot{m}_{azi}$'s. Further, the $\dot{m}_{as}$ used to calculate $\dot{m}_{as}^{max}$ is delayed from the $\dot{m}_{as}$ in the fan subsystem by a length of $t_{dls} = 61.0/\dot{m}_{as}$ secs due to the length of supply duct between the fan and the zones.

When the reheat coil in a zone is operating, the change in $\dot{m}_{azi}$ has another effect which is described in a manner similar to the relation between T_{cool} and $\dot{m}_{as}$. The transfer function between T_{zdi} and $\dot{m}_{azi}$ is given by

$$\frac{T_{zdi}(s)}{M_{azi}(s)} = \frac{\delta_{azi} + \delta_{1zi} \cdot s + \delta_{2zi} s^2}{\alpha_{2zi} s^2 + \alpha_{1zi} s + \alpha_{ozi}} \qquad \text{(IV-15)}$$

where the α's are the same as in equation III-12 and the δ's depend upon the same quantities as the α's and β's. Also, if the heating coil is on, any change in T_{cool} will affect T_{zdi} in a manner similar to the way T_{am} affects T_{cool}; that is, the description is

$$\frac{T_{zdi}(s)}{T_{cool}(s)} = \frac{G_z}{(1 + t_{hz}s)} \qquad \text{(IV-16)}$$

where t_{hz} = 4.0 secs is the same constant as in IV-4. The value of G_z, which was obtained from G in IV-4 with the aid of the Gartner-Harrison transfer functions for T_{cool} vs. T_{am} and T_{zdi} vs. T_{cool}, which have reasonable final values, was calculated by using the final-value theorem of Laplace transforms, i.e.,

$$G_z = G \cdot \frac{\lim_{s \to 0}\left[s \cdot \frac{T_{zdi}(s)}{T_{cool}(s)}\right]}{\lim_{s \to 0}\left[s \cdot \frac{T_{cool}(s)}{T_{am}(s)}\right]} \qquad \text{(IV-17)}$$

This resulted in the value $G_z = 0.8$. If the heating coil is not in use, then any change in T_{cool} will produce an equal change in T_{zdi}. That is, $T_{zdi} = T_{cool}$ when the coil's effect is absent. In either case, coil or no coil, the changes in T_{cool} at the cooling coil are delayed by time $t_{dls} = 61.0/\dot{m}_{as}$ secs before they reach the zone duct.

At this point, all of the necessary relations have been presented that were required to write a simulation program of the entire HVAC system. This was done with the Advanced Continuous Simulation Language simulation package which included the pure time delays, the single pole transfer functions, the quadratic transfer functions, and the hysteresis. This simulation will be used in the next chapters.

B. Transfer Function Matrix Description

In order to use a frequency analysis technique to determine the sensitivity of the seven subsystems to interconnection, it is necessary to derive a matrix transfer function description of the system. The MIMO system will now be described as having vector inputs and outputs and by describing the elements of the transfer function matrices. In order that the effect of the interconnections may be studied, the MIMO system plant transfer function matrix, P' (a 7 by 7 matrix) will be decomposed into two parts as

$$P' = P + \Delta P \qquad \text{(IV-18)}$$

where P is the nominal plant containing the disconnected subsystems and ΔP is the additive plant perturbation (see Figure 16). This figure also shows the controller transfer function matrix, G, and the feedback transfer function matrix, H, which also need to be described.

The approach of this section will be to derive the matrix P' by using a signal flow graph of the system plant. The matrix P will be given without need of derivation because its diagonal elements have already been derived in Chapter II, and its off-diagonal elements are all zero by the assumption that the SISO subsystems are isolated or non-interacting. This will then have determined the perturbation matrix by $\Delta P = P'-P$. The controller and feedback matrices, whose on-diagonal elements have also been given in Chapter II and whose off-diagonal elements are zero because the SISO subsystems do not have interconnections in sensing or control, will then be given.

In order that the system plant matrix, P', be derived, it is necessary to draw the signal flow graph of the system plant (see Figure 17). Recall from the first chapter that the plant input vector U in the summer is,

$$U = (P_{ad}\ P_{vc}\ f_1\ P_{dz1}\ P_{dz2}\ P_{dz3}\ P_{dz4})^T \qquad \text{(II-1)}$$

and in winter, it is

$$U = (P_{ad}\ P_{vc}\ f_1\ P_{vz1}\ P_{vz2}\ P_{vz3}\ P_{vz4})^T \qquad \text{(II-2)}$$

and the output is always

$$Y = (T_{am}\ T_{cool}\ P_c\ T_{z1}\ T_{z2}\ T_{z3}\ T_{z4})^T \qquad \text{(II-3)}$$

Because the use of P_{vzi} and P_{dzi} are made mutually exclusive by the ZET, the artifice of the zone mode matrix - M(i,j):i=1,2,3,4;j=1,2 - was introduced into the system plant signal flow graph to eliminate the necessity of making the input vector have 11 elements. If the zone i is modulating its water valve, i.e., $18.3°C < T_{zi} < 20.0$, then M(i,1) = 1 and M(i,2) = 0; if the zone i is modulating the air damper, i.e., $24.2 < T_{zi} < 25.6°C$, then M(i,1)=0, M(i,2) = 1; and for all other T_{zi}, M(i,1)=M(i,2)=0. By including the zone mode matrix in the transfer functions which have P_{vzi} or P_{dzi} as the input, the matrix P' has the dimensions of 7 by 7.

The signal flow graph branches are labeled by the transfer function's P's and T's. The input and output nodes of these branches are given in Table 1.

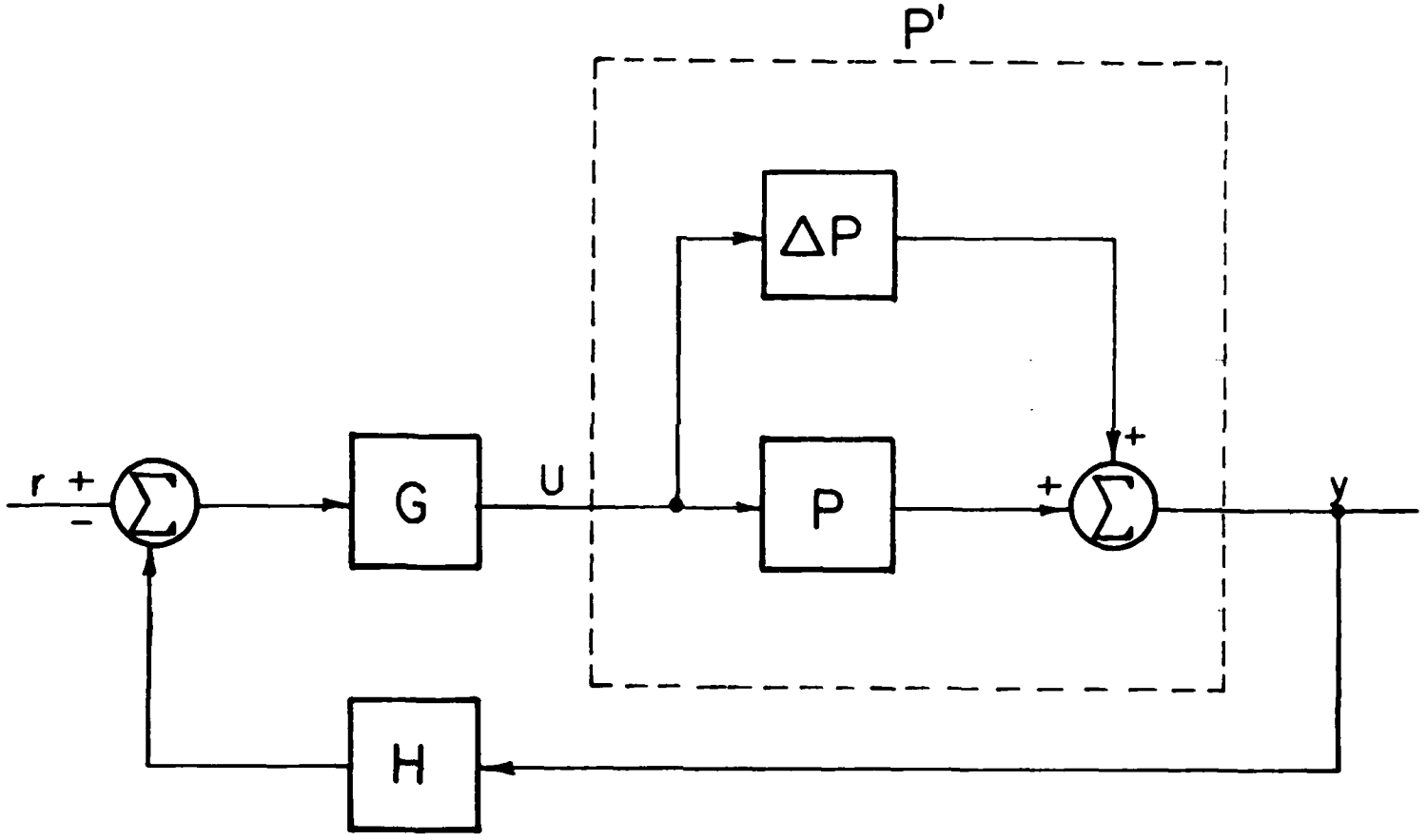

Figure 16. Additive plant perturbations.

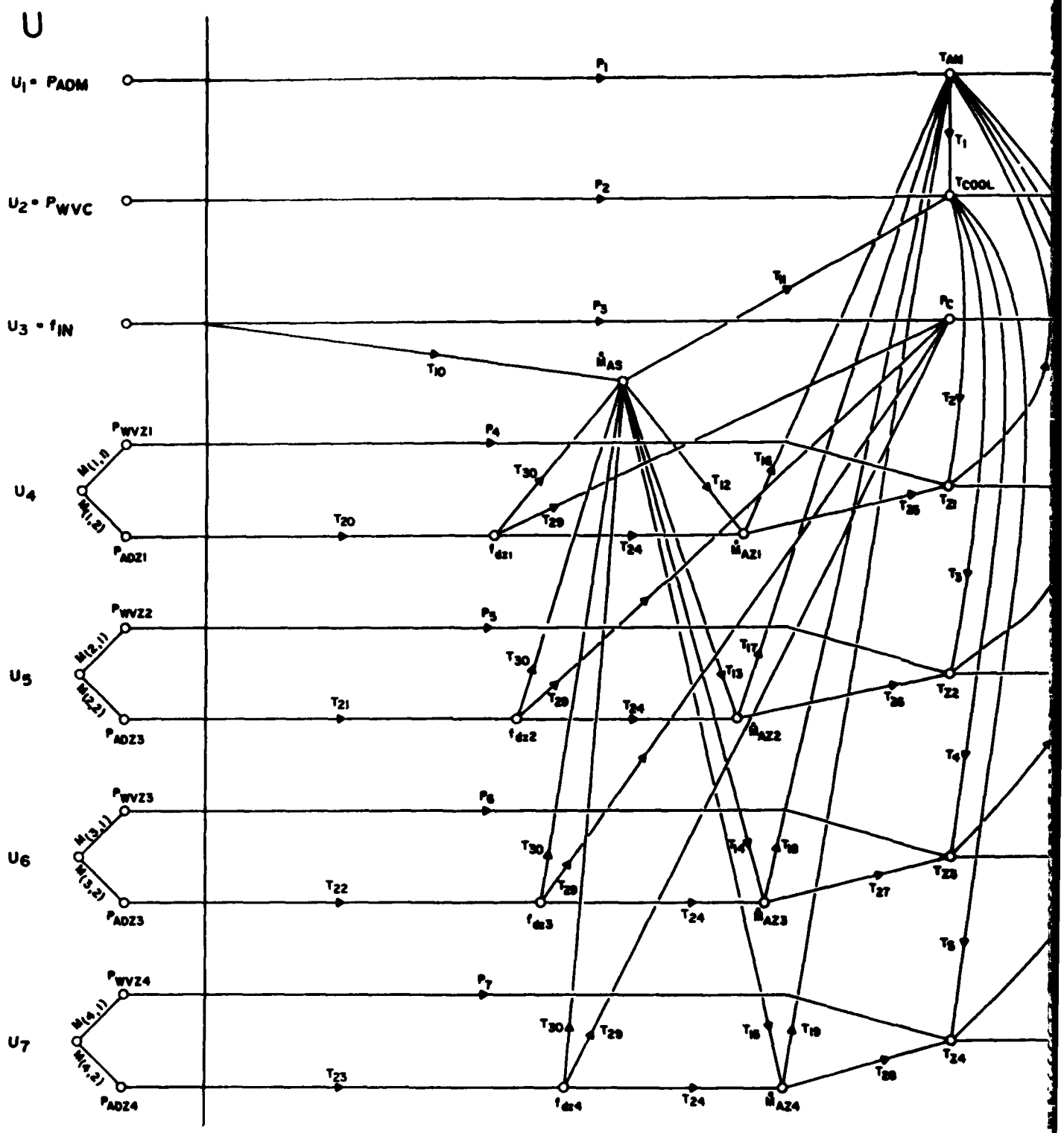

Figure 17. System plant signal flow chart.

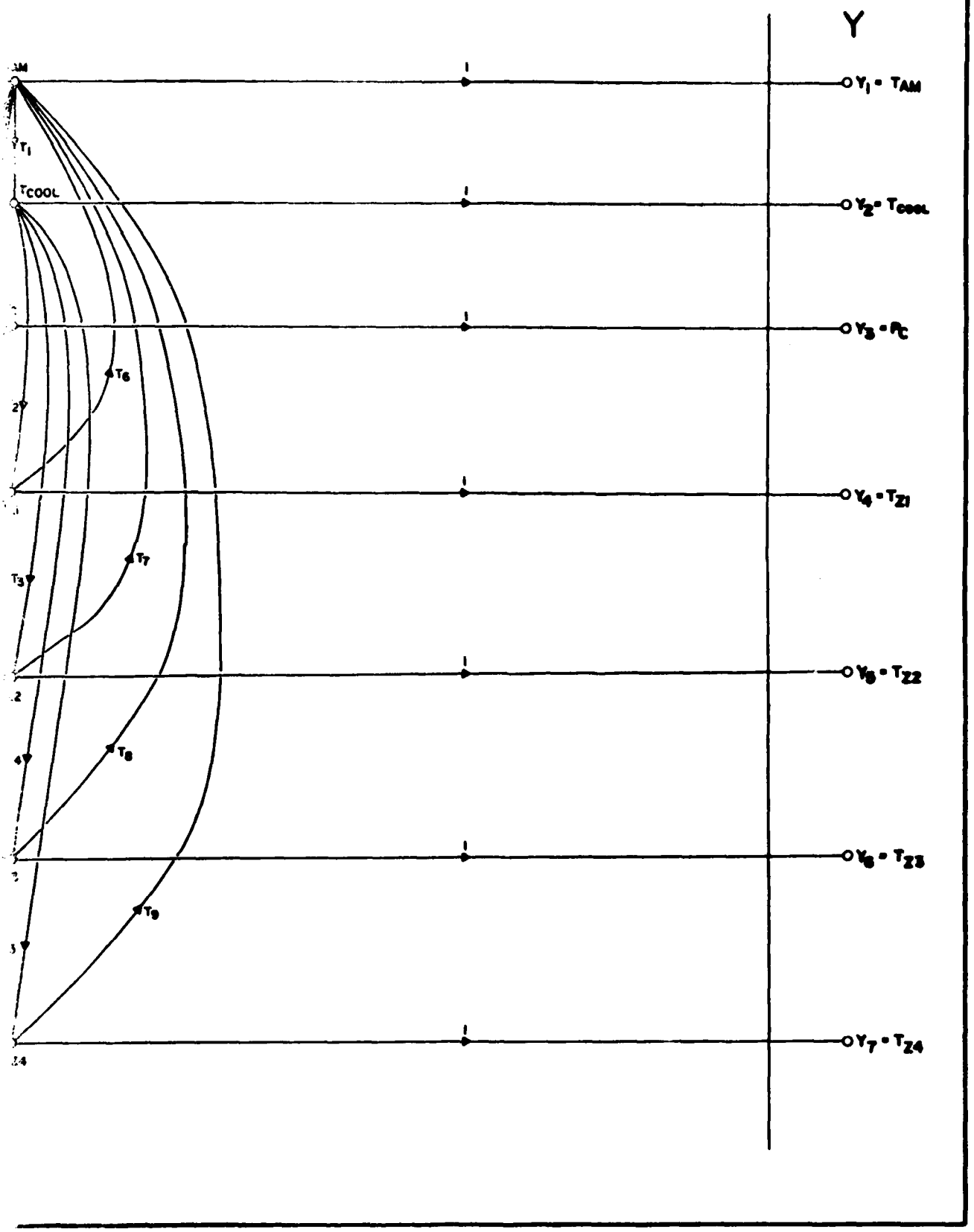

Table 1. System Plant Transfer Functions

BRANCH GAIN	OUTPUT NODE	INPUT NODE
P_1	T_{am}	P_{ad}
P_2	T_{COOL}	P_{VC}
P_3	P_c	f_{IN}
P_{3+j}; $j=1,2,3,4$	T_{zj}	P_{vzj}
T_1	T_{COOL}	T_{am}
T_{1+j}; $j=1,2,3,4$	T_{zj}	T_{COOL}
T_{5+j}; $j=1,2,3,4$	T_{am}	T_{zj}
T_{10}	$\dot{m}_{as}$	f_{IN}
T_{11}	T_{COOL}	$\dot{m}_{as}$
T_{11+j}; $j=1,2,3,4$,	$\dot{m}_{azj}$	$\dot{m}_{as}$
T_{15+j}; $j=1,2,3,4$	T_{am}	$\dot{m}_{azj}$
T_{19+j}; $j=1,2,3,4$	f_{dzj}	P_{dzj}
T_{24}	$\dot{m}_{azj}$	f_{dzj}
T_{24+j}; $j=1,2,3,4$	T_{zj}	$\dot{m}_{azj}$
T_{29}	P_c	f_{dzj}
T_{30}	$\dot{m}_{as}$	f_{dzj}

The transfer functions were derived in the previous chapter and the first part of this chapter. They will now be summarized here:

$$P_1(s) = \frac{T^o_{ret} - T_{out}}{P^{mx}_{ad} - P^{mn}_{ad}} \cdot \frac{1}{1 + t_{am} \cdot s} \cdot \frac{1}{1 + t_{bm} s} \qquad \text{(IV-19)}$$

$$P_2(s) = \frac{\dot{m}^{max}_{wc}}{P^{max}_{wv} \; P^{min}_{wv}} \cdot \frac{1}{1 + t_{as} s} \cdot \frac{\beta_o + \beta_1 s}{\alpha_2 s^2 + \alpha_1 s + \alpha_o} \qquad \text{(IV-20)}$$

$$P_{(s)} = \frac{12.28 - 11.30 \cdot f^o_{wo}}{1 + t_m \cdot s} \qquad \text{(IV-21)}$$

$$P_{3+j}(s) = \frac{\dot{m}^{mx}_{wz}}{P^{max}_{wv} - P^{min}_{wv}} \cdot \frac{\dot{m}^{o}_{azj}}{C_{zj} s + \dot{m}^{o}_{azj} + \mu + C_{zj} \cdot F_1} \cdot \frac{1}{1 + t_{wvz} s}$$

$$\cdot \frac{\beta_o + \beta_1 s}{\alpha_{2zj} s^2 + \alpha_{1z2} \cdot s + \alpha_{ozj}} : \; j = 1,2,3,4 \qquad \text{(IV-22)}$$

$$T_1(s) = \frac{G}{1 + s/b} \cdot EXP(-s \cdot t_{dlm}) \qquad \text{(IV-23)}$$

$$T_{5+j}(s) = f^o_{dzj} \cdot f^o_{ret} \cdot EXP(-s \cdot t_{dlm}) : \quad j = 1,2,3,4 \qquad \text{(IV-24)}$$

$$T_{10}(s) = \frac{-4.075 \cdot 10^{-4} + 0.1523 \cdot f^o_{wo}}{1 + t_m \cdot s} \qquad \text{(IV-25)}$$

$$T_{11}(s) = \frac{\delta_o + \delta_1 s + \delta_2 s^2}{\alpha_2 s^2 + \alpha_1 s + \alpha_o} \qquad \text{(IV-26)}$$

$$T_{11+j}(s) = \frac{f^o_{ret}}{\dot{m}_{as}} \cdot (T^o_{zj} - T^o_{ret}) \cdot EXP(-s \cdot t_{dlr}): \quad j = 1,2,3,4 \qquad \text{(IV-27)}$$

$$T_{19+j}(s) = \frac{1 - f_{dz}^{min}}{p_{ad}^{max} - p_{ad}^{min}} \cdot \frac{1}{1 + t_{az}S} : \quad j = 1,2,3,4 \qquad \text{(IV-28)}$$

$$T_{24}(s) = \dot{m}_{az}^{max} \qquad \text{(IV-29)}$$

$$T_{28}(s) = 17.06 - 0.02782 \cdot \dot{\Theta}_f^o \qquad \text{(IV-30)}$$

Eight of the T's depend upon the steady-state zone temperature and must be specified in two modes:

a) if $T_{zj}^o < 20^oC$

$$T_{1+j}(s) = \frac{\dot{m}_{azj} \cdot EXP(-s \cdot t_{dls})}{C_{zj} \cdot s + \dot{m}_{azj} + \mu + C_{zj} \cdot F_i} \cdot \frac{G_z}{1 + t_{hz} \cdot s} : \quad j = 1,2,3,4 \qquad \text{(IV-31)}$$

$$T_{24+j}(s) = [(T_{zdj}^o - T_{zj}^o) + \dot{m}_{azj}^o \cdot (\delta_{ozj} + \delta_{1zj} \cdot s + \delta_{2zj} \cdot s^2)/$$

$$(\alpha_{2zj} \cdot s^2 + \alpha_{1zj} \cdot s + \alpha_{ozj})]$$

$$/(C_{zj} \cdot s + \dot{m}_{azj}^o + \mu + C_{zj} \cdot F_I): \quad j = 1,2,3,4 \qquad \text{(IV-32)}$$

and

b) if $T_{zj}^o > 20^oC$

$$T_{i+j}(s) = \frac{\dot{m}_{azj}^o \cdot EXP(-s \cdot t_{dls})}{(C_{zj} \cdot s + \dot{m}_{azj} + \mu + C_{zj} \cdot F_I)} : \quad j = 1,2,3,4 \qquad \text{(IV-33)}$$

$$T_{24+j}(s) = \frac{T_{zdj}^o - T_{zj}^o}{(C_{zj} s + \dot{m}_{azj}^o + \mu + C_{zj} \cdot F_I)} : \quad j = 1,2,3,4 \qquad \text{(IV-34)}$$

Having presented the detail of the transfer functions, it is now possible to derive, using Mason's gain formula[5], the elements of the matrix P'. In order to contain the size of the expressions, a few auxiliary functions will be defined. First, the loops on the plant signal flow graph will be designated by L's.

$$\begin{aligned} L_1(s) &= T_1T_2T_6 \\ L_2(s) &= T_1T_3T_7 \\ L_3(s) &= T_1T_4T_8 \\ L_4(s) &= T_1T_5T_9 \end{aligned} \tag{IV-35}$$

The denominator in all of the gains to be derived will be D (sometimes labeled Δ),

$$D(s) = 1-L_1L_2L_3L_4 \tag{IV-36}$$

The last auxiliary functions are the S's:

$$S_1(s) = \sum_{j=1}^{4} T_{5+j}T_{11+j}T_{24j} \tag{IV-37}$$

$$S_2(s) = \sum_{j=1}^{4} T_{1+j}T_{5+j} \tag{IV-38}$$

$$S_{2+i}(s) = S_1 - T_{5+i}T_{11+i}\cdot T_{24+i} : \quad i = 1,2,3,4 \tag{IV-39}$$

$$S_{6+i}(s) = T_{1+i}T_{11} + T_1T_{1+i} + T_{11+i}T_{24+i}\left(1-\prod_{j=1}^{4} L_j\right): \; i=1,2,3,4 \tag{IV-40}$$

$$S_{10+i}(s) = T_1T_{24}(T_{15+i} + T_{5+i}T_{24+i}): \quad i = 1,2,3,4 \tag{IV-41}$$

With the aid of D and the L's and S's, it is now possible to present P', the MIMO system plant transfer function matrix (see Figure 18).

The next matrix to be presented is the nominal system plant transfer function matrix, P. This matrix, although in MIMO form, represents the seven isolated SISO subsystems. This matrix is shown in Figure 19.

$$
\begin{bmatrix}
P_1\frac{1}{\Delta} & P_2\frac{S_2}{\Delta} & T_{10}\frac{T_{11}S_2+S_1}{\Delta} & M(1,1)P_4\frac{T_8}{\Delta}+M(1,2)T_{20}\frac{T_{30}(S_1+T_{11}S_2)+T_{24}(T_{16}+T_8T_{25})}{\Delta} & M(2,1)P_5\frac{T_7}{\Delta}+M(2,2)T_{21}\frac{T_{30}(S_1+T_{11}S_2)+T_{25}(T_{17}+T_7T_{25})}{\Delta} \\
P_1\frac{1}{\Delta} & P_2\frac{1}{\Delta} & T_{10}\frac{T_{11}+T_1S_1}{\Delta} & M(1,1)P_4\frac{T_1T_8}{\Delta}+M(1,2)T_{20}\frac{T_{30}(T_1S_1+T_{11}S_2)+S_{11}}{\Delta} & M(2,1)P_5\frac{T_1T_7}{\Delta}+M(2,2)T_{21}\frac{T_{30}(T_1S_1+T_1S_2)+S_{12}}{\Delta} \\
0 & 0 & P_3 & M(1,2)T_{20}T_{29} & M(2,2)T_{21}T_{29} \\
P_1\frac{T_1T_2}{\Delta} & P_2\frac{T_2}{\Delta} & T_{10}\frac{S_7}{\Delta} & M(1,1)P_4\frac{1-L_2L_3L_4}{\Delta}+M(1,2)T_{20}\frac{T_{30}S_7+T_{24}(T_1T_2T_{18}+T_{29}(1-L_2L_3L_4))}{\Delta} & M(2,1)P_5\frac{T_1T_2T_7}{\Delta}+M(2,2)T_{21}\frac{T_{30}S_7+T_2S_{12}}{\Delta} \\
P_1\frac{T_1T_3}{\Delta} & P_2\frac{T_3}{\Delta} & T_{10}\frac{S_8}{\Delta} & M(1,1)P_4\frac{T_1T_3T_8}{\Delta}+M(1,2)T_{20}\frac{T_{30}S_8+T_3S_{11}}{\Delta} & M(2,1)P_5\frac{1-L_1L_2L_4}{\Delta}+M(2,2)T_{21}\frac{T_{30}S_8+T_{24}(T_1T_3T_7+T_{29}(1-L_1L_3L_4}{\Delta} \\
P_1\frac{T_1T_4}{\Delta} & P_2\frac{T_4}{\Delta} & T_{10}\frac{S_9}{\Delta} & M(1,1)P_4\frac{T_1T_4T_8}{\Delta}+M(1,2)T_{20}\frac{T_{30}S_9+T_4S_{11}}{\Delta} & M(2,1)P_5\frac{T_1T_4T_7}{\Delta}+M(2,2)T_{21}\frac{T_{30}S_9+T_4S_{12}}{\Delta} \\
P_1\frac{T_1T_5}{\Delta} & P_3\frac{T_5}{\Delta} & T_{10}\frac{S_{10}}{\Delta} & M(1,1)P_4\frac{T_1T_5T_8}{\Delta}+M(1,2)T_{20}\frac{T_{30}S_{10}+T_5S_{11}}{\Delta} & M(2,1)P_5\frac{T_1T_5T_7}{\Delta}+M(2,2)T_{21}\frac{T_{30}S_{10}+T_5S_{12}}{\Delta}
\end{bmatrix}
$$

Figure 18. System plant transfer function matrix - P^1.

$\dots) P_5 \frac{T_7}{\Delta}$	$M(3,1)\, P_6 \frac{T_8}{\Delta}$	$M(4,1)\, P_7 \frac{T_9}{\Delta}$
$\frac{\dots S_1+T_{11}S_2)+T_{24}(T_7+T_7T_{26})}{\Delta}$	$+M(3,2)T_{22}\frac{T_{30}(S_1+T_{11}S_2)+T_{24}(T_8+T_8T_{27})}{\Delta}$	$M(4,2)T_{23}\frac{T_{30}(S_1+T_{11}S_2)+T_{25}(T_9+T_9T_{28})}{\Delta}$
$\dots 2)T_{21}\frac{T_{30}(T_1S_1+T_{11}S_2)+S_{12}}{\Delta}$	$M(3,1)\,P_6\frac{T_1T_8}{\Delta}+M(2,2)T_{22}\frac{T_{30}(T_1S_1+T_{11}S_2)+S_{13}}{\Delta}$	$M(4,1)\,P_7\frac{T_1T_9}{\Delta}+M(2,2)T_{23}\frac{T_{30}(T_1S_1+T_{11}S_2)+S_{14}}{\Delta}$
$\dots 2)\, T_{21}T_{29}$	$M(3,2)\, T_{22}T_{29}$	$M(4,2)\, T_{23}T_{29}$
$\dots_3 \frac{T_1T_2T_7}{\Delta}$	$M(3,1)\,P_6\frac{T_1T_2T_8}{\Delta}$	$M(4,1)\,P_7\frac{T_1T_2T_9}{\Delta}$
$\frac{T_{30}S_7+T_2S_{12}}{\Delta}$	$+M(3,2)\,T_{22}\frac{T_{30}S_7+T_2S_{13}}{\Delta}$	$+M(4,2)\,T_{22}\frac{T_{30}S_7+T_2S_{14}}{\Delta}$
$\dots \frac{1-L_1L_3L_4}{\Delta}$	$M(3,1)\,P_6\frac{T_1T_3T_8}{\Delta}$	$M(4,1)\,P_7\frac{T_1T_3T_9}{\Delta}$
$\dots \frac{(T_1T_3T_7+T_{26}(1-L_1L_3L_4))}{\Delta}$	$+M(3,2)\,T_{22}\frac{T_{30}S_8+T_3S_{13}}{\Delta}$	$+M(4,2)\,T_{22}\frac{T_{30}S_8+T_3S_{14}}{\Delta}$
$\dots \frac{T_1T_4T_7}{\Delta}$	$M(3,1)\,P_6\frac{1-L_1L_2L_4}{\Delta}$	$M(4,1)\,P_7\frac{T_1T_4T_9}{\Delta}$
$\dots \frac{T_{30}S_9+T_4S_{12}}{\Delta}$	$+M(3,2)\,T_{22}\frac{T_{30}S_9+T_{24}(T_1T_4T_8+T_{27}(1-L_1L_2L_4))}{\Delta}$	$+M(4,2)\,T_{22}\frac{T_{30}S_9+T_4S_{14}}{\Delta}$
$\dots_5 \frac{T_1T_5T_7}{\Delta}$	$M(3,1)\,P_6\frac{T_1T_5T_8}{\Delta}$	$M(4,1)\,P_7\frac{1-L_1L_2L_3}{\Delta}$
$\dots \frac{T_{30}S_{10}+T_5S_{12}}{\Delta}$	$+M(3,2)\,T_{22}\frac{T_{30}S_{10}+T_5S_{13}}{\Delta}$	$+M(4,2)\,T_{23}\frac{T_{30}S_{10}+T_{24}(T_1T_5T_9+T_{28}(1-L_1L_2L_3))}{\Delta}$

P_1	0	0	0	0	0	0
0	P_2	0	0	0	0	0
0	0	P_3	0	0	0	0
0	0	0	$m(1,1) - P_4$ $+m(1,2)\ T_{20}\ T_{24}\ T_{25}$	0	0	0
0	0	0	0	$m(2,1) - P_5$ $+m(2,2)\ T_{21}\ T_{24}\ T_{26}$	0	0
0	0	0	0	0	$m(3,1) - P_6$ $+ m(3,2)\ T_{22}\ T_{24}\ T_{27}$	0
0	0	0	0	0	0	$m(4,1) - P_7$ $+ m(4,2)\ T_{23}\ T_{24}\ T_{28}$

Figure 19. Nominal system plant - P.

The additive perturbation matrix ΔP has now been determined. Using P' and P,

$$\Delta P = P' - P \tag{IV-42}$$

performed by simple matrix addition.

The two remaining matrices are the feedforward and feedback transfer function matrices, G and H, respectively. These are presented in Figures 20 and 21. The symbols in columns (or rows) four through seven of H need to be defined. The ΔP are related to the limits of the pneumatic pressure as

$$\Delta P = \begin{cases} P_{wv}^{max} - P_{wv}^{min} & \text{if } M(j,1)=1 \\ P_{ad}^{max} - P_{ad}^{min} & \text{if } M(j,2)=1 \end{cases} \tag{IV-43}$$

The symbol ΔT_z is associated with the width of the temperature bands in the ZET, as

$$\Delta T_z = \begin{cases} -1.7^{o}C = (18.3-20.0) & \text{if } M(j,1)=1 \\ 1.4^{o}C = (25.6-24.2) & \text{if } M(j,2)=1 \end{cases} \tag{IV-44}$$

This concludes the derivation of the MIMO description using transfer function matrices. This description will be used in Chapter VI to implement a frequency domain analysis technique to determine the effect of the interconnections, as a perturbation, upon the sensitivity of the control of the system output.

C. Modes of Operation: The Steady-State Values

From the presentation of the transfer function matrices it is obvious that the steady-state values, e.g., T_{ret}^{o}, $\dot{m}_{as}^{o}$, f_{dzi}^{o}, are crucial to the description of the system. In addition, the coefficients of the coil transfer functions, the α, β, and δ's, depend upon the steady-state values. And when the simulations are performed, the steady-state values become so important that when a coil is not in operation, it must be deleted from the computer input deck lest the simulation would diverge, producing erroneous results.

In an attempt to order the steady-state values in a manner relevant to the operation of the HVAC system, a mnemonic was invented which reflects the outdoor temperature, T_{out}, whether or not the cooling coil is in operation, and how many of the zone temperatures fall in each of the bands of the ZET. This device will be called the "mode of operation" and will have the form mXXLYZ, where m indicates that this is the mode of operation mnemonic, XX is the outdoor temperature, L is a logical symbol indicating whether the cooling

$$
\begin{bmatrix}
\dfrac{K_p^m + K_x^m S^{-1}}{1 + t_{ep} S} & 0 & 0 & 0 & 0 & 0 & 0 \\
0 & \dfrac{K_p^c + K_i^c S^{-1}}{1 + t_{ep} S} & 0 & 0 & 0 & 0 & 0 \\
0 & 0 & \dfrac{K_p^f + K_x^f S^{-1}}{1 + t_{msc} S} & 0 & 0 & 0 & 0 \\
0 & 0 & 0 & \dfrac{\Delta P}{\Delta T_z (1 + t_{cz} S)} & 0 & 0 & 0 \\
0 & 0 & 0 & 0 & \dfrac{\Delta P}{\Delta T_z (1 + t_{cz} S)} & 0 & 0 \\
0 & 0 & 0 & 0 & 0 & \dfrac{\Delta P}{\Delta T_z (1 + t_{cz} S)} & 0 \\
0 & 0 & 0 & 0 & 0 & 0 & \dfrac{\Delta P}{\Delta T_z (1 + t_{cz} S)}
\end{bmatrix}
$$

Figure 20. Feedforward compensator - G.

$\frac{1}{1+t_{sm}S}$	0	0	0	0	0	0
0	$\frac{1}{1+t_{sc}S}$	0	0	0	0	0
0	0	$\frac{1}{1+t_{bf}S}$	0	0	0	0
0	0	0	1	0	0	0
0	0	0	0	1	0	0
0	0	0	0	0	1	0
0	0	0	0	0	0	1

Figure 21. Feedback compensator - H.

coil is operating or not (it can take values of 'Y'-Yes, the coil is operating or 'N'-No, the cooling coil is not operating), and YZ which indicates how many zones are heating-Y or cooling-Z (where zone i heating means T^{o}_{zi}<20.0 ^{o}C and zone i cooling means T^{o}_{zi} > 24.2). The sum of Y and Z need not equal four; in fact, the number of zones in the "zero energy band" is precisely 4-(Y+Z).

The selection of which modes of operation were to be studied was made in an attempt to represent those modes of operation that an actual HVAC system of this type would require for a climatic year. The modes of operation which were studied are presented in Table 2.

There are two subsystems whose operational status are not reflected in the mode of operation mnemonic: the fan and the mixing box. The fan is always operating, so inclusion of its operation would be redundant. The status of the mixing box was left to being more or less a byproduct of the mode of operation development procedure.

The modes of operation were developed by selecting an outdoor temperature and the number of zones which would be heating or cooling. This determined what the desired zone temperatures should be which, via the cold deck reset, would determine the steady-state cold deck temperature. So, knowing T^{o}_{zi}, T^{o}_{cool}, and T^{o}_{out}, and by setting the derivative in III-9 equal to zero, it was possible to find the internal loads of the zones, the L_i's, that were needed to maintain T^{o}_{zi}. Knowing T^{o}_{zi} also allowed for determination of T^{o}_{ret}. Because the fan setpoint was always P^{sp}_{c}=622 pa, knowing T^{o}_{zi} determined $\dot{m}^{o}_{as}$ through f^{o}_{dzi} and f^{o}_{wo}. By this procedure the resulting f^{o}_{dzi} and f^{o}_{wo} were determined. Further, if the mixing box could achieve its setpoint, the cooling coil, by the setpoint selection procedure, was not required to operate. Because of this, it was not possible to have the mixing box and cooling coil operating simultaneously.

The purpose for defining the mode of operation mnemonic was to improve organization. This will be seen in the following chapters where the steady-state values which were determined by the whole system will be used in the individual subsystems. This insures that the tuning of the subsystems was not performed vacuously but rather, with respect to the values the interconnections will have when operating with the total system.

Table 2. System Modes of Operation: The Steady-State Values

MODE	T_{OUT}	ZONES								FAN			COOLING COIL			MIXING BOX		
			L_1 [kW]	T^0_{Z2} [°C]	L_2 [kW]	T^0_{Z3} [°C]	L_3 [kW]	T^0_{Z4} [°C]	L_4 [kW]	P_C [Pa]	f_{WO}	$\dot{m}_{as}$ [Kg/sec]	T^0_{COOL} [°C]	T^{SP}_{COOL} [°C]	$\dot{m}_{wc}$ [Kg/sec]	T^0_{am} [°C]	T^0_{RET} [°C]	T^{SP}_{am} [°C]
mM5n40	-15.	18.6	16.0	18.6	16.0	18.6	16.0	18.6	16.0	622	0.500	2.850	14.62	18.3	0	13.52	18.6	17.2
m00n40	0.0	19.9	11.2	19.9	11.2	19.9	11.2	19.9	11.2	622	0.500	2.900	18.00	18.3	0	16.9	19.9	17.2
m10n00	10.	22.5	12.8	22.5	12.8	22.5	12.8	22.5	12.8	622	0.500	2.452	18.3	18.3	0	17.2	22.5	17.2
m10n21	10.	19.7	3.0	19.7	3.0	21.9	14.0	24.9	22.7	622	0.521	2.955	15.5	15.5	0	14.4	22.1	14.4
m15n04	14.5	24.8	12.9	24.8	12.9	24.8	12.9	24.8	12.9	622	0.571	1.942	16.0	16.0	0	14.9	24.8	14.9
m20y00	20.	22.1	4.5	22.1	4.5	22.1	4.5	22.1	4.5	622	0.500	2.900	18.3	18.3	0.172	20.0	22.1	17.2
m20y03	20.	21.3	4.1	24.9	12.9	24.9	12.9	24.9	12.9	622	0.533	3.329	15.5	15.5	0.533	20.0	24.3	14.4
m30y04	30.	24.9	3.7	24.9	3.7	24.9	3.7	24.9	3.7	622	0.581	3.467	15.7	15.7	0.993	25.6	24.9	14.6
m40y04	40.	25.5	1.0	25.5	1.0	25.5	1.0	25.5	1.0	622	0.662	4.210	13.1	13.1	2.116	27.7	25.5	12.0

V. IMPLEMENTING THE CONTROL DESIGN: SELECTION OF THE CONTROLLER PARAMETER VALUES BY THE ZIEGLER-NICHOLS TECHNIQUE

Once the PI controllers have been installed on the HVAC system, the problem becomes how to determine the gain settings for some "optimum" response. A practical method which takes account of the variations from system to system by performing a simple experiment is the Ziegler-Nichols technique.

J. Ziegler and N. Nichols[1] in a 1942 paper entitled "Optimum Settings for Automatic Controllers" proposed "Practical names and units of measurement...for the two principal characteristics affecting [the] controllability [of industrial processes]." Although the authors speak of automatic reset control, this is equivalent to the present terminology of integral control.

The technique is performed by first turning off the reset or integral control and then finding the proportional control value entitled the "Ultimate Sensitivity" (Su), above which the output oscillations will continue to increase in amplitude and below which oscillations will diminish to straight line control. At ultimate sensitivity, the amplitude ratio, the relative amplitude of any wave to that of the wave which preceded it, is maintained at unity. From the value of Su and the period of the oscillations (Pu) at that gain setting, the authors proposed that optimal settings for K_p and K_I can be derived. The optimality of the settings is a qualitative tradeoff resulting in "reasonably rapid [response] without excessive loss of stability or excessive increase in period."

The steps to implement this technique are clearly presented in the literature which is provided by the controller manufacturers.

1. Lock out integral and derivative control.

2. Set proportional gain K_p at sufficiently small value to rule out any oscillation.

3. Increase K_p until the control variable starts to oscillate, i.e., oscillation once started does not die down but is sustained (this value of K_p is Su).

4. Measure the period of oscillation at this setting (this is Pu) (see Figure 22).

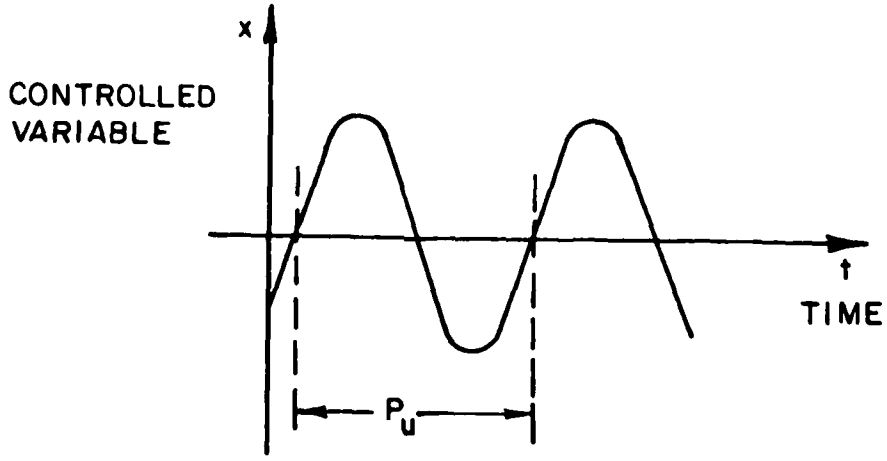

Figure 22. Ziegler-Nichols oscillation test.

5. The optimum values for K_p and K_I can then be calculated according to the following formulas:

$$K_p = 0.45 \cdot Su \qquad (V\text{-}1)$$
$$K_I = 0.54 \cdot Su/Pu$$

or if the integral time constant is used it is

$$T_I = 0.83\ P_u \qquad (V\text{-}2)$$

This technique for control parameter selection will be used on the mixing box, cooling coil, and fan subsystems. The steady-state data will be used for the constant input values which would be variable if the subsystems were interconnected. The effects of seasonal changes of the subsystem components on the optimum parameter values can then be seen. Also, the effect of hysteresis will be shown by finding optimum parameter values for both the linear and non-linear subsystems. Finally, it will be found that Equation (V-1) results in a response which is highly oscillatory or underdamped, whereas a critically damped or 1/4-wave response is more desirable. By changing the fractions in (V-1), parameter values resulting in this 1/4-wave response can be found.

The first subsystem to be presented is the mixing box. The control action is operative during three of the modes of operation: m10n00, m10n21, m15n04. The results of performing the Z-N test on these three sets of steady-state values are shown in Table 3. From these results it can be seen that the introduction of an E/P and a damper with hysteresis reduces the ultimate sensitivity by 26% and slightly more than doubles the ultimate period, P_u. The change in mode of operation changes S_u at most by 15% and the effect on P_u is less than 6%. More dramatic is the need to reduce the gains to achieve a 1/4-wave response. In the linear case, the reduction is 80% and in the nonlinear, 60%. Plots of the response of T_{oam} to a 1°C increase in the setpoint for the linear and nonlinear systems with both underdamped and critically damped control parameter settings for the m10n00 mode of operation are shown in Figures 23, 24, 25, and 26. From the results of these tests a revised formula for obtaining the settings necessary for a 1/4-wave response from the linear system is

$$K_p = 0.09 \cdot S_u \qquad (V\text{-}3)$$

$$K_I = 0.11 \cdot S_u/P_u$$

Table 3. Mixing Box Subsystem Controller Parameter Value Selection

MODE	f^{o}_{RET}	T^{spo}_{AM}	T^{o}_{RET}	T^{o}_{OUT}	LINEAR			HYSTERESIS		
					Z-N OSCILLATION	Z-N STEP	1/4 WAVE	Z-N OSCILLATION	Z-N STEP	1/4 WAVE
m10n00	0.577	17.2	22.47	10.0	Su=26.7 Pu=14.85	Kp=12.02 KI=0.97	Kp= 2.4 KI=0.19	Su=19.96 Pu=31.6	Kp=8.98 KI=0.341	Kp=3.59 KI=0.137
m10n21	0.367	14.44	22.07	10.0	Su=27.6 Pu=14.3	Kp=12.4 KI= 1.04	Kp=2.48 KI=0.21	Su=20.30 Pu=29.6	Kp=9.135 KI=0.370	Kp=3.654 KI=0.148
m15n04	0.038	14.89	24.79	14.5	Su=31.4 Pu=14.8	Kp=14.1 KI=1.15	Kp=1.15 KI=0.23	Su=23.3 Pu=30.9	Kp=10.5 KI=0.41	Kp=4.73 KI=0.18

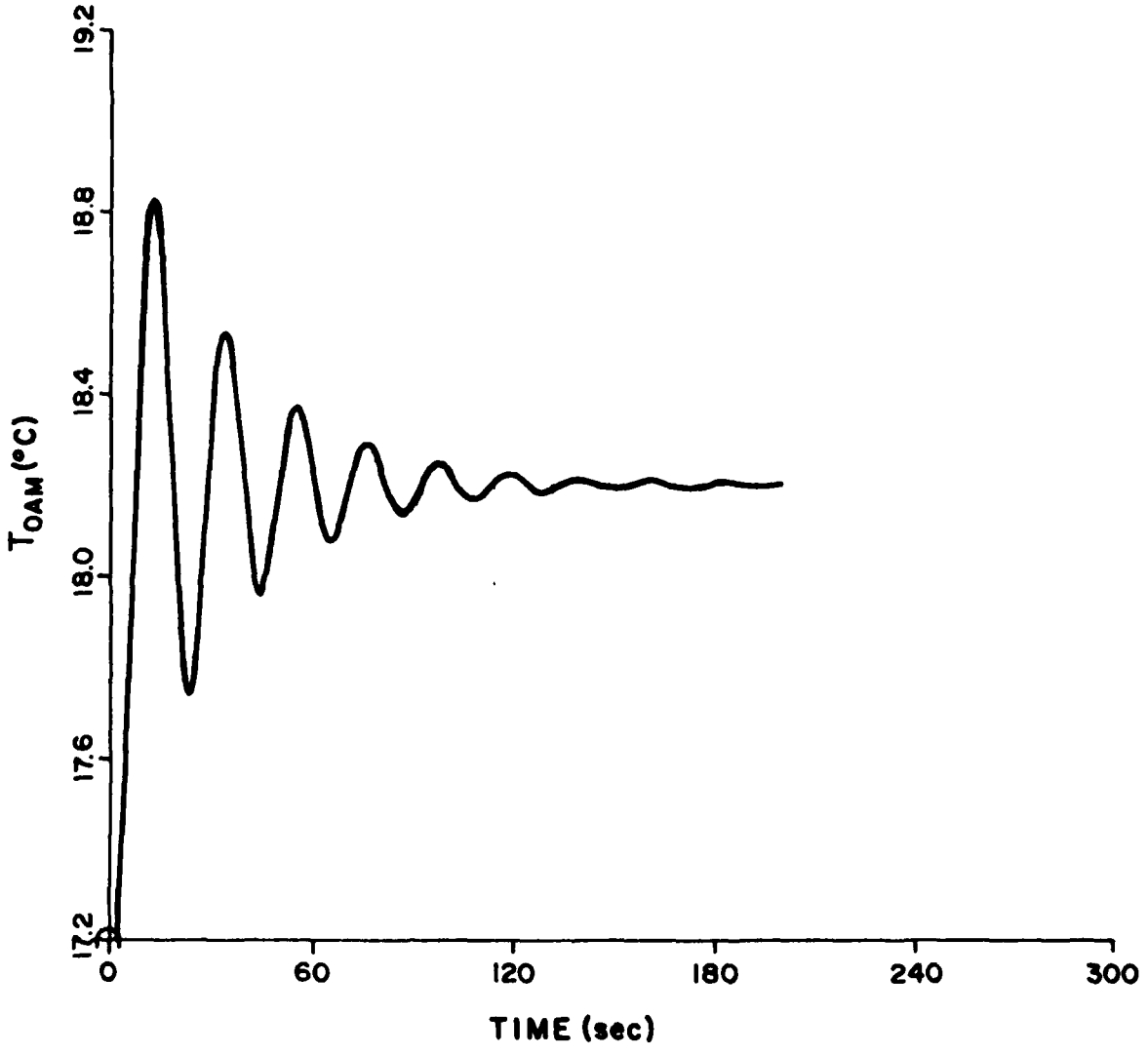

Figure 23. Linear mixing box setpoint step change - underdamped response.

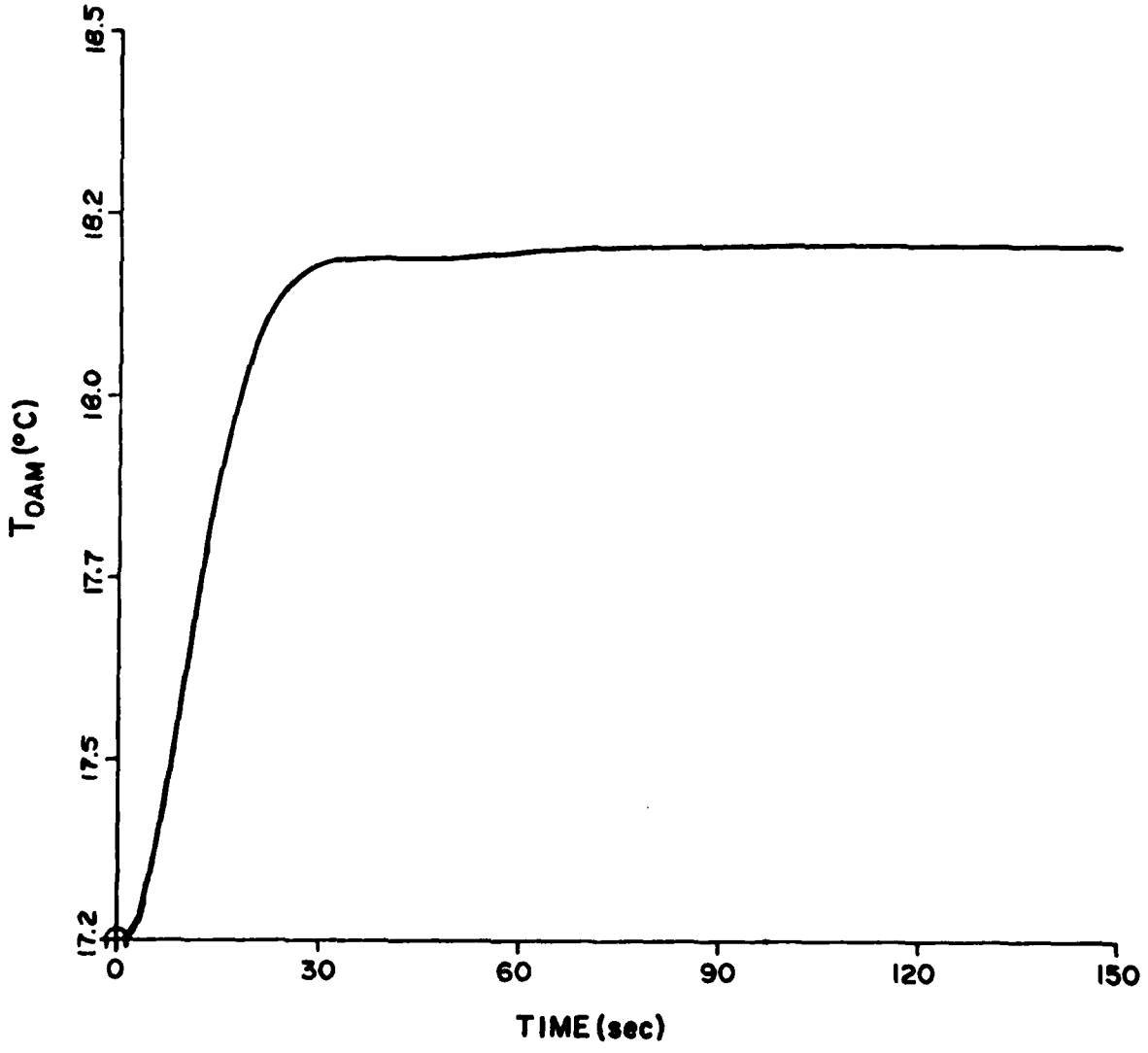

Figure 24. Linear mixing box setpoint step change - critically damped response.

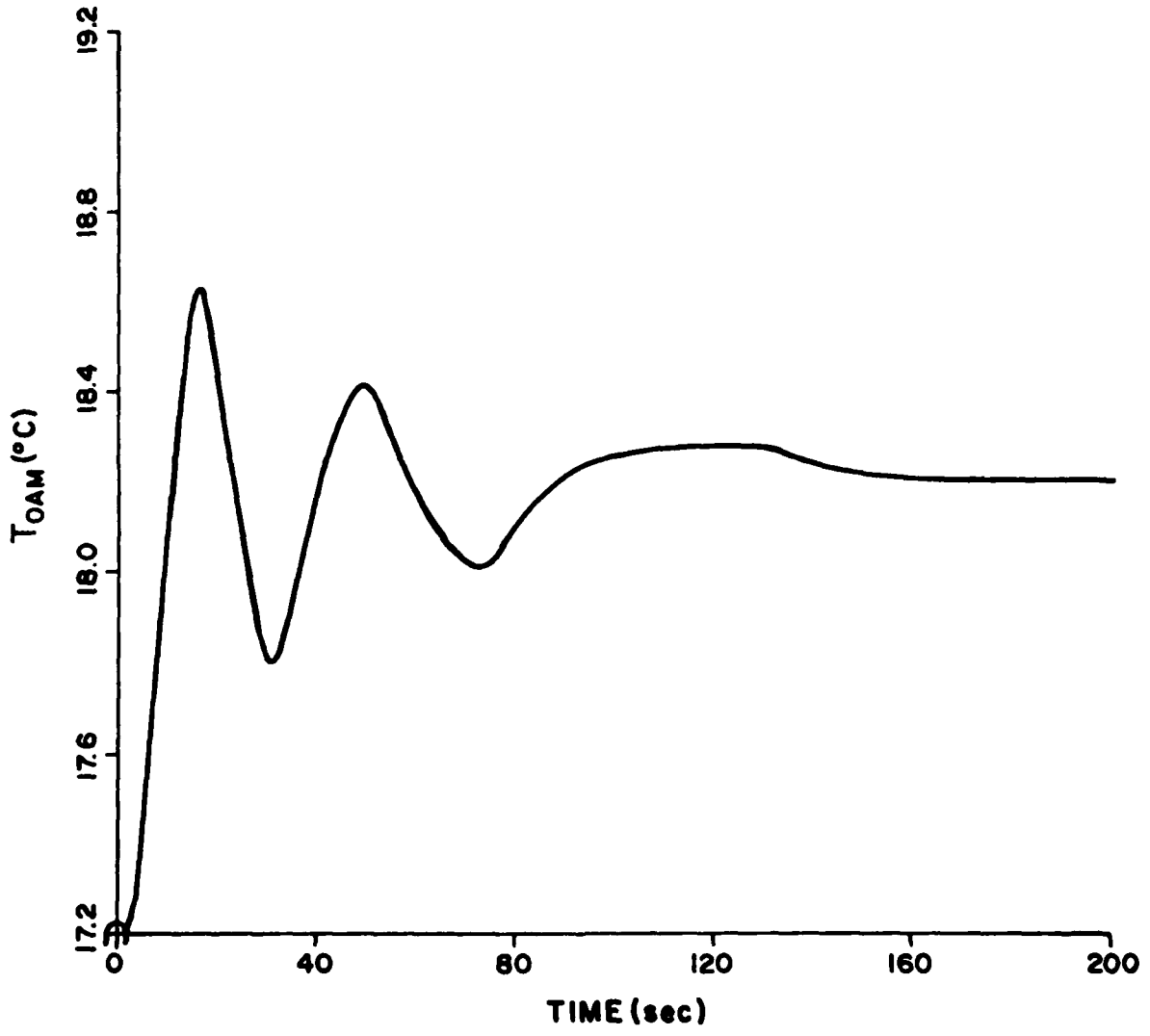

Figure 25. Nonlinear mixing box setpoint step change - underdamped response.

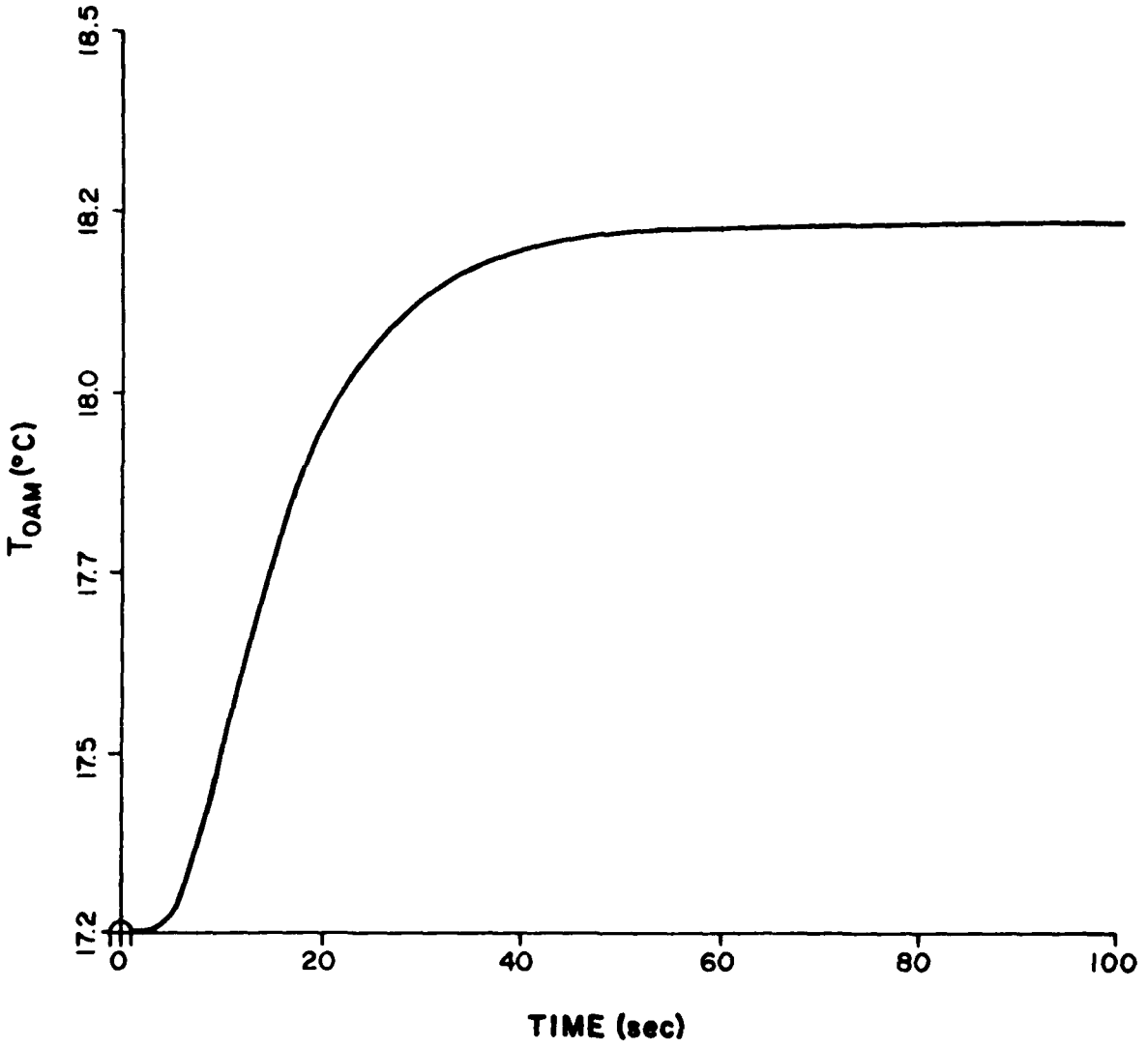

Figure 26. Nonlinear mixing box setpoint step change - critically damped response.

For the nonlinear system, a quarter-wave response could be obtained by using

$$K_p = 0.18 \cdot S_u \qquad \text{(V-4)}$$

$$K_I = 0.22 \cdot S_u / P_u$$

The next subsystem is the cooling coil. The coil is in operation during four modes of operation: m20y00, m20y03, m30y04, m40y04. The results of performing the Z-N test on these sets of steady-state values are shown in Table 4. From these results it can be seen that the introduction of hysteresis in the E/P and the water valve reduces S_u by 10, 16, 17, and 18% and increases P_u by 59, 41, 40, and 27% for the modes m20y00, m20y03, m30y04, and m40y04, respectively. The changes in S_u and P_u for different modes of operation are quite large; the maximum change for S_u is more than 200% and for P_u more than 20%. Again, there was a need to drastically reduce the control parameter settings from the value suggested by Z-N to achieve a 1/4-wave response. A 60% reduction was necessary for the linear system. A 50% decrease was needed for the system with hysteresis. This suggests a revised formula set to obtain a critically damped response to a step change in the setpoint. For the linear system, they are:

$$K_p = 0.18 \cdot S_u \qquad \text{(V-5)}$$

$$K_I = 0.22 \cdot S_u / P_u$$

and for the nonlinear system,

$$K_p = 0.23 \cdot S_u \qquad \text{(V-6)}$$

$$K_I = 0.27 \cdot S_u / P_u$$

Plots of cooling coil output, T_{ocol}, for a step change of 1°C in the setpoint when the system is operating in the mode m20y03 for the linear and nonlinear components and underdamped and critically damped settings are shown in Figures 27, 28, 29, and 30.

The next subsystem is the fan. The fan is in operation during all the modes, although four modes have the same steady-state conditions for the fan. The results of performing the Z-N test on the different sets of steady-state values are shown in Table 5. For this subsystem, the maximum change, due to different modes, is 14% for S_u whereas P_u is the same for all the modes. The need to reduce the gains to achieve a 1/4-wave response was again

Table 4. Cooling Coil Subsystem Controller Parameter Value Selection

MODE	M^{o}_{WC}	T^{o}_{MIX}	T^{spo}_{COOL}	M^{o}_{AS}	LINEAR			HYSTERESIS		
					Z-N OSCILLATION	Z-N STEP	1/4 WAVE	Z-N OSCILLATION	Z-N STEP	1/4 WAVE
m20y00	0.1724	21.10	18.3	2.8997	Su=-4.6 Pu=-39.2	Kp=-2.07 KI=-0.063	Kp=-0.83 KI=-0.025	Su=-4.14 Pu=-62.5	Kp=-1.86 KI=-0.036	Kp=-0.93 KI=-0.018
m20y03	0.5332	21.10	15.5	3.329	Su=-7.8 Pu=-37.3	Kp=-3.5 KI=-0.11	Kp=-1.40 KI=-0.044	Su=-6.55 Pu=-52.7	Kp=-2.95 KI=-0.067	Kp=-1.48 KI=-0.034
m30y04	0.9927	26.74	15.67	3.467	Su=-8.3 Pu=-35.7	Kp=-3.7 KI=-0.13	Kp=-1.49 KI=-0.05	Su=-6.85 Pu=-50.0	Kp=-3.08 KI=-0.074	Kp=-1.87 KI=-0.034
m40y04	2.116	28.80	13.06	4.210	Su=-14.1 Pu=-32.5	Kp=-6.35 KI=-0.23	Kp=-2.54 KI=-0.094	Su=-11.5 Pu=-41.4	Kp=-5.18 KI=-0.15	Kp=-2.56 KI=-0.075

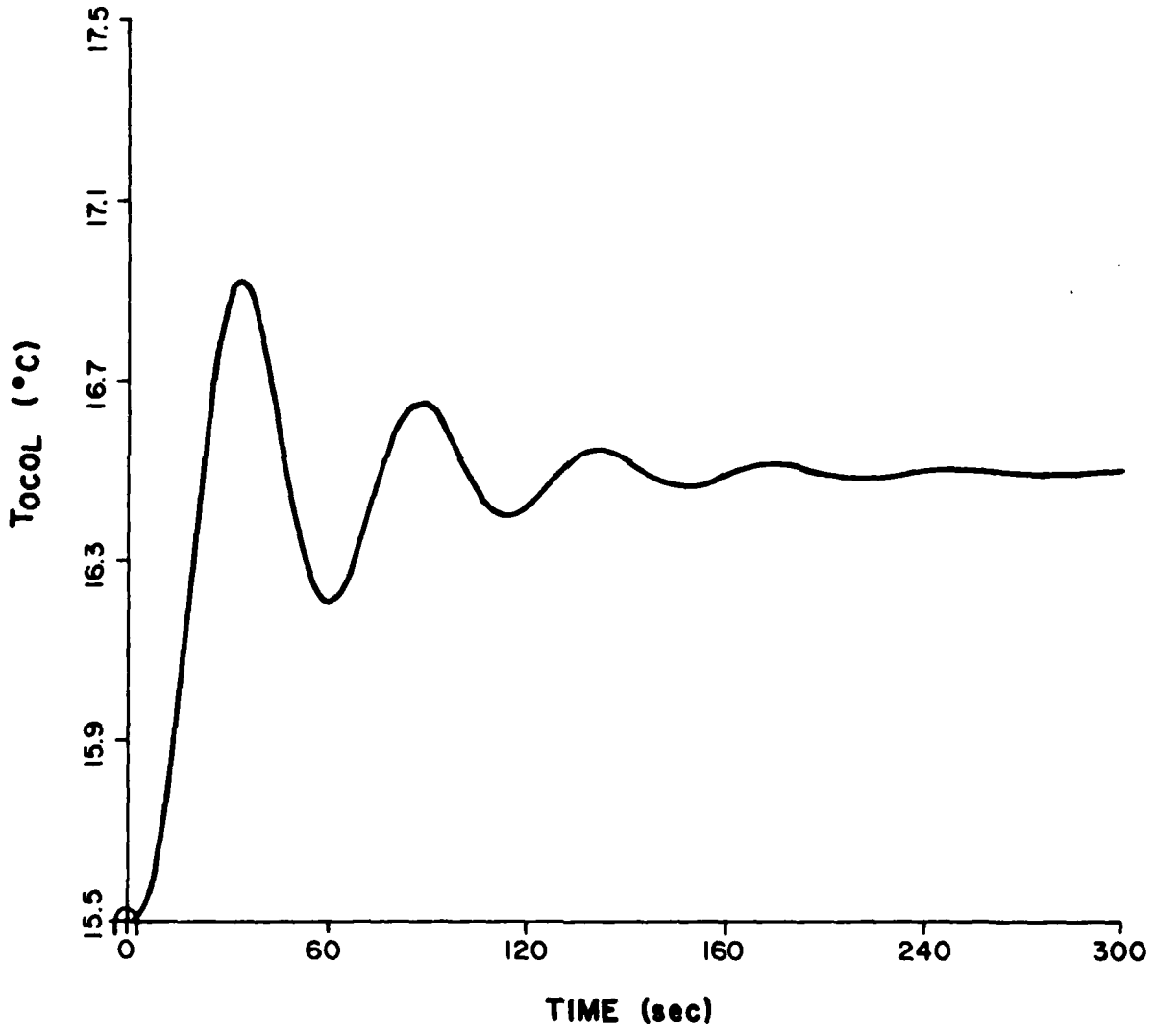

Figure 27. Linear cooling coil setpoint step change - underdamped response.

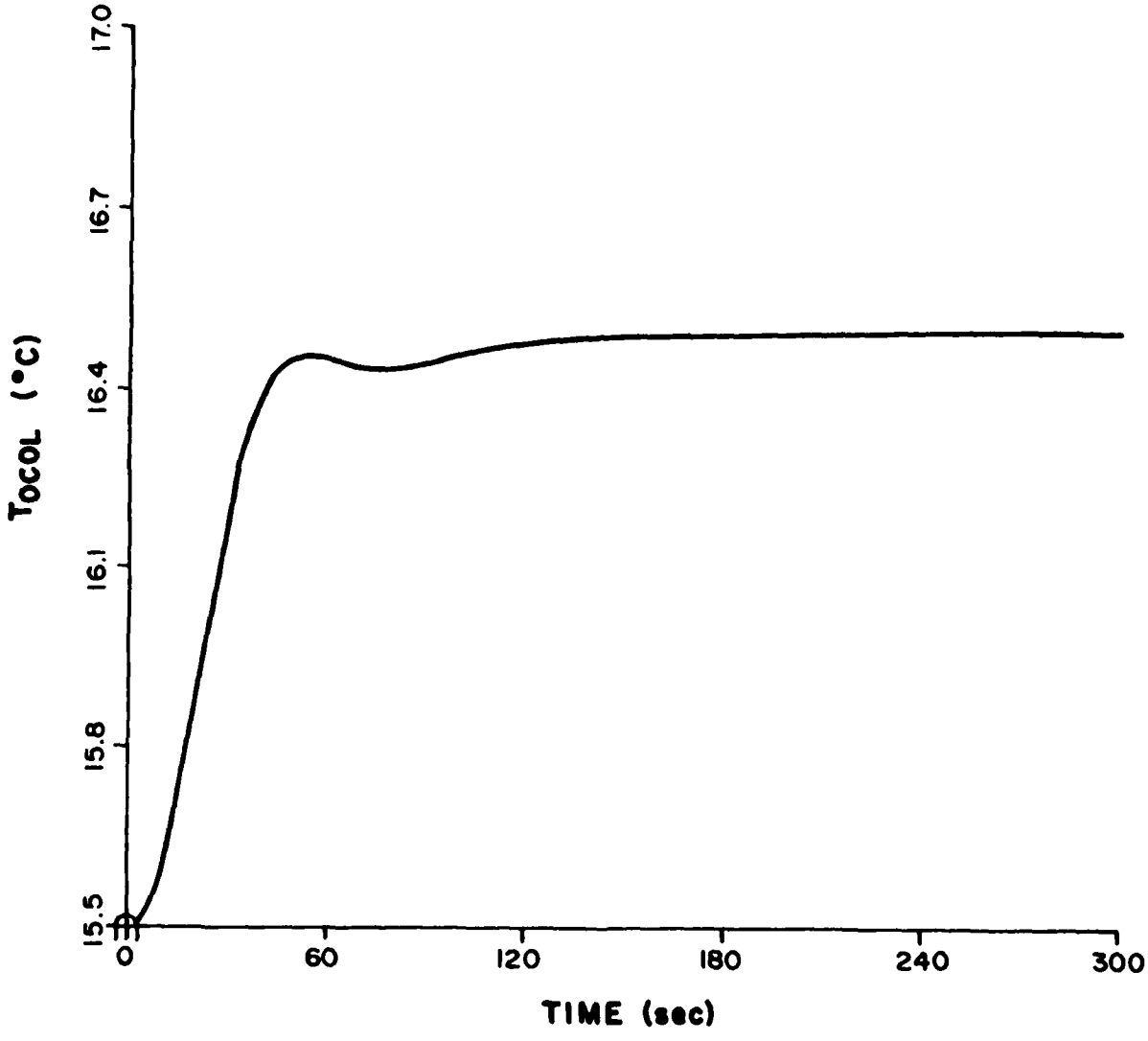

Figure 28. Linear cooling coil setpoint step change - critically damped response.

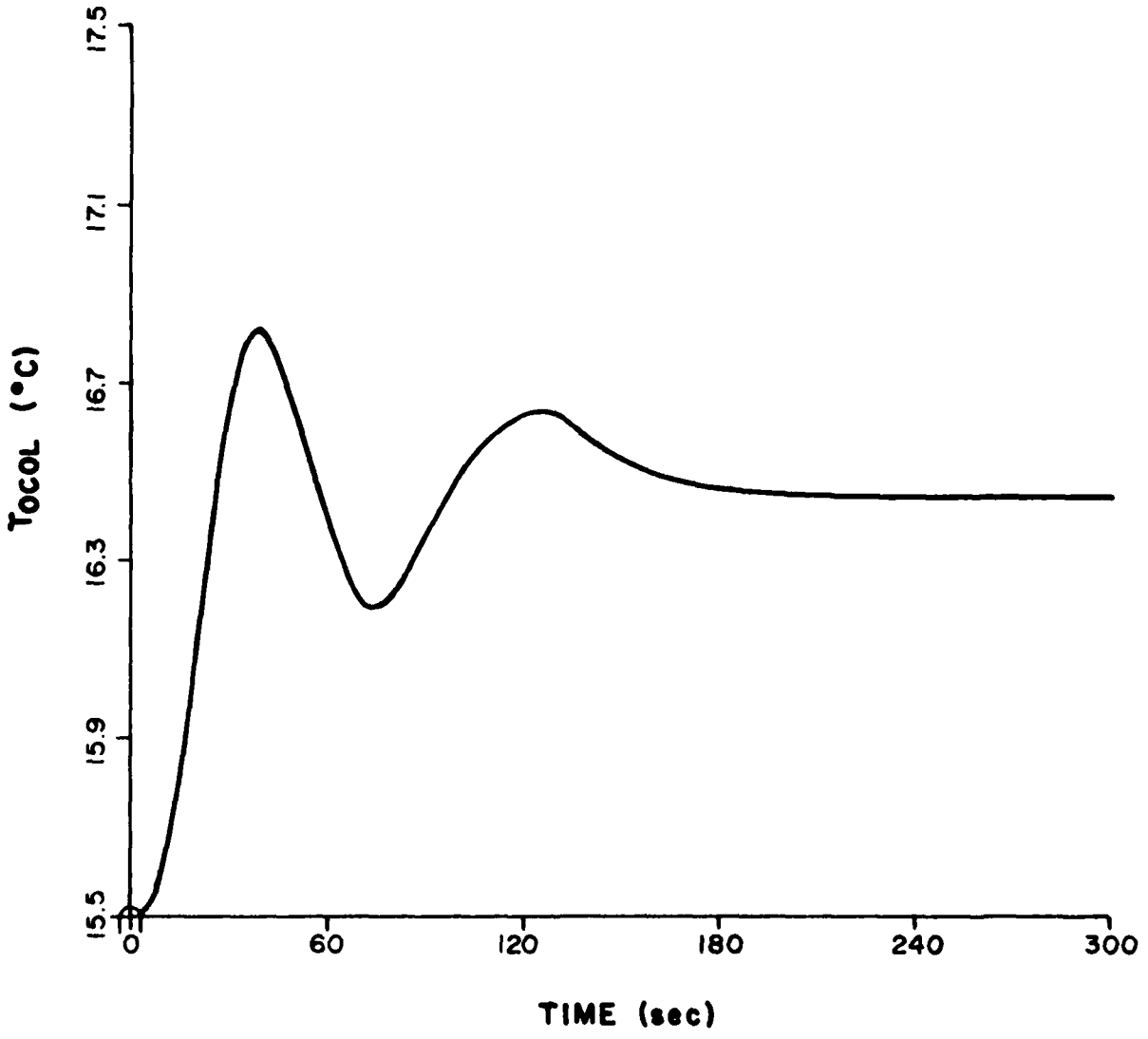

Figure 29. Nonlinear cooling coil setpoint step change - underdamped response.

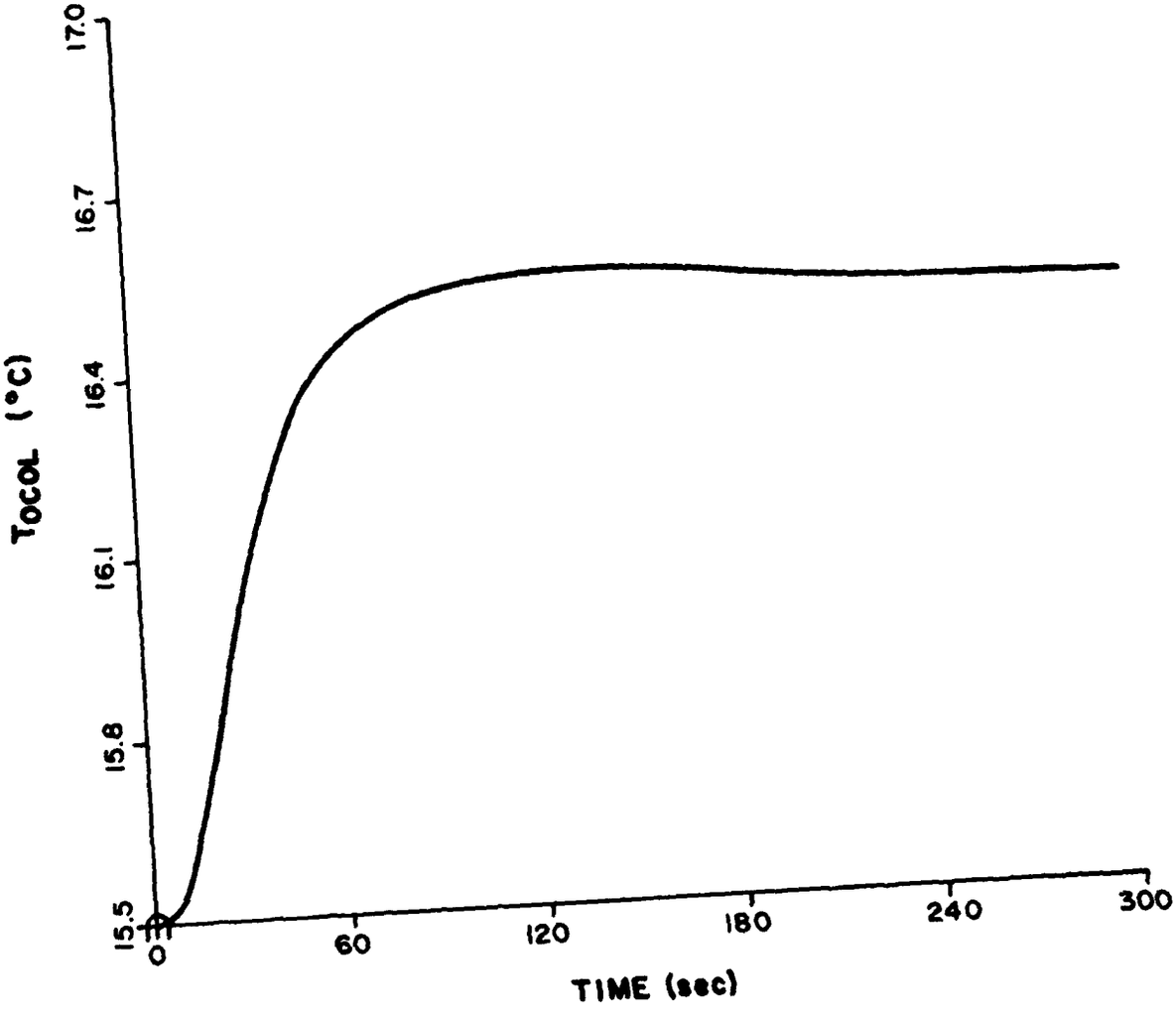

Figure 30. Nonlinear cooling coil setpoint step change - critically damped response.

Table 5. Fan Subsystem Controller Parameter Value Selection

MODE	f_{wo} FDTO	NON-LINEAR M.S.C.			LINEAR M.S.C.		
		Z-N OSCILLATION	Z-N STEP	1/4 WAVE	Z-N OSCILLATION	Z-N STEP	1/4 WAVE
mM5n10 m00n40 m10n00 m20y00	0.5000	Su=0.469 Pu=0.64	Kp=0.211 K_I=0.396	Kp=0.042 K_I=0.079	Su=2.9 Pu=1.68	Kp=0.76 K_I=0.54	Kp=0.38 K_I=0.05
m10n21	0.5213	Su=0.479 Pu=0.64	Kp=0.216 K_I=0.404	Kp=0.043 K_I=0.081	Su=3.0 Pu=1.68	Kp=1.35 K_I=0.96	Kp=0.68 K_I=0.10
m20y03	0.5648	Su=0.499 Pu=0.64	Kp=0.225 K_I=0.421	Kp=0.045 K_I=0.084	Su=3.2 Pu=1.68	Kp=1.44 K_I=1.03	Kp=0.72 K_I=0.10
m15n04	0.5714	Su=0.502 Pu=0.64	Kp=0.226 K_I=0.424	Kp=0.045 K_I=0.085	Su=3.3 Pu=1.68	Kp=1.49 K_I=1.06	Kp=0.745 K_I=0.106
m30y04	0.5812	Su=0.507 Pu=0.64	Kp=0.227 K_I=0.428	Kp=0.046 K_I=0.086	Su=3.5 Pu=1.68	Kp=1.58 K_I=1.13	Kp=0.79 K_I=0.11
m40y04	0.6619	Su=0.537 Pu=0.64	Kp=0242 K_I=0.453	Kp=0.048 K_I=0.091	Su=4.0 Pu=1.68	Kp=1.80 K_I=1.29	Kp=0.9 K_I=0.13

present. Here, the reduction was 80%. So, the revised formula for achieving a 1/4-wave response in the isolated fan subsystem is

$$K_p = 0.09 \cdot S_u \qquad (V\text{-}7)$$

$$K_I = 0.11 \cdot S_u / P_u$$

Plots of the response of P_{oc} and $\dot{m}_{as}$ to a step change in setpoint for the mode of operation m30y04 are shown in Figures 31 and 32 for the underdamped case and in Figures 33 and 34 for the critically damped case.

The final subsystem is the zone. This subsystem is controlled by the zero energy band thermostat (ZET) which is a proportional controller. The gains are set by the widths of the temperature bands in which the valve and damper are modulated. The temperatures at the extremes of these bands are set at the factory. Further, because these controllers are relatively cheap and serve an energy conservation purpose beyond that of dynamic control, they were the only controllers for the zones considered in this study.

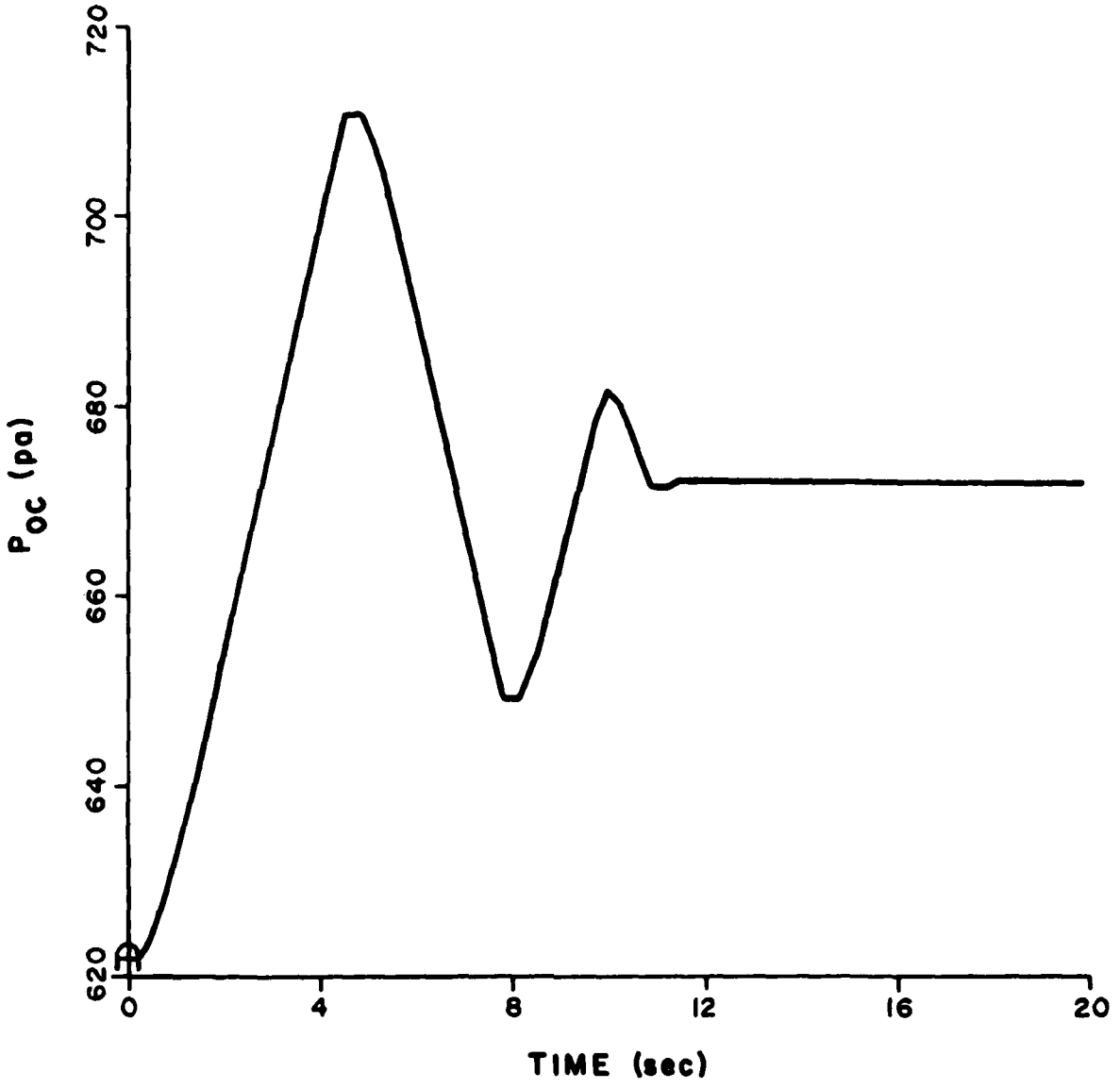

Figure 31. Fan underdamped response to a setpoint step change - P_{OC}.

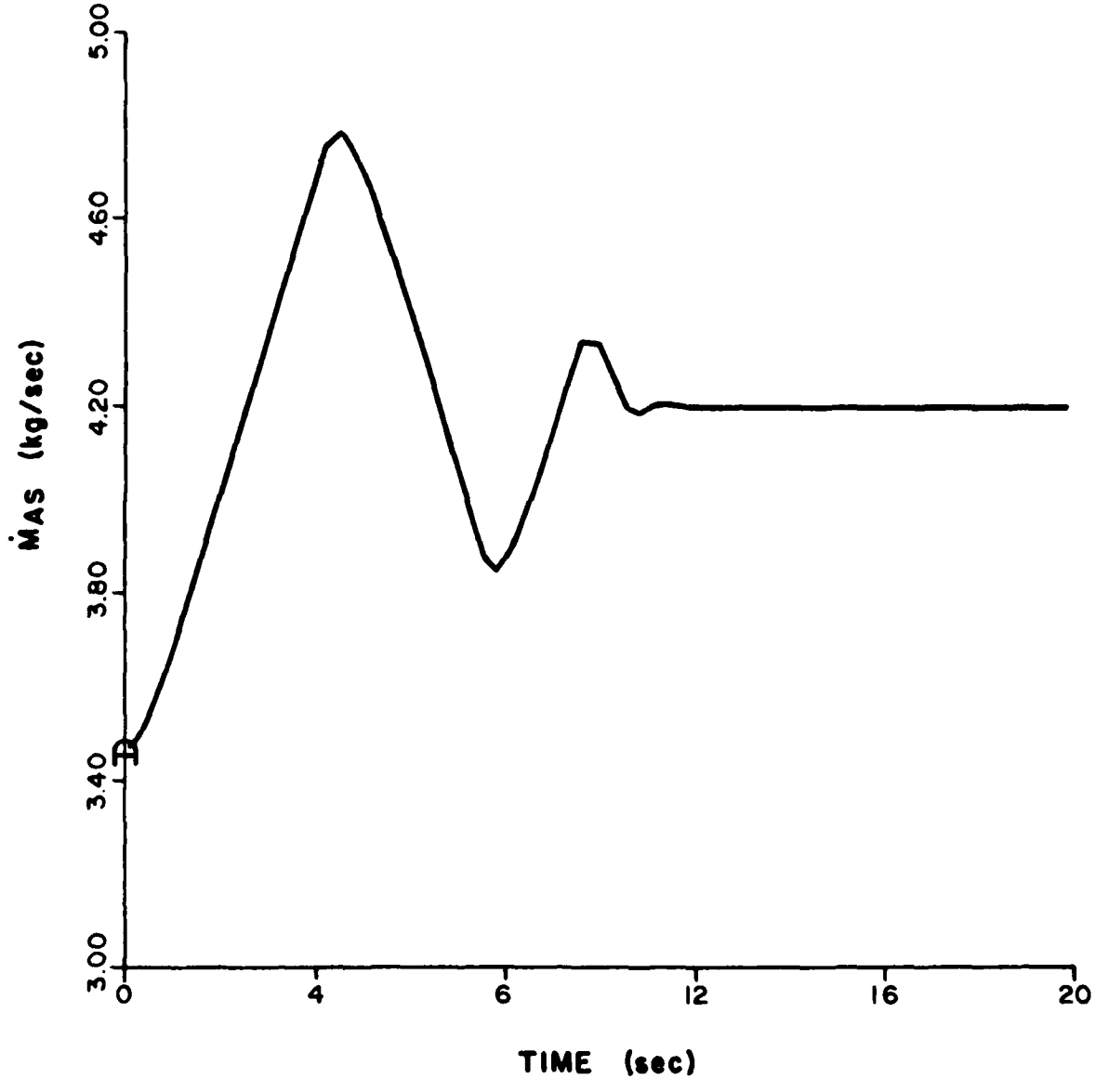

Figure 32. Fan underdamped response to a setpoint step change - $\dot{m}_{as}$.

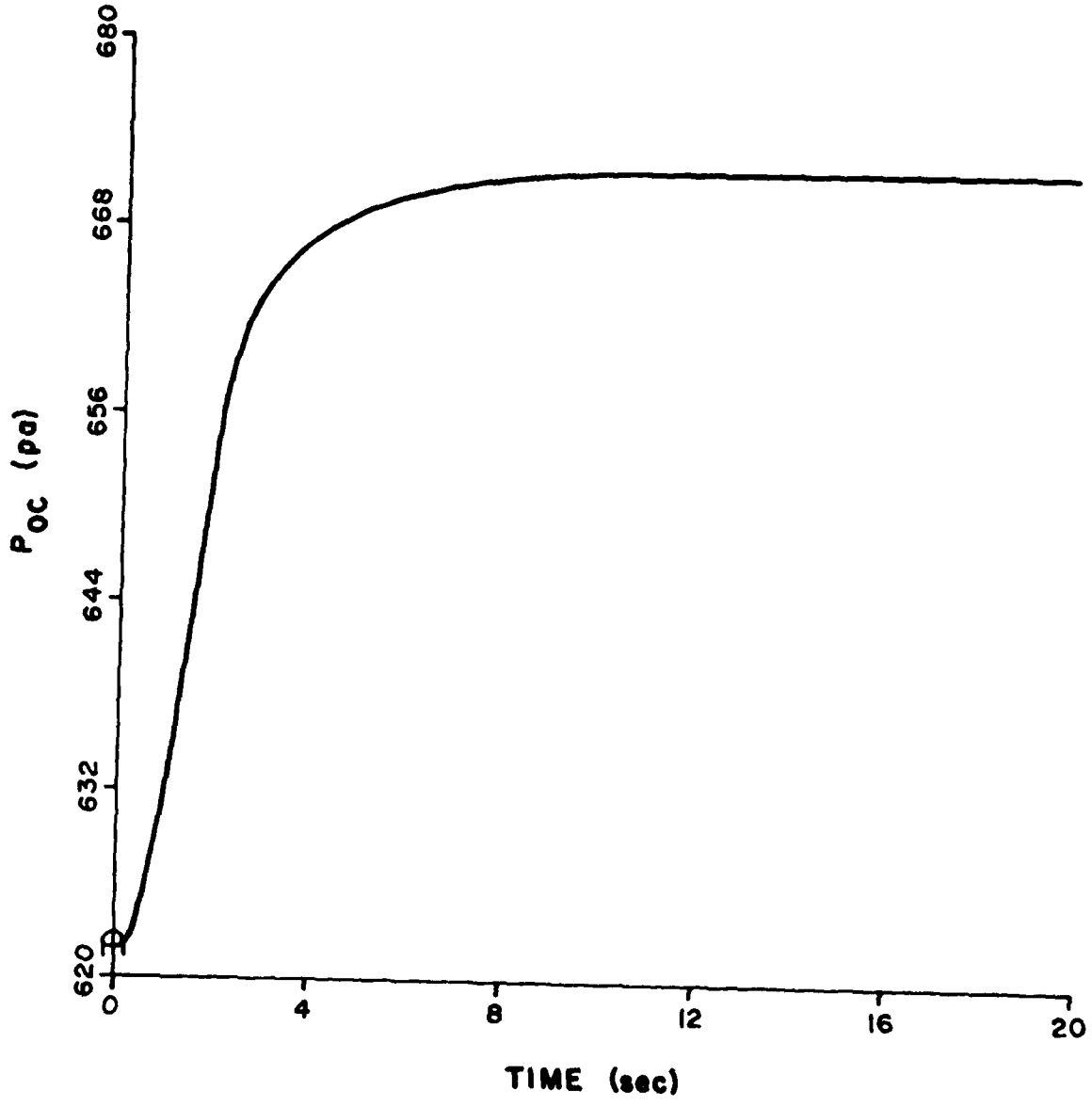

Figure 33. Fan critically damped response to a setpoint step change - P_{oc}.

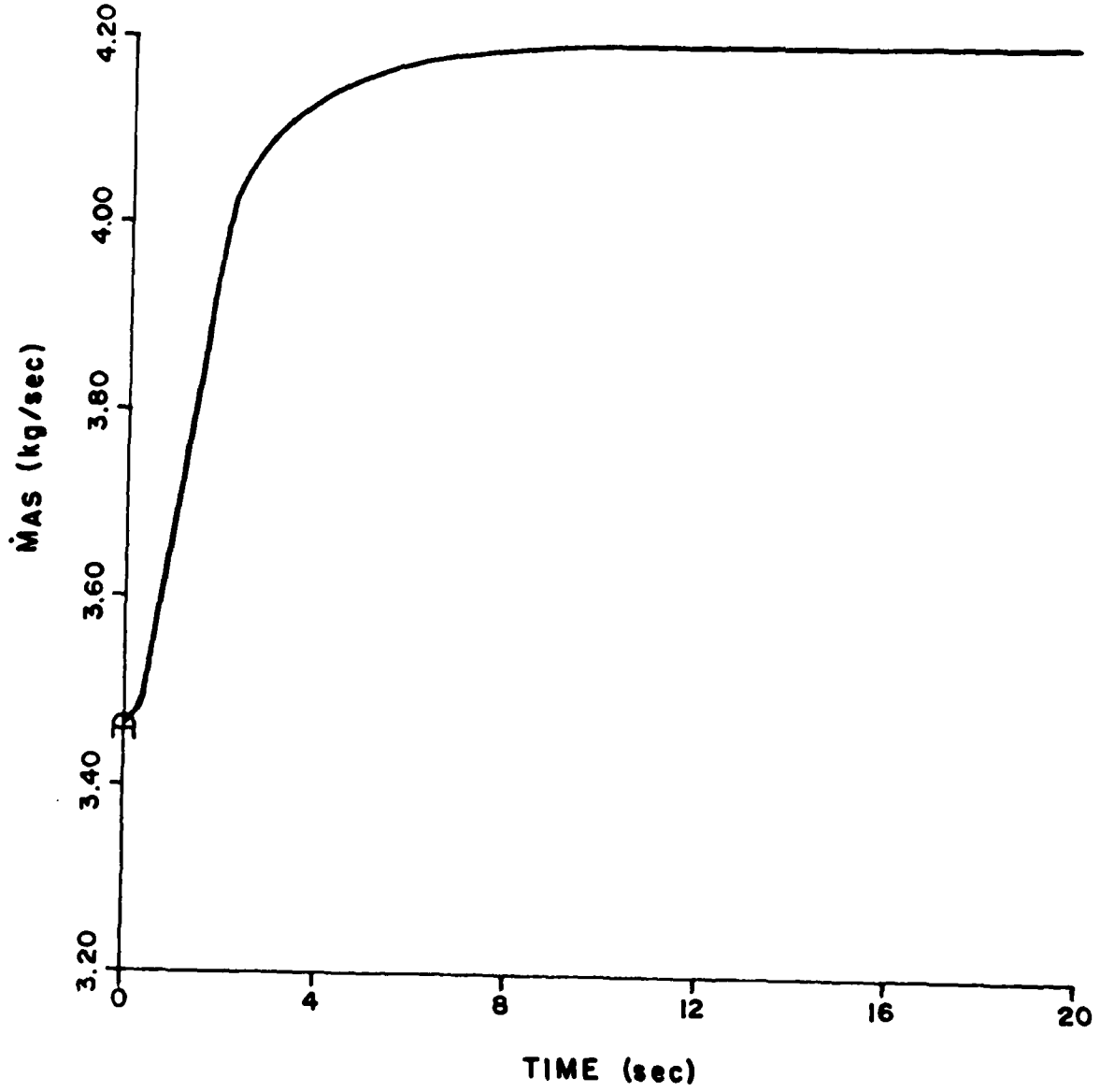

Figure 34. Fan critically damped response to a setpoint step change - $\dot{m}_{as}$.

VI. THE EFFECTS OF INTERCONNECTION: SINGULAR VALUES BOUNDS FOR COMPARISON SENSITIVITY

This chapter will present a technique for determining whether a condition on the sensitivity of the SISO design is met when the interconnections are considered to be present. The condition on the sensitivity is called comparison sensitivity. When the comparison sensitivity condition for the system is met, the sensitivity to modeling errors of the closed loop system is less than for an open-loop system which, without the modeling errors, has the same overall transfer function as the closed-loop system. So, if the comparison sensitivity is not met, there exists an open-loop system with the desired (by design) overall transfer function which is less sensitive to modeling errors than the designed closed-loop transfer function of the total system. Obviously, comparison sensitivity is a desired goal of a closed loop system. In fact, Bode, a pioneer in the design of feedback systems, considered compensation for unmodeled dynamics to be the primary motivation for closed-loop control.[6] For a more technical derivation of the comparison sensitivity, see Cruz, Freudenberg, and Looze.[7] Leave it to be said that for comparison sensitivity to be met is to assure that the inequality

$$\int_0^\infty e_c^T(t)e_c(t)dt \leq \int_0^\infty e_o^T(t)e_o(t)dt \qquad \text{(VI-1)}$$

holds, where $e_c(t)$ is the error vector of the difference between the modeled plant and the true plant for the closed-loop system and $e_o(t)$ is the error vector for the open-loop system.

The errors in modeling a plant are commonly described in two ways: multiplicative or additive perturbations to the nominal plant model. For the present system, the additive perturbation description will be used (see Figure 16). It is now necessary to have a test for comparison sensitivity when the plant perturbations are additive. This is given by Cruz, et al.[8], using singular values.[i] The test is:

Theorem: Consider a nominal plant P, the additive plant perturbation ΔP, the feedback compensator H and the feedforward compensator G. Assume that $(I+PGH)^{-1}$ and ΔP are asymptotically stable. If ΔP satisfies

[i] The notation for a singular value of the matrix A is given by $\sigma_i[A]$, and is the positive square roots of the eigenvalues of A^HA (where A^H is the conjugate transpose of A).

$$\min \sigma_i [I+P(j\omega)G(j\omega)H(j\omega)]$$

$$\geq \max \sigma_i [\Delta P(j\omega)] \cdot \max \sigma_i [G(j\omega)H(j\omega)] + 1 \qquad \text{(VI-2)}$$

for all $\omega<\omega_c$ and the additively perturbed system is asymptotically stable for $\omega \geq \omega_c$, then the additively perturbed system is asymptotically stable and satisfies the sensitivity condition (VI-1) for all reference inputs r(t) such that

$$R(j\omega) = 0 \text{ for } \omega > \omega_c \qquad \text{(VI-3)}$$

where R(s) is the transform of r(t).

An interpretation of VI-2 is that the smallest singular value of I + PGH - the distance in n-space to the nearest singular matrix, where n is the largest dimension of the matrices - must be larger than the product of the largest singular values of ΔP and GH - the distance to the furthest singular matrices - plus an amount necessary to insure the sensitivity condition. (Note that without the addition of unity, VI-2 would express the condition necessary to insure asymptotic stability of the perturbed system.) It is important to note that the test is sufficient but not necessary. If the inequality in VI-2 is satisfied, the comparison sensitivity is guaranteed; the converse, however, does not hold. If the test fails (the inequality in IV-2 is not met for some $\omega < \omega_c$), the comparison sensitivity may, in fact, hold.

Now that the test has been presented, it will be used on the system under study. Recall that the matrices, P',P, ΔP, G, and H have already been derived (see Chapter IV). Using the steady-state data of the various modes of operation and the controller parameter values of Chapter V, the quantities on the right- and left-hand sides of VI-2 must be computed and compared.

For some modes of operation, some of the columns (or rows) of G will contain all zeros. This happens because one of the control variables is uncontrolled for the specific mode of operation, e.g., when T_{zi} falls in the dead band, the cooling coil is not on, or $T_{out} > T_{ret}$ which sets $f_{ret} = 0.85$. Because this results in both sides of VI-2 equaling unity, the test is of no value. In order to use the test, only the variables which, for the present mode, are being controlled should be considered as elements of the output vector Y. This is done by deleting rows and columns from P, P', ΔP, G, and H. Note that because all of the forward path gains were considered in deriving P', deletion of the row and column associated with the mixing box when it is not controlling will not result in deletion of the effect of changes in T_{ret} on T_{cool}. Likewise, this is true of deleting any row and column pair when it is not controlling.

So, for the m10n00 mode, where the cooling coil and the zones are not controlling, the matrices have a dimension of 2x2 corresponding to the fan and mixing box working. The results of the comparison sensitivity test are shown in Figure 35. For m15n04 the matrices are 6x6 because the cooling coil is off. Results of the test for this mode are shown in Figure 36. For m20y00 the matrices are 2x2 and the test results are shown in Figure 37. The M40y04 mode has 6x6 matrices and the test results are shown in Figure 38.

By inspecting the Figures 35, 36, 37, and 38 and referring to Equation VI-2 it can be seen that the test failed on every try. In fact, the system in every mode of operation failed to satisfy this test for comparison sensitivity. Of course, this does not mean that the system necessarily fails to meet the comparison sensitivity condition (Equation VI-1); this test simply fails to prove it.

These results should not be construed to imply that the test is not useful. In fact, an option is to now consider this test as a design criterion, i.e., devise new G and H's, possibly with non-zero off-diagonal elements, which along with P and ΔP, satisfy the test given in Equation VI-1. The procedure would then insure that the comparison sensitivity condition was met.

One method of proceeding to find new G and H's would be to keep the SISO design of the controllers in G but also include precompensation in G and H which would anticipate the perturbative effects of ΔP, the interconnections. Although this may be analytically possible and, with the advent of Direct Digital Control in HVAC systems, be technically feasible, it may lead to a highly conservative design. This has been a criticism of singular value techniques in the past.[9]

Before we embark upon this formidable task, perhaps the present SISO design can, by another method, be shown to result in good control.

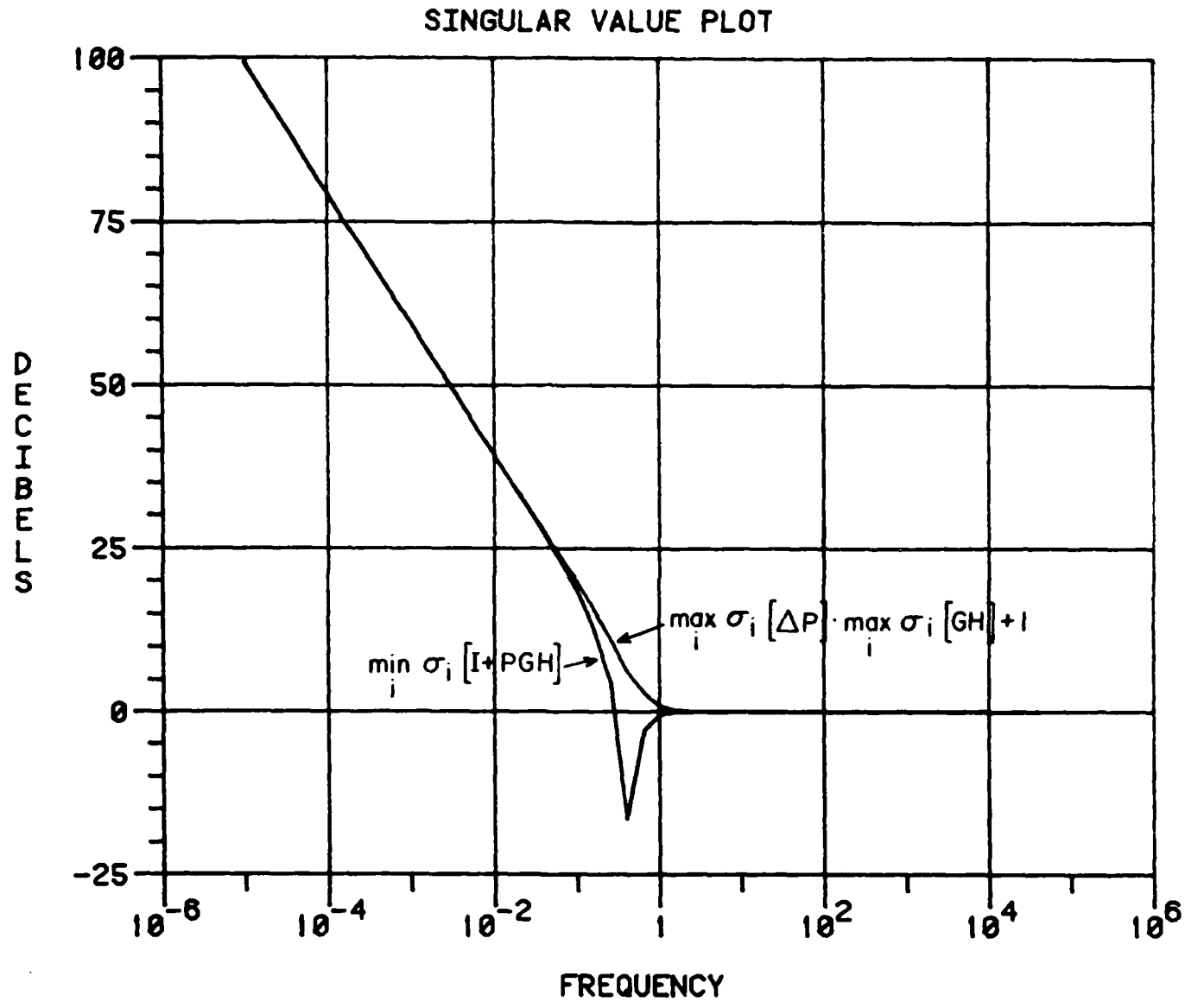

Figure 35. Comparison sensitivity test - m10n00.

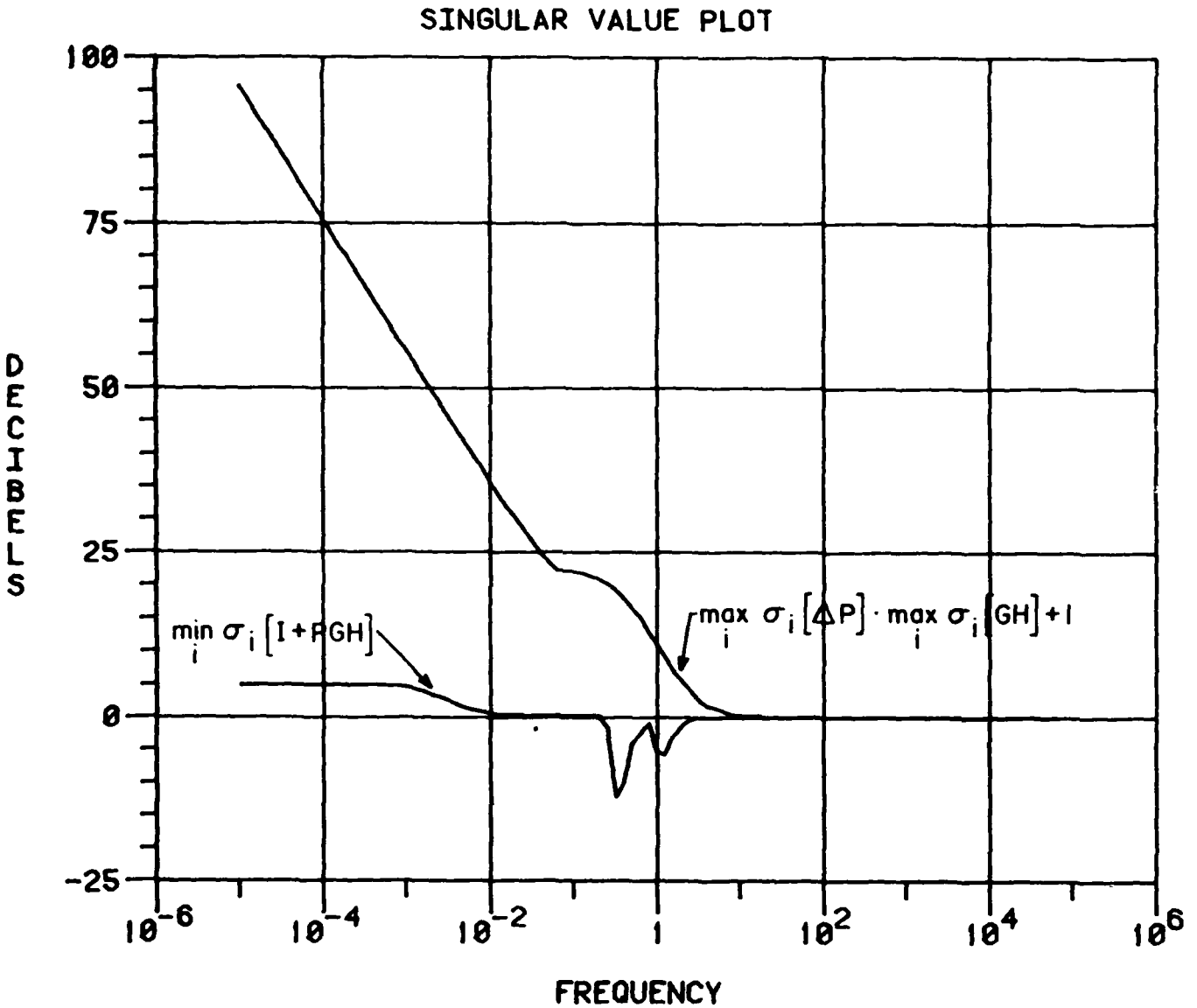

Figure 36. Comparison sensitivity test - m15n04.

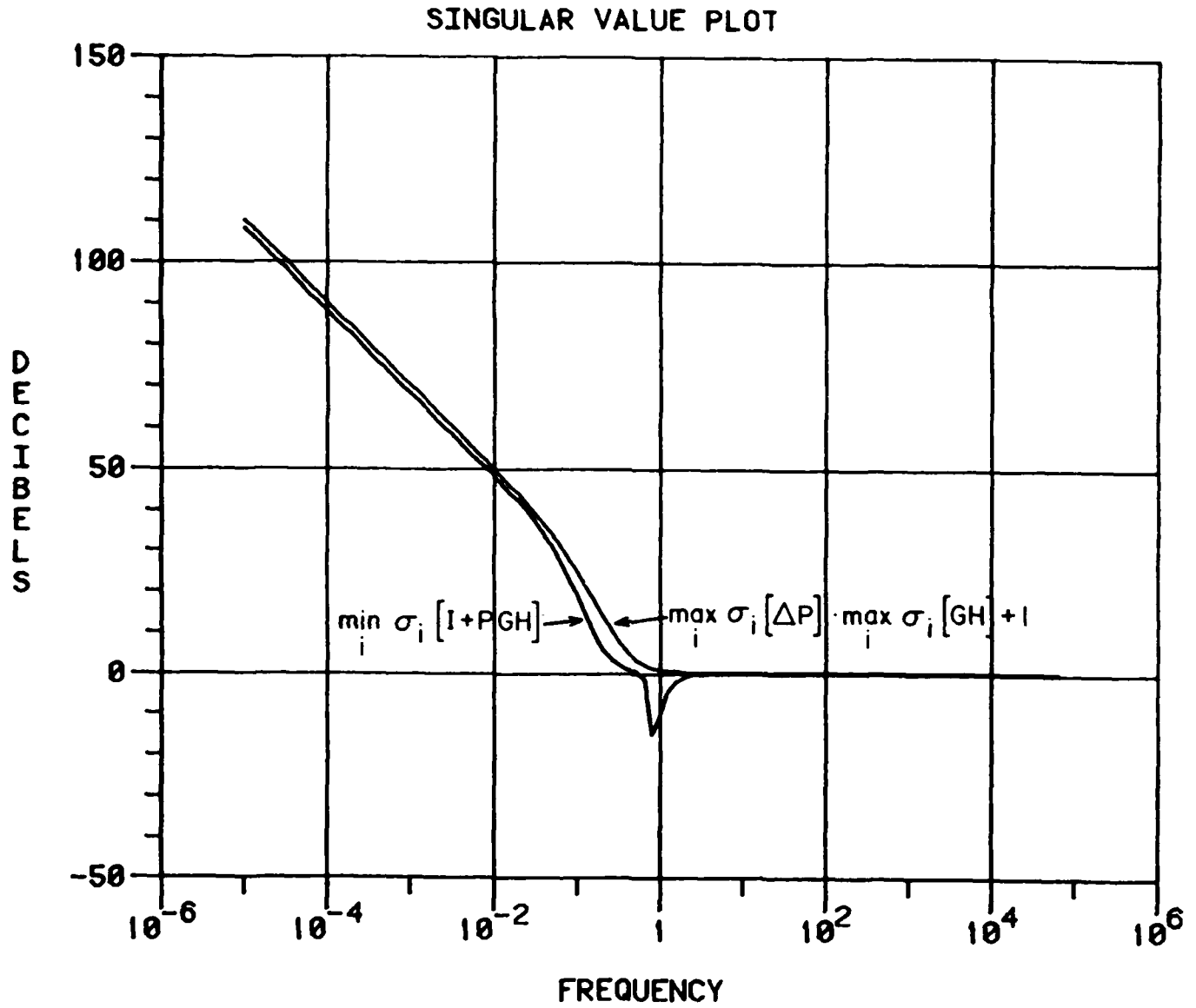

Figure 37. Comparison sensitivity test - m20y00.

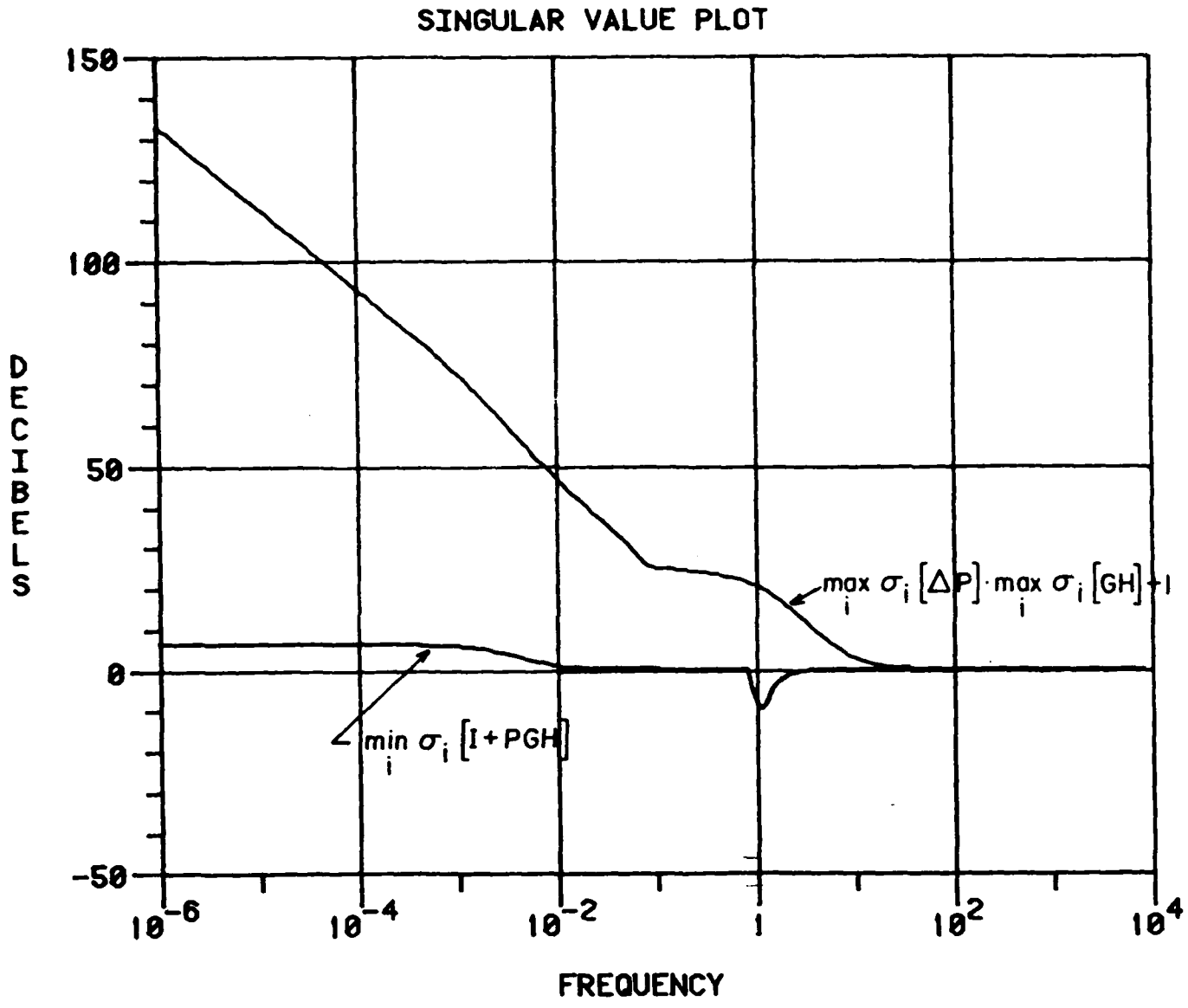

Figure 38. Comparison sensitivity test - m40y04.

VII. THE EFFECTS OF INTERCONNECTION: COMPUTER SIMULATION

This chapter, like the previous, will attempt to discern the effects of the presence of the interconnections on the SISO designed control of the subsystem control variables. Having seen the comparison sensitivity technique fail to establish knowledge of these effects for our present system, it is necessary to choose a different approach. This approach will utilize the computer simulation developed in Chapters III and IV along with steady-state modes of operation and the controller parameter values found in Chapter V. As in Chapter V, step changes will be made in the setpoints of the mixing box, cooling coil, and fan subsystems; additionally, load changes will be made to occur in the zones. By recording the response of the control variable in the primary subsystem[i] and the variations of the secondary subsystems[ii] control variables, due to the interconnections to the primary subsystem, it will be possible to see the effects of interconnection, as calculated by the simulation. The effect of the interconnection will be seen in two ways. First, by comparing the response of the primary subsystem to the isolated subsystem response, it will be possible to observe the degradation of the response from the 1/4-wave response. Second, any variation in the secondary subsystem control variables will be different from the SISO design where, by assuming the interconnection variables to be constant, it was assumed that the secondary subsystem control variables maintained their constant steady-state values. Again, the SISO design of the controllers will be tested for MIMO quality by observing: 1) the degradation of the primary subsystem response to a step change and 2) the variations of the secondary subsystems control variables.

The chapter will proceed by considering step changes in the setpoints of the mixing box, the cooling coil, and the fan. Then a step change will be made to occur in one of the zones.[iii]

A. Mixing Box Setpoint Step Change

The mixing box underwent a setpoint step change during two modes of operation: m10n00 and m15n04.

A summary of the result of these simulations is shown in Table 6. For m15n04, the step change to the setpoint was $\Delta T_{am}^{sp} = 0.5$; there was no degradation from design of the primary subsystem response: the zone temperatures

---

[i] Primary subsystem: The subsystem which incurs the step change in set point or load.

[ii] Secondary subsystem: A non-primary subsystem.

[iii] The reset of the cooling coil setpoint by the highest zone temperature was not considered in this chapter.

Table 6. Mixing Box Setpoint Step Change Response

MODE	T_{AM} [°C]	ΔT_{AM} [°C]	CHANGE IN RESPONSE?	ZONE T_{Z° [°C]	ZONE ΔT_Z [°C]	FAN ΔP_C [Pa]	FAN δ	FAN $\dot{M}_{AS^\circ}$ [kg/sec]	FAN $\Delta\dot{M}_{AS}$ [kg/sec]
m10n00	17.2	-1.0	YES	22.47	-0.48		No Change		No Change
m15n04	14.9	+0.5	NO	24.79	0.07	RTSP	<0.1%	1.942	0.071

(all responding identically) changed by 0.3%, the pressure in the duct varied <0.1%[iv], and the supply air mass flow increased by 4%. Overall, for this mode, the variations were very small and there was no degradation. (It should be noted that $\dot{m}_{as}$ is not a control variable but is presented because it is the link between the fan and the other subsystems.)

For the m10n00 mode, the only secondary subsystems affected were the zones. This was because the zones were in the zero-energy band and were not modulating their dampers. The change in T_{zi} was -2%, but from energy considerations, this is considered acceptable. There was a slight degradation of the mixing box step response. To see this, observe Figure 39, for the isolated subsystem response; Figure 40, for the primary subsystem response; and Figure 41, for the secondary subsystem response.

This concludes the mixing box setpoint step change simulations. In summary, a change in the mixing box subsystem seems to have either minimal or acceptable effects on the secondary subsystems.

B. Cooling Coil Setpoint Step Change

The same procedure just described for the mixing box subsystem was performed on the cooling coil. The results of the simulations are summarized in Table 7. For all the simulations, the step change had a magnitude of unity. Most of the primary responses suffered degradation, due to $\Delta\dot{m}_{as} \neq 0$ because the zone dampers moved. The variance of P_c was less than a single Pascal, the maximum $\Delta\dot{m}_{as}$ was $-0.200 \frac{ka}{sec}$ for m40y04 with $\Delta T^{sp}_{cool} = -1$, and the maximum Δt_{zi} was +0.4°C change for m40y04 with $\Delta T^{sp}_{cool} = -1$.

An example of the effect of the interconnections between the cooling coil, the zone, the fan, and back to the cooling coil by virtue of T_{cool} being affected by a $\Delta\dot{m}_{as} \neq 0$ was observed in the m20y03 mode simulation. A plot of the isolated subsystem response is shown in Figure 42. The primary subsystem response is shown in Figure 43. The secondary subsystem responses are shown in Figures 44, 45, and 46. To obtain a measure of the degradation, the settling time, t_{set} (the time required for the control variable to stay within 10 percent of the final value), for the two responses was estimated. For the isolated subsystem $t_{set} \approx 70$ secs and for the primary subsystem, $t_{set} \approx 400$ secs. Note, however, that they both eventually assume the setpoint. Also, the variations, although noticeable, do not appear to be significant.

[iv] As a point of clarification, the S's in the associated tables are the maximum changes of the value divided by its steady-state value, whereas the Δ's, e.g. Δ_{pas}, are the differences between the final value and the initial value of the variable.

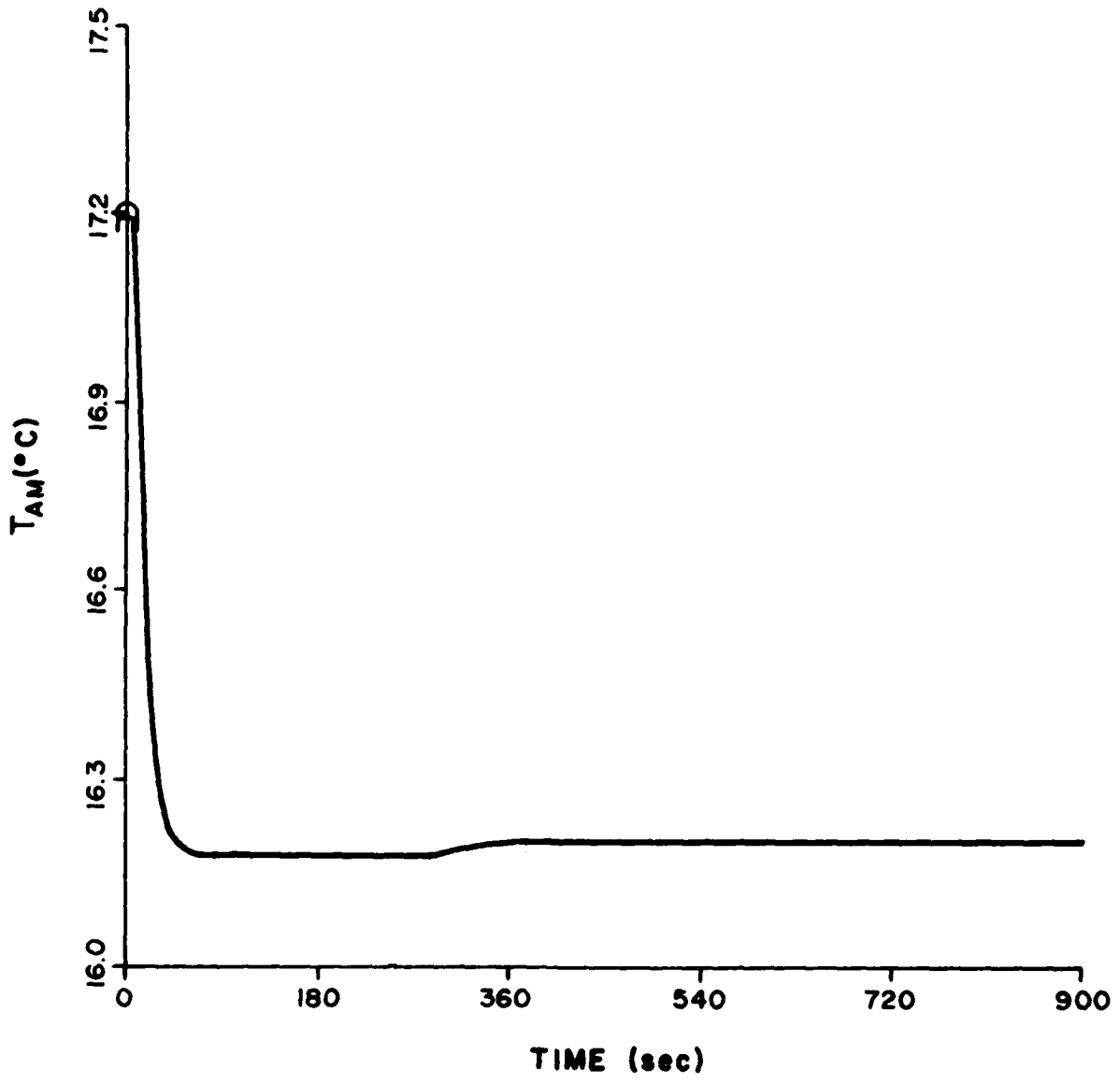

Figure 39. Mixing box (m10n00) setpoint step change - isolated subsystem response.

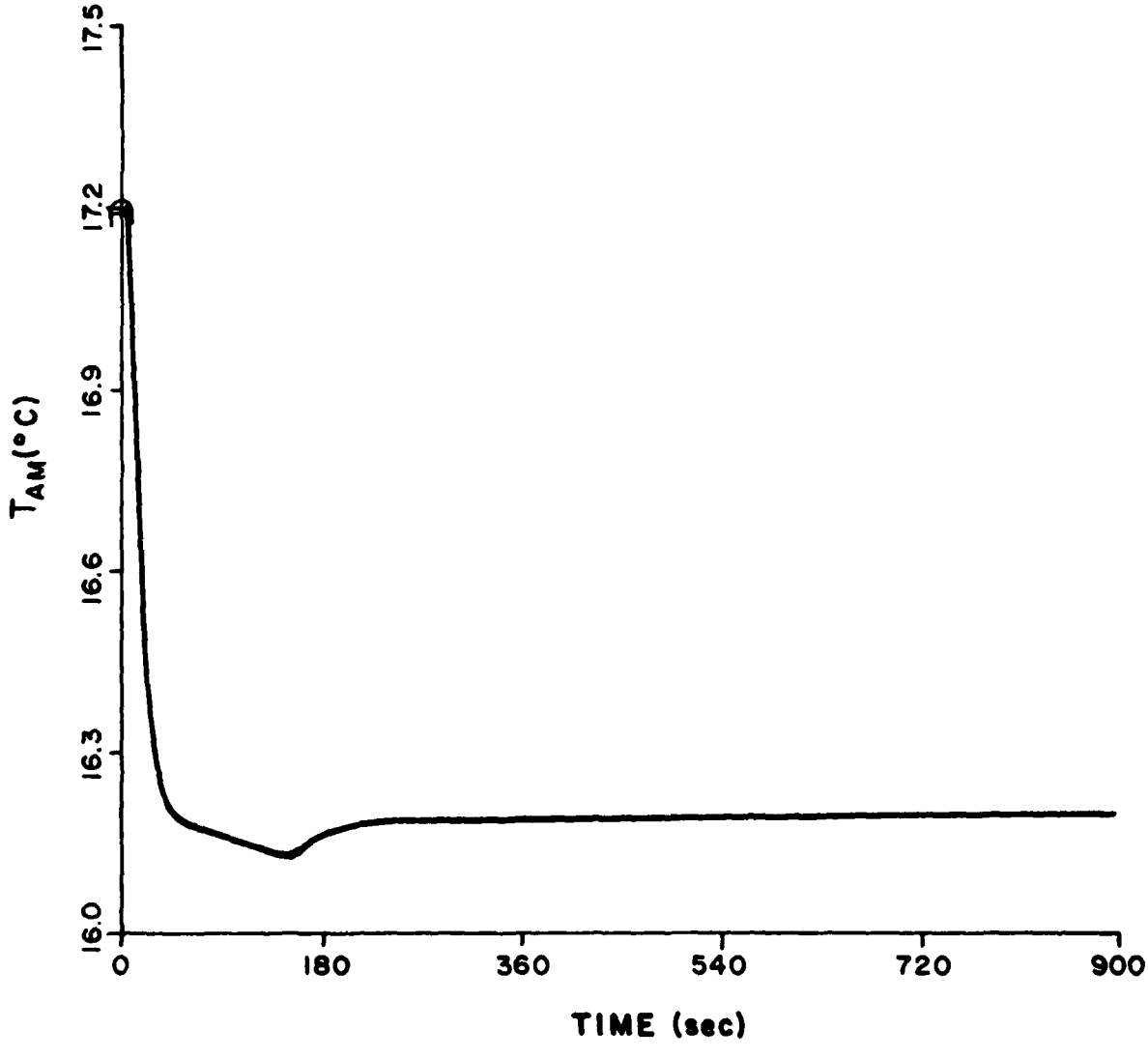

Figure 40. Mixing box (m10n00) setpoint step change - primary subsystem response.

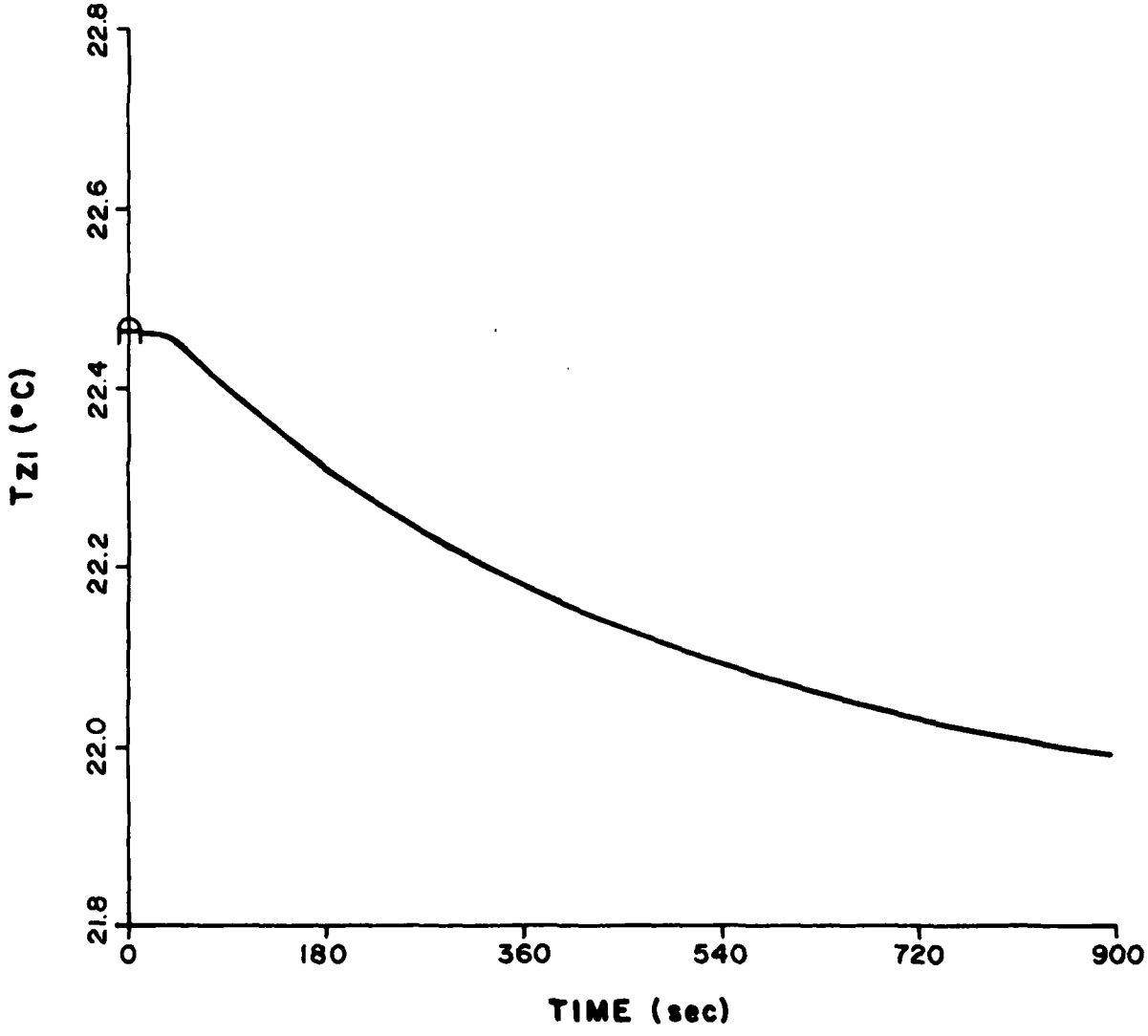

Figure 41. Mixing box (m10n00) setpoint step change - secondary subsystem response T_{zi}.

Table 7. Cooling Coil Setpoint Step Change Response

MODE	T_{COOL}^{spo} [°C]	ΔT_{COOL}^{sp} [°C]	CHANGE IN RESPONSE	FAN ΔP_c [Pa]	FAN δ	FAN $\dot{M}_{AS}^{o}$ [kg/sec]	FAN $\Delta\dot{M}_{AS}$ [kg/sec]	ZONE T_z^o [°C]	ZONE ΔT_z [°C]	ZONE T_z^o [°C]	ZONE ΔT_z [°C]
m20y00	18.3	+1.0	NO		No Change		No Change	22.10	+0.38		
m20y03	15.5	+1.0	YES	RTSP	<0.1%	3.329	+0.158	21.3	+0.34	24.91	+0.21
m40y04	13.1	+1.0	YES	RTSP	<0.1%	4.210	+0.086	25.53	+0.40		
m40y04	13.1	-1.0	YES	RTSP	<0.1%	4.210	-0.220	25.53	-0.16		

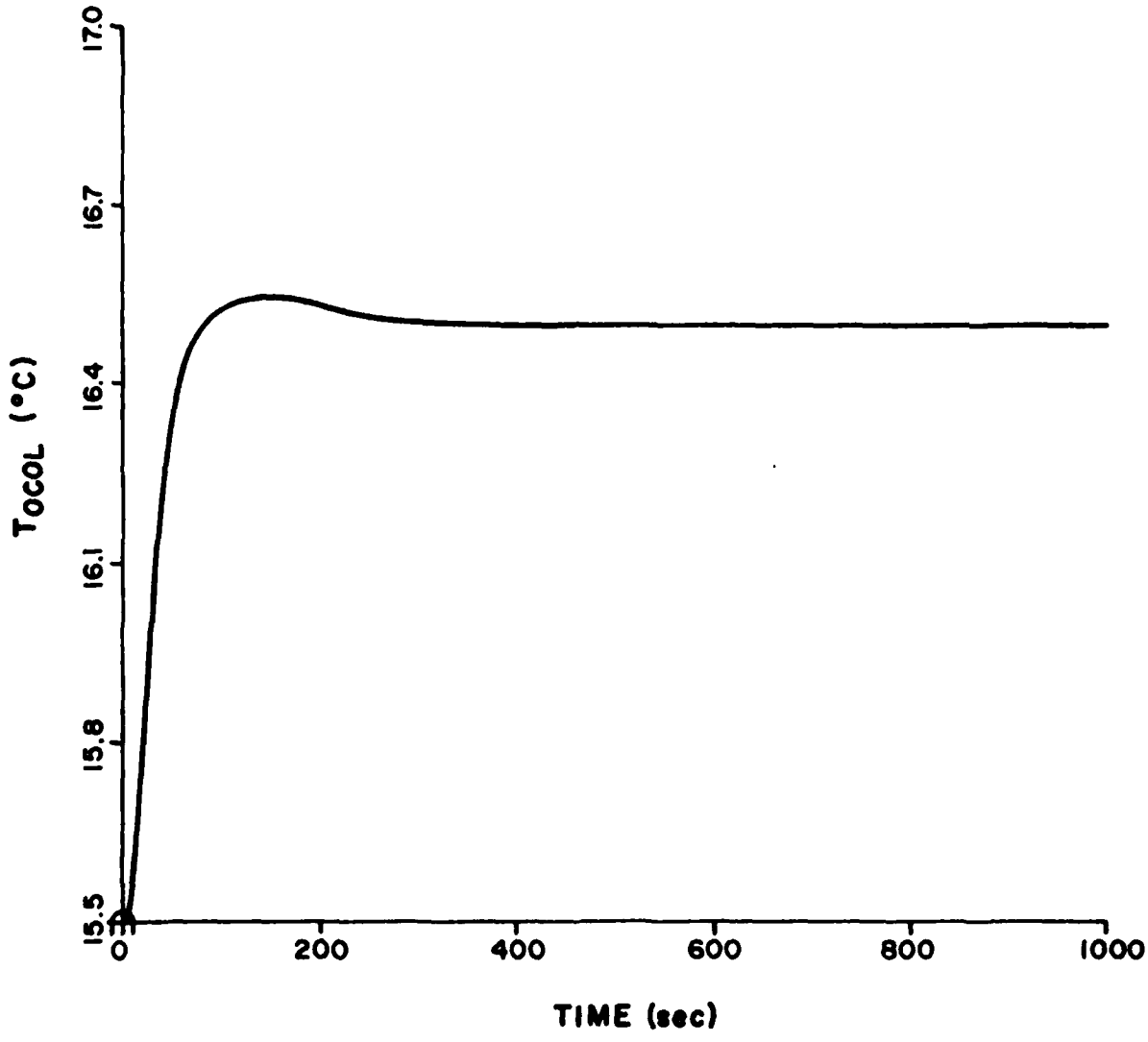

Figure 42. Cooling coil (m20y03) setpoint step change - isolated subsystem response.

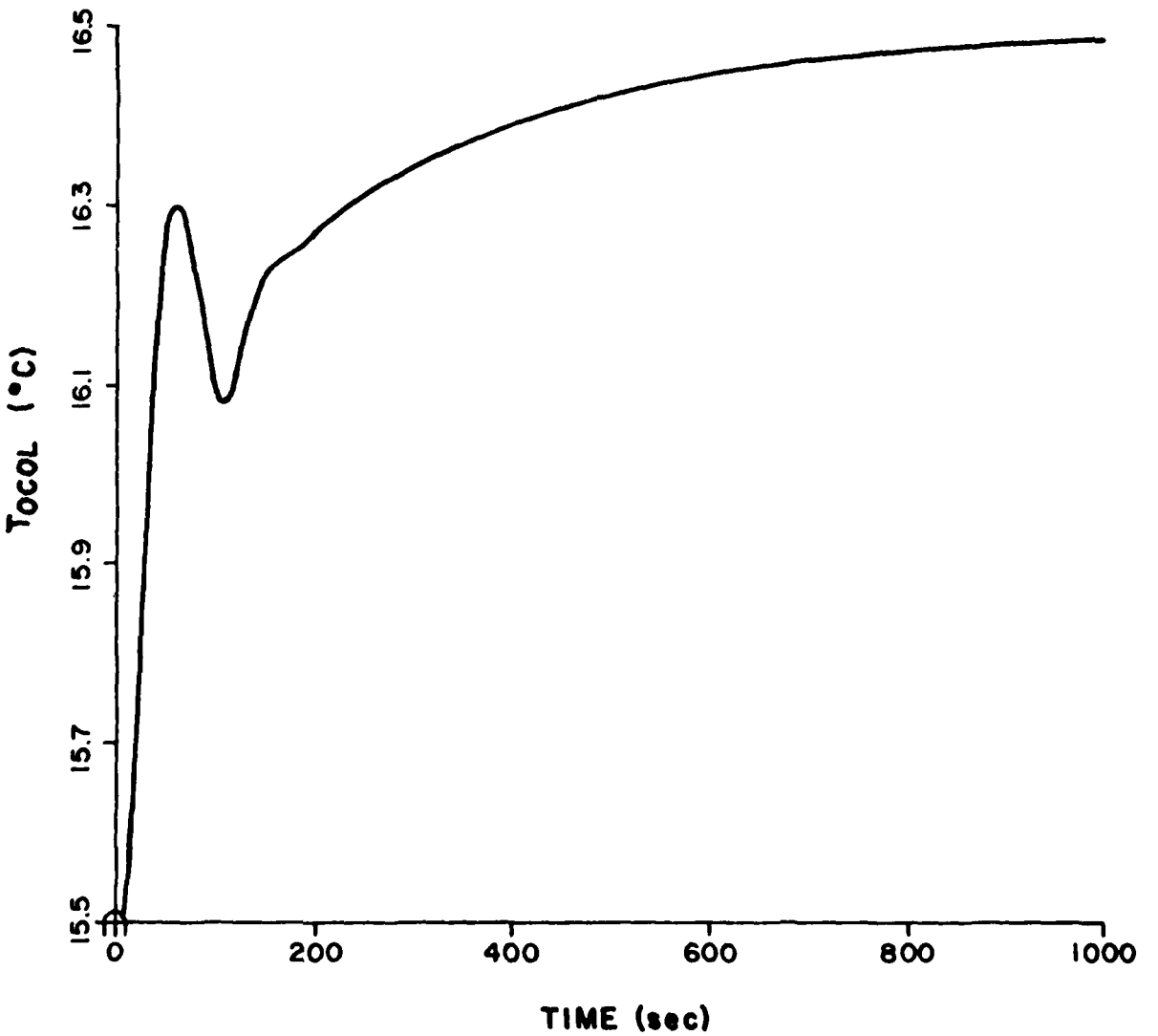

Figure 43. Cooling coil (m20y03) setpoint step change - primary subsystem response.

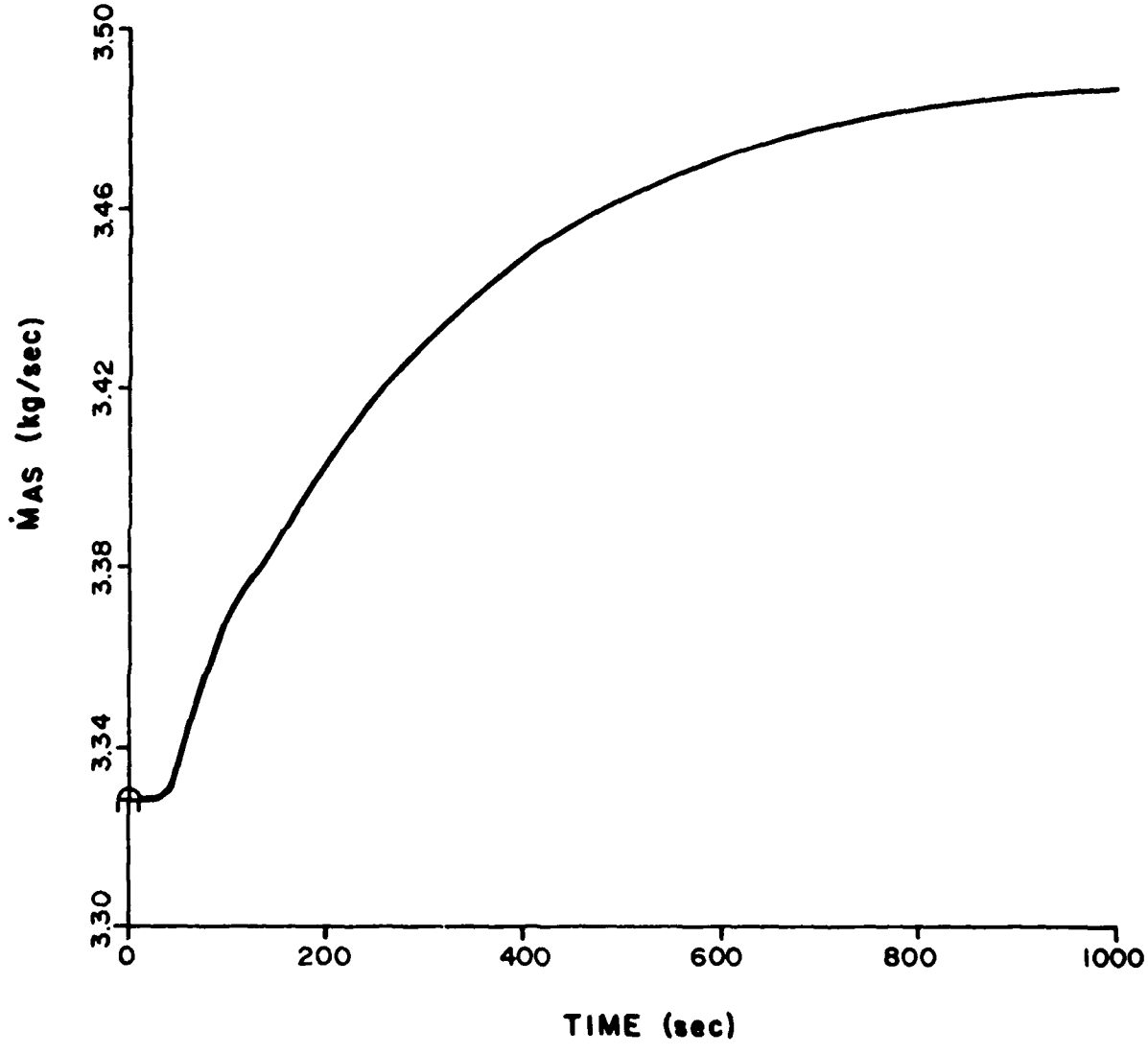

Figure 44. Cooling coil (m20y03) setpoint step change - secondary subsystem response $\dot{m}_{as}$.

AD-A159 049 PI CONTROL OF A SINGLE-DUCT VAV (VARIABLE AIR VOLUME) HVAC (HEATING VENTI (U) CONSTRUCTION ENGINEERING RESEARCH LAB (ARMY) CHAMPAIGN IL G PERCIVALL JUN 85 2/2

UNCLASSIFIED CERL-TM-E-85/05 F/G 13/1 NL

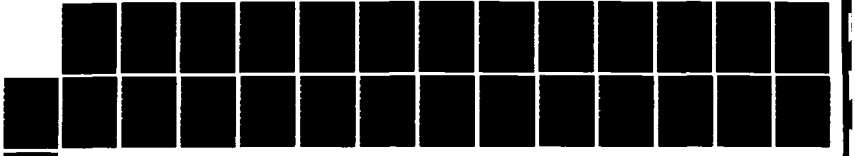

END

FILMED

DTIC

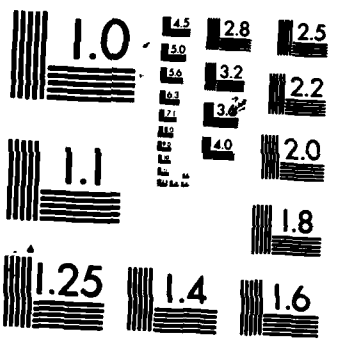

MICROCOPY RESOLUTION TEST CHART
NATIONAL BUREAU OF STANDARDS-1963-A

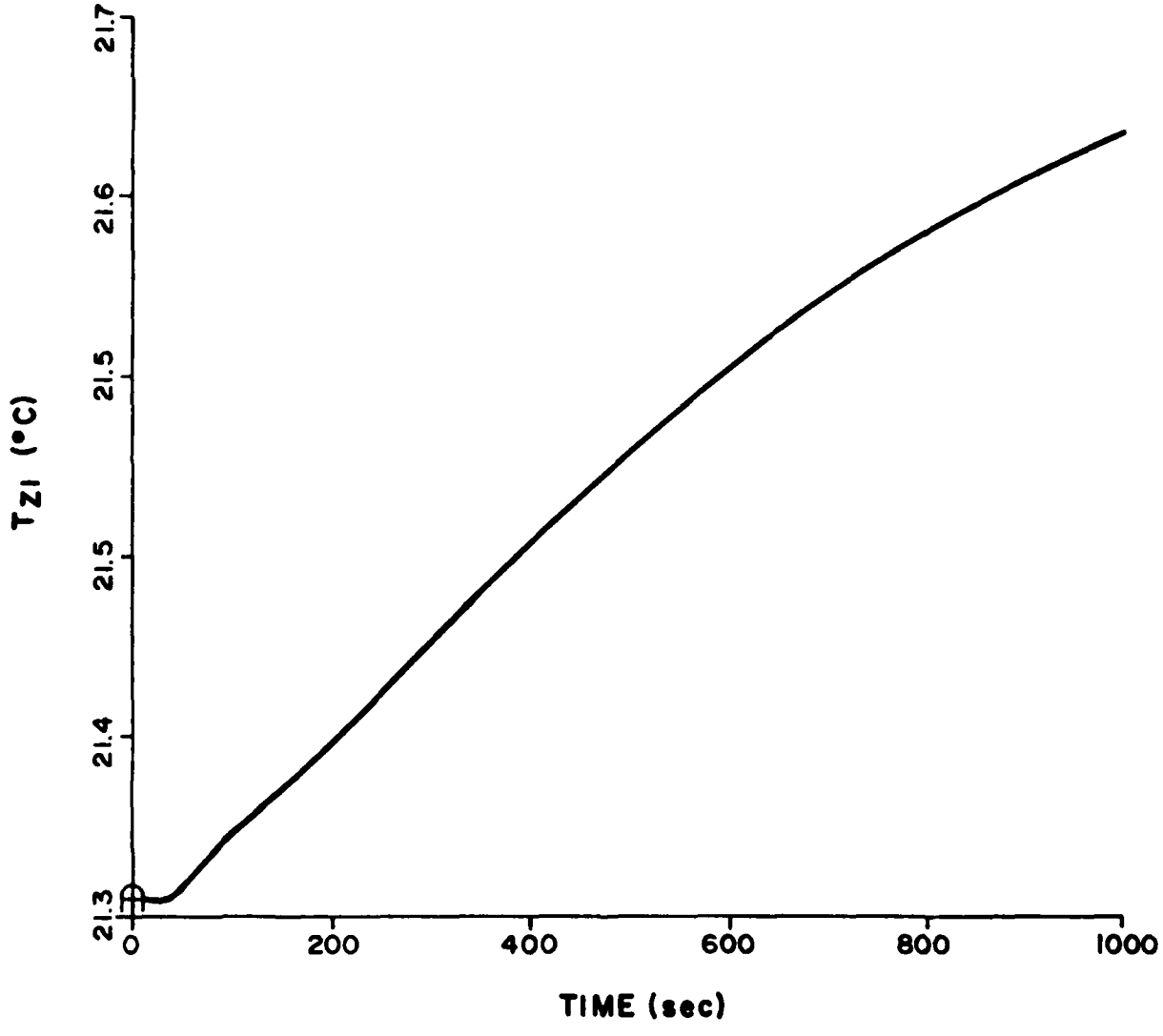

Figure 45. Cooling coil (m20y03) setpoint step change - secondary subsystem response - T_{21}.

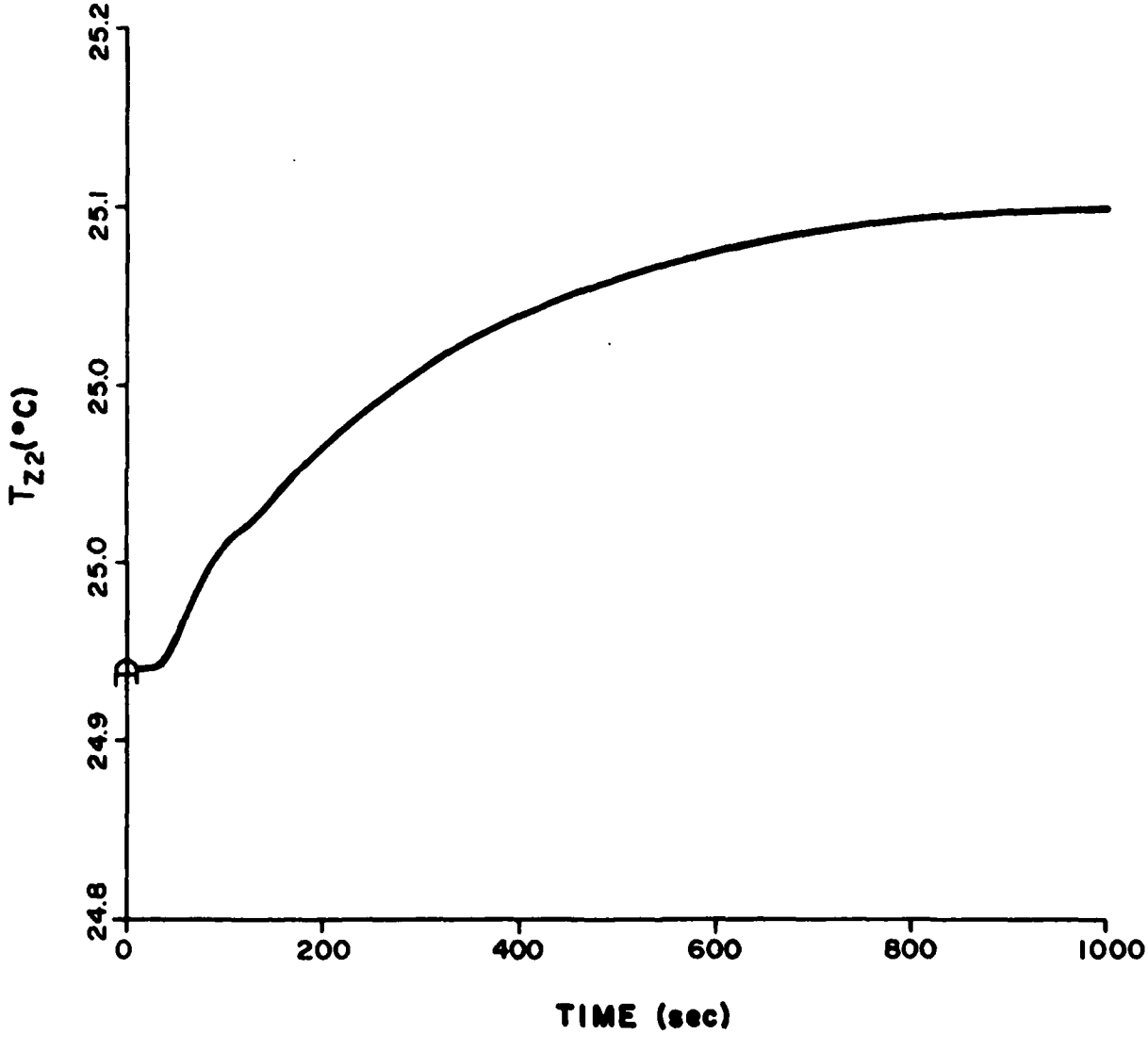

Figure 46. Cooling coil (m20y03) setpoint step change - secondary subsystem response - T_{z2}.

Overall, m20y03, just observed, was one of the worst cases, using degradation and variation as measures, and this mode was seen not to suffer intolerably from the disruption of a cooling coil setpoint step change. It seems fair to conclude that the system is fairly insensitive to this change.

C. Fan Setpoint Step Change

The procedure used in the previous two sections will be used again here to examine the results of a step change of the setpoint for the fan subsystem. This test was performed using five of the steady-state modes of operation. The results of these tests are summarized in Table 8. All of the step changes were the same, ΔP_c^{sp} = 50 pa. The maximum of the recorded mass flow changes, 22%, occurred when the dampers in the zones were not operating (m10n00). The maximum change in T_{zi}, 6%, also occurred when f_{wo} did not change (m00n40). The mixing box was not operating for three modes, suffered no change for another, and varied 6% for m10n00, but returned to the setpoint with a settling time (10% of maximum deviation) of 300 secs. The cooling coil was operating during two of the modes tested, and, although the cold deck temperature did return to the setpoint, the variations were rather large, 40% and 43%. This effect was due to the change in air mass flow across the coil.

As an example of this setpoint change, the simulated outputs for m40y04 are presented in Figure 47 for P_c and Figure 48 for $\dot{m}_{as}$ in the isolated subsystem, Figures 49 and 50 for P_c and $\dot{m}_{as}$ in the primary subsystem, and Figures 51 and 52 for the secondary subsystems. The P_c responses were indistinguishable; this was the case for every mode. The $\dot{m}_{as}$'s have the same initial response, but the primary subsystem does not stay at the steady-state value of isolated response; it again begins to decrease due to the closing of the zone dampers. The cooling coil is again affected by $\Delta\dot{m}_{as}$ but returns to the setpoint. The zone temperature is lowered by the increase in $\Delta\dot{m}_{as}$ and the decrease in T_{cool}.

In this subsystem setpoint step change, there is evidence of variations in the secondary control variables. But, because the control variables with integral control return to their setpoint and because those with proportional have only small changes, the variations may be considered acceptable. And again, there was no degradation of the primary control variable response.

D. Zone Load Step Change

To test the effect of interconnection by changes in the zone subsystem, the zone load L_i was given a step change and the system control variables were observed. This test was performed using seven of the modes of operation. The results of these tests are summarized in Table 9. The maximum change in T_{zi} for the smallest load change, ΔLOAD, was 9% for m10n00. The secondary zone

Table 8. Fan Setpoint Step Change Response

	P_C^{spo} [kW]	ΔP_C^{sp} [kW]	ISOLATED SUBSYSTEM $\dot{M}_{AS}^{O}$ [kg/sec]	ISOLATED SUBSYSTEM $\Delta\dot{M}_{AS}$ [kg/sec]	PRIMARY SUBSYSTEM $\dot{M}_{AS}^{O}$ [kg/sec]	PRIMARY SUBSYSTEM $\Delta\dot{M}_{AS}^{F}$ [kg/sec]	ZONE T_Z^U [°C]	ZONE ΔT_Z [°C]	ZONE T_Z^O [°C]	ZONE ΔT_Z [°C]	MIXING BOX ΔT_{AM}^{F} [°C]	MIXING BOX δ	COOLING COIL ΔT_{COOL}^{F} [°C]	COOLING COIL δ
m00n40	622	+50	2.900	+0.544	2.900	+0.540	19.73	+1.28				Not Oper.		Not Oper.
m10n00	622	+50	2.900	+0.544	2.452	+0.548	22.47	-0.33			RTSP	6%		Not Oper.
m15n04	622	+50	3.382	0.713	1.942	No Record	24.79	-0.42				No Change		Not Oper.
m20y03	622	+50	3.331	0.696	3.329	0.302	21.31	-1.24	24.91	-0.52		Not Oper.	RTSP	-40%
m40y04	622	+50	4.260	+1.009	4.210	+0.300	25.53	-0.52				Not Oper	RTSP	-43%

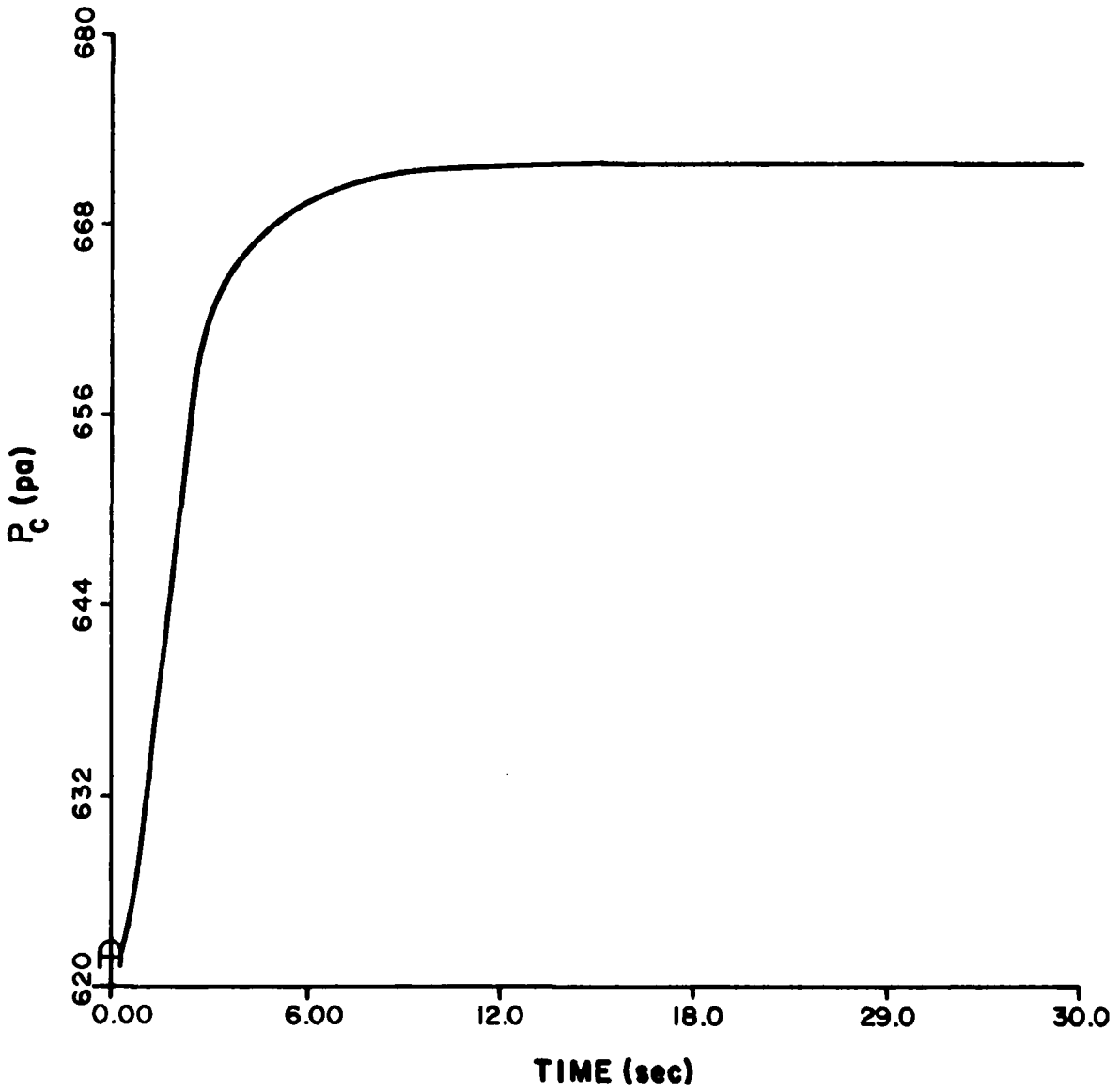

Figure 47. Fan (m40y04) setpoint step change - isolated subsystem response - P_c.

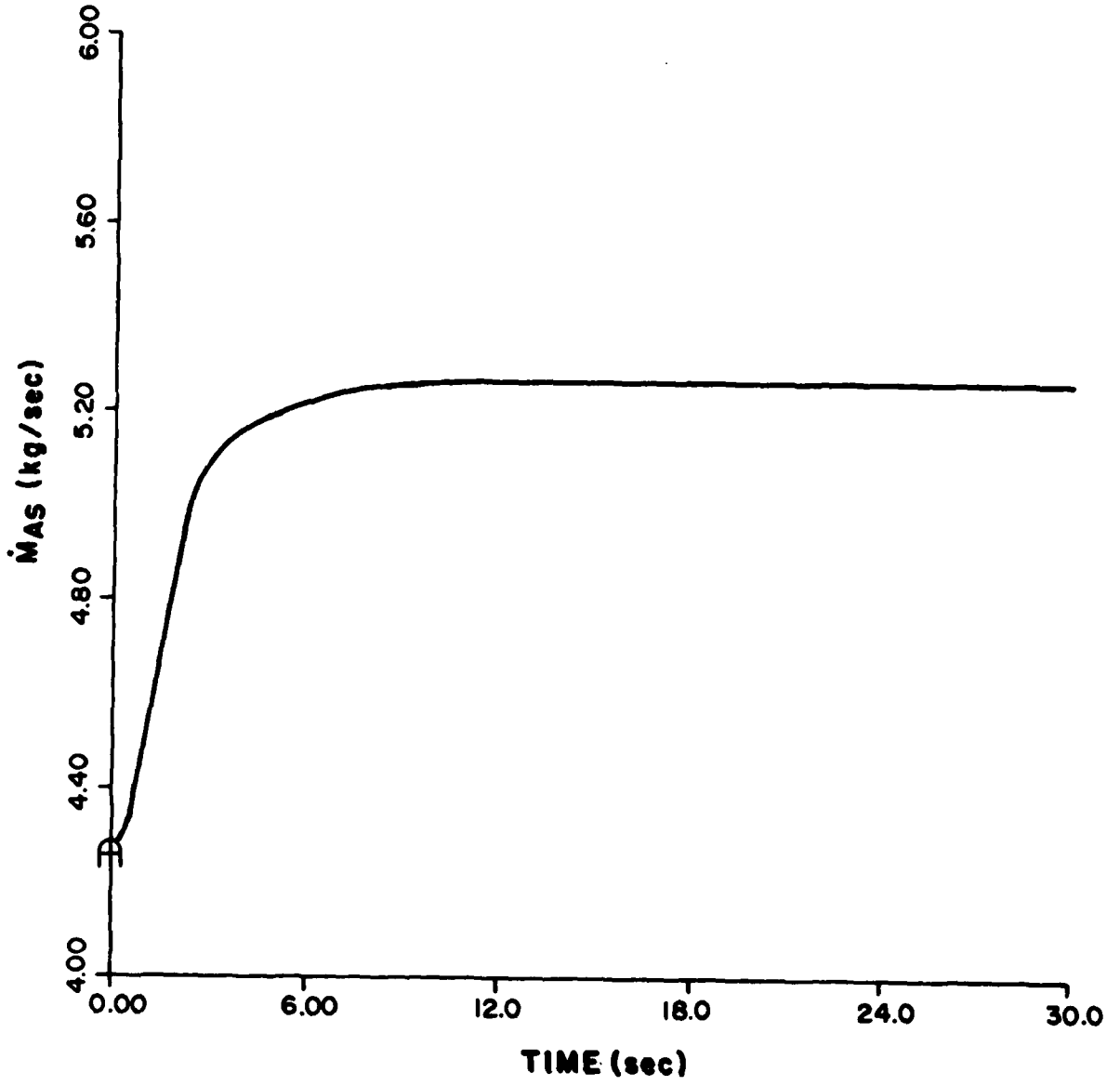

Figure 48. Fan (m40y04) setpoint step change - isolated subsystem response - $\dot{m}_{as}$.

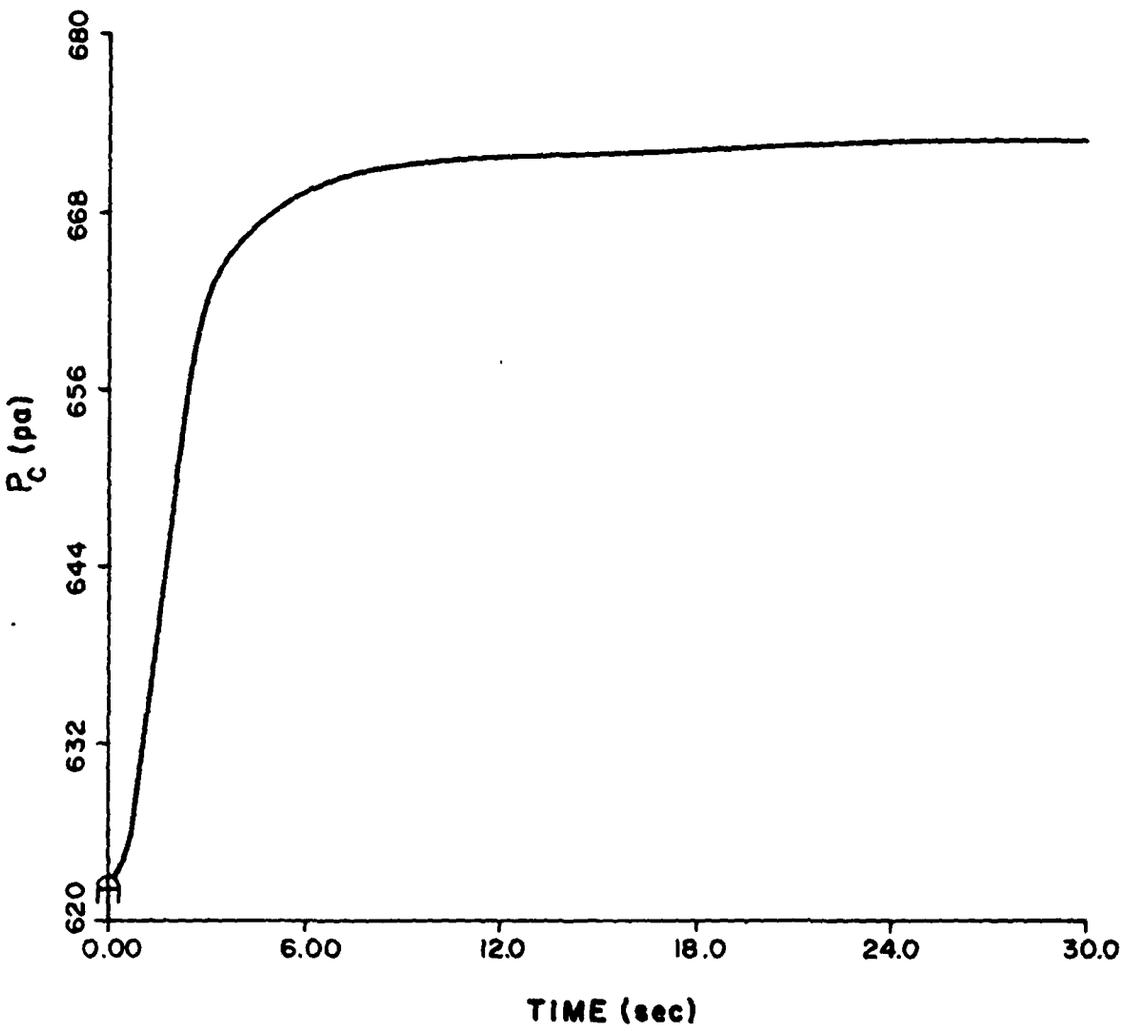

Figure 49. Fan (m40y04) setpoint step change - primary subsystem response - P_c.

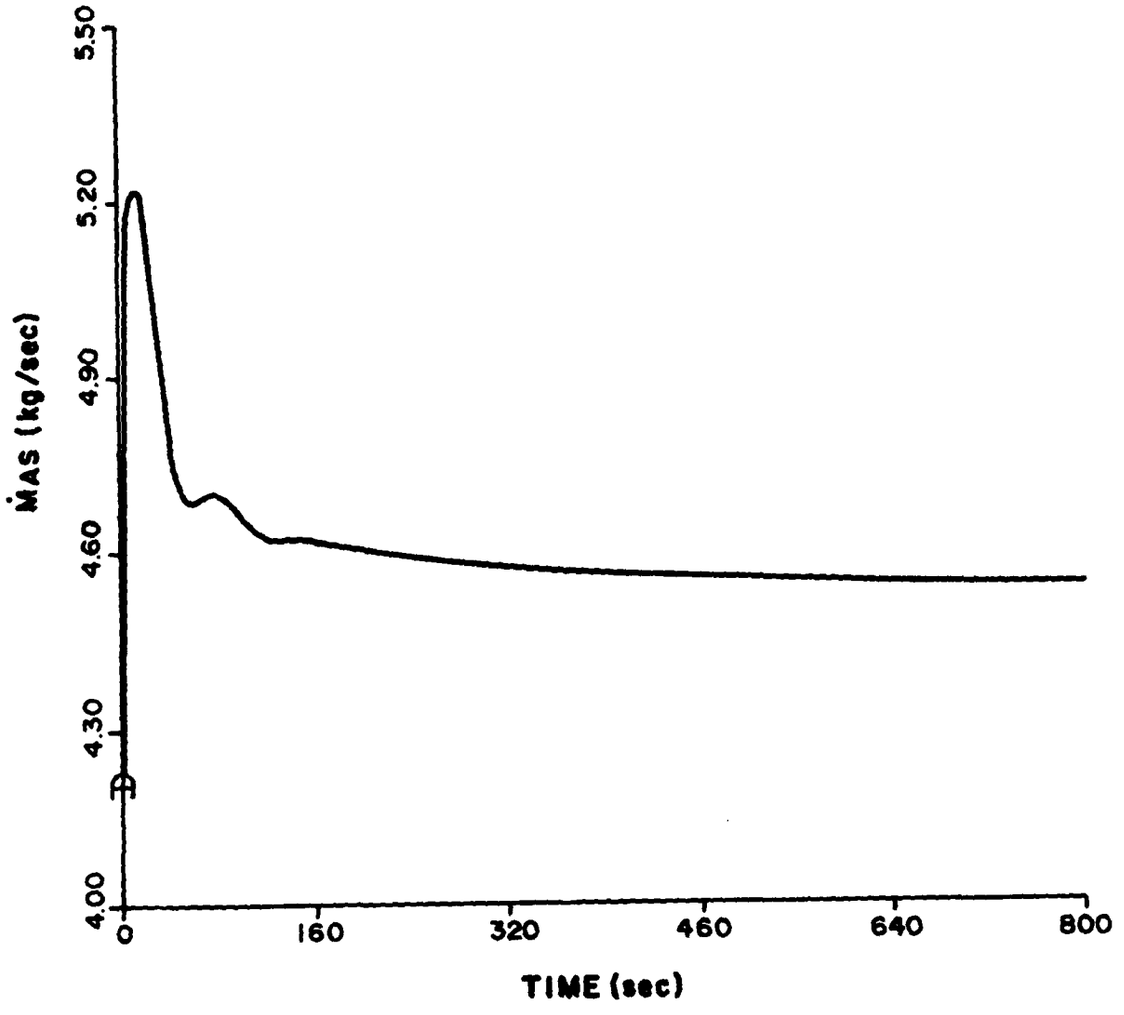

Figure 50. Fan (m40y04) setpoint step change - primary subsystem response - $\dot{m}_{as}$.

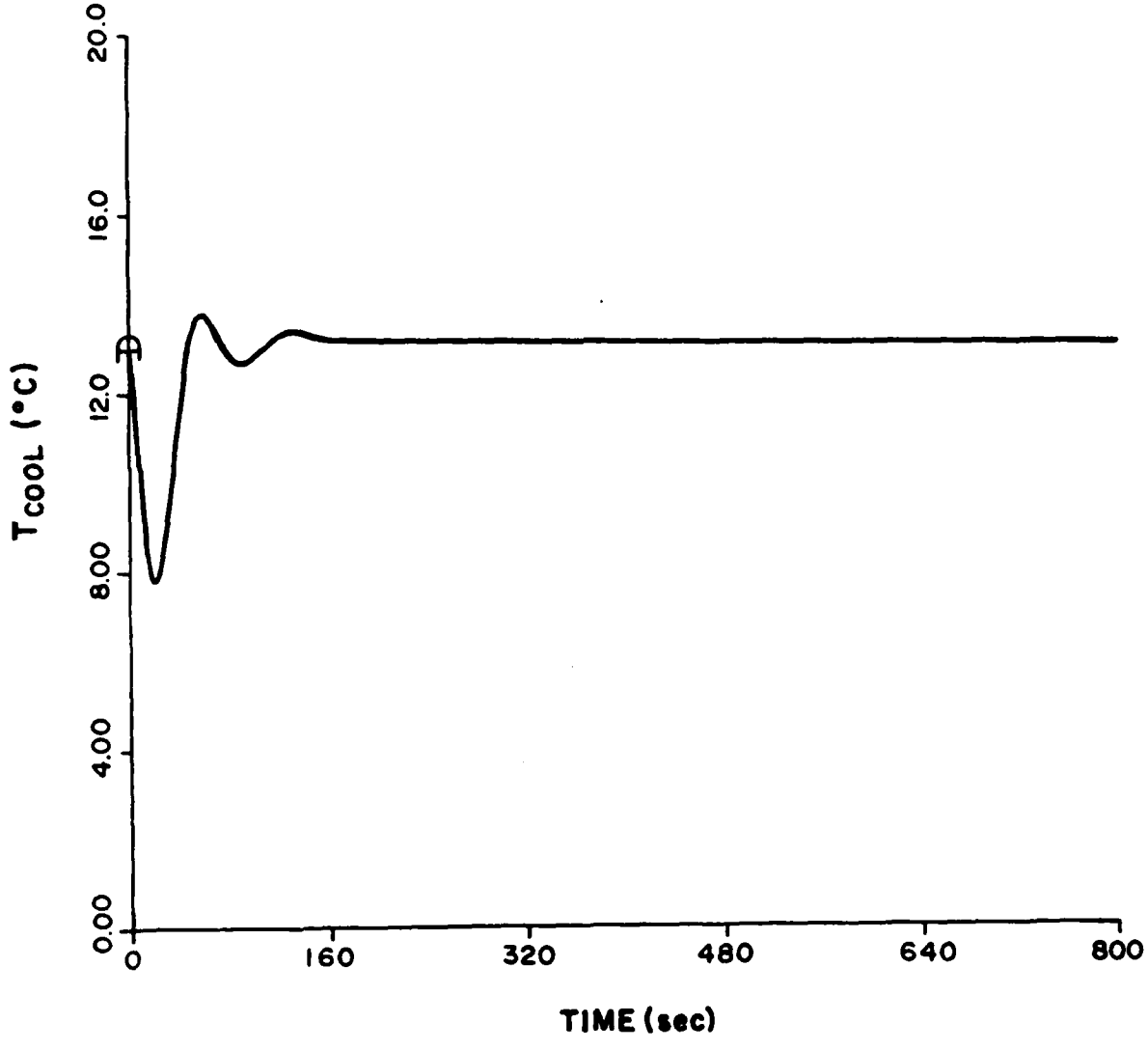

Figure 51. Fan (m40y04) setpoint step change - secondary subsystem response - T_{cool}.

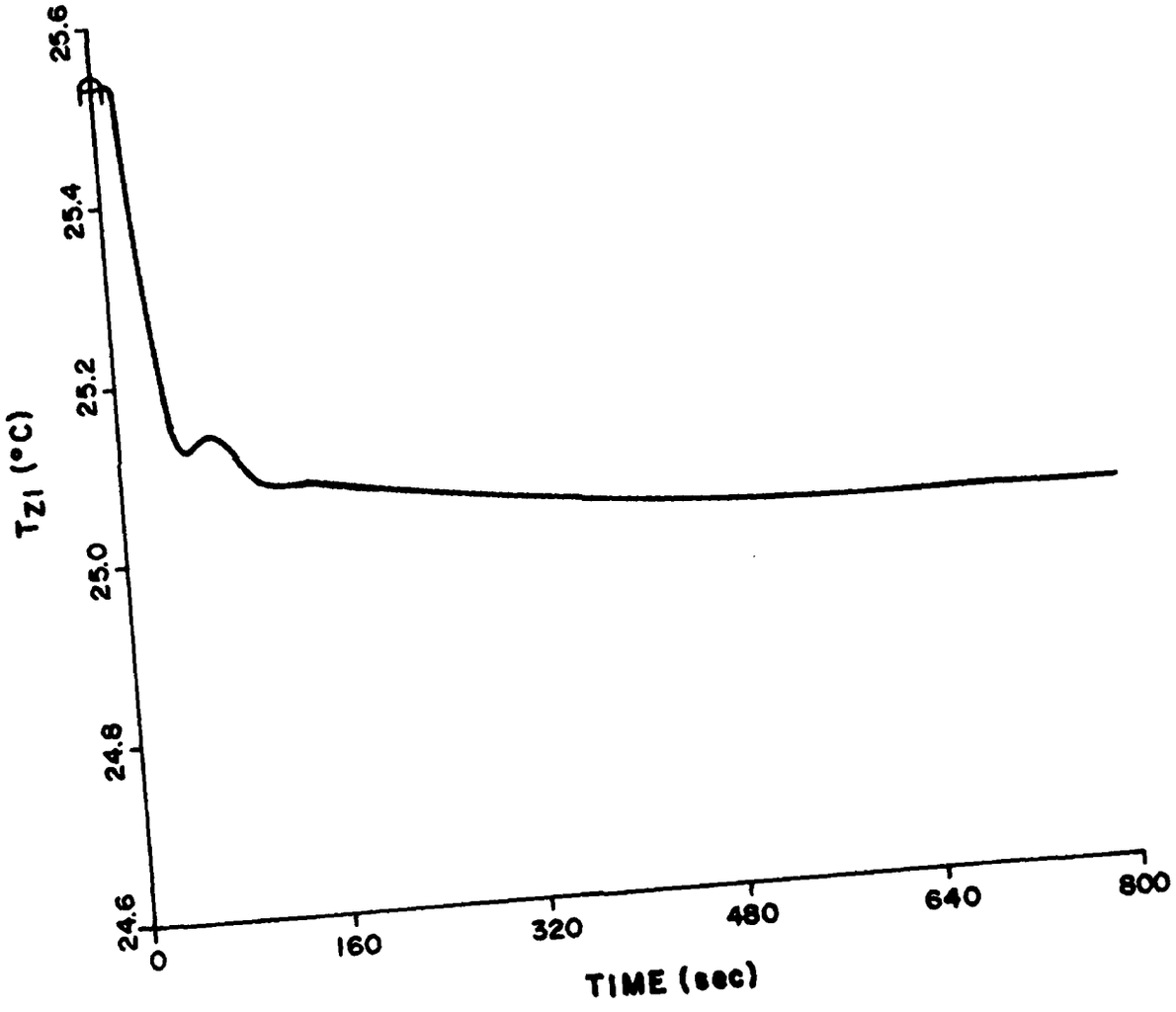

Figure 52. Fan (m40y04) setpoint step change - secondary subsystem response - T_{Z1}.

Table 9. Zone Load Step Change Response

MODE	ΔLOAD [kW]	Tz° [°C]	ISOLATED ZONE SUBSYSTEM Tz' [°C]	ISOLATED ZONE SUBSYSTEM ΔTz [°C]	PRIMARY ZONE SUBSYSTEM Tz' [°C]	PRIMARY ZONE SUBSYSTEM ΔTz [°C]	SECONDARY ZONE Tz° [°C]	SECONDARY ZONE ΔTz [°C]	MIXING BOX ΔTAM [°C]	MIXING BOX δ	COOLING COIL ΔTCOOL [°C]	COOLING COIL δ	FAN ΔPc [Pa]	FAN δ	FAN Ṁas° [kg/sec]	FAN ΔṀas [kg/sec]
m00n40	+5	19.73	19.89	0.16	19.98	0.25	N.C.			Not Oper.	N.O.	Not Oper.		No Change		No Change
m10n00	-3	22.47	20.59	-1.94	20.59	-1.88	22.47	-0.12	RTSP	<0.9%	N.O.	Not Oper.		No Change		No Change
m15n04	-3	24.79	23.78	-1.01	23.74	-1.05	24.79	-0.03	0.4%	0.4%	N.O.	Not Oper.	RTSP	<0.1%	1.942	-8.8%
m20y00	-7	22.10	24.76	2.66	24.68	2.58	22.1	-0.26		Not Oper.	-1.06	-5.8%	RTSP	<0.1%	2.900	+4%
m20y03	-3	22.10	20.36	1.74	20.36	1.74	N.C.			Not Oper.		No Change		No Change		No Change
m20y03	+3	24.91	25.32	0.41	25.40	0.49	21.31	0.04		Not Oper.	RTSP	3.2%	RTSP	<0.1%	3.329	+4.7%
m40y04	+3	25.53	26.64	1.12	26.76	1.23	25.53	0.01		Not Oper.	RTSP	1.5%	RTSP	<0.1%	4.210	+0.6%

subsystem temperature changes were barely perceptible, the maximum being 1% for m20y00.

For two of the modes, the mixing box was operating. For m10n00 the T_{am} deviated by < 0.9% and returned to the setpoint. For m15n04 the deviation was so small that the value of the integral in the controller did not become large enough to overcome the hysteresis within the duration of the simulation (1000 secs); hence the deviation δ equals the changes ΔT_z in percentage.

The cooling coil was operating during four modes. For m20y03, with a load change in zone 1, there was no change. For m20y03, with a load change in zone 2, and for m40y04, the cold deck temperature deviated from the setpoint by a small amount due mainly to $\Delta\dot{m}_{as}$, and then returned to the setpoint. For m20y00, the steady-state chilled water mass flow is low, resulting in large gains in T_{cool} vs. $\Delta\dot{m}_{as}$ (as simulated by the transfer functions). This change is so large that T_{cool} could not be forced to return to the setpoint by opening the water valve to full flow.

The fan was operating in all of the modes tested. For three modes the zone damper positions did not change so the fan speed did not change. For the modes where the fan was active, the pressure in the duct deviated from the set point by < 0.1%. The air mass flow had large changes of up to 8.8%, but $\dot{m}_{as}$ is not a control variable so this change is important only in that it affects the other subsystems.

Two examples of this test will be presented. The first is the m10n00 mode with a -3.0 kW step change. The plots are shown in Figure 53 for the isolated zone, Figure 54 for the primary zone, and Figures 55 and 56 for the secondary zones. Comparing Figures 53 and 54 reveals that the interconnections had little effect on the zone response. The secondary zone is seen to decrease slightly due to a decrease in T_{cool} due to the decrease in T_{zi}. The mixing box response is again small, but the effects of hysteresis are clearly evident.

The second mode to be presented is m40y04 with a +3.0 kW step change in the load of zone 1. The plots are shown in Figure 57 for the isolated zone, Figure 58 for the primary zone and Figures 59 and 60 for the secondary subsystems. Again the difference in response for the primary subsystem is indistinguishable from that for the isolated subsystem. The deviations in T_{cool} are clearly evident and so too is the return to the setpoint. Finally, the air mass flow change is seen to be small, but it is large enough to produce the changes in T_{cool}.

Overall, the variations in secondary subsystem control variables are small and, except for one questionable case, the variables return to the

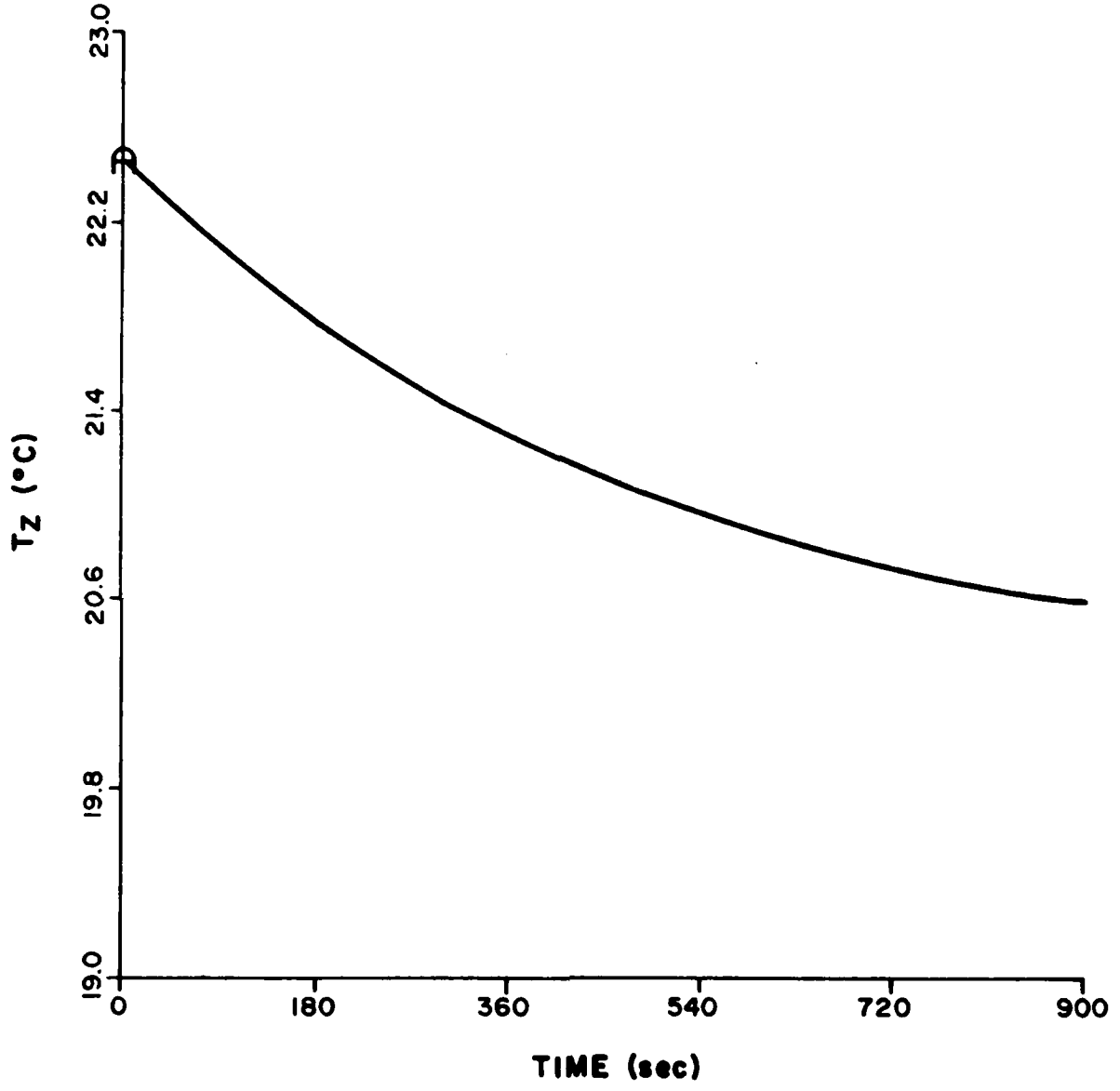

Figure 53. Zone (m10n00) load step change - isolated subsystem response.

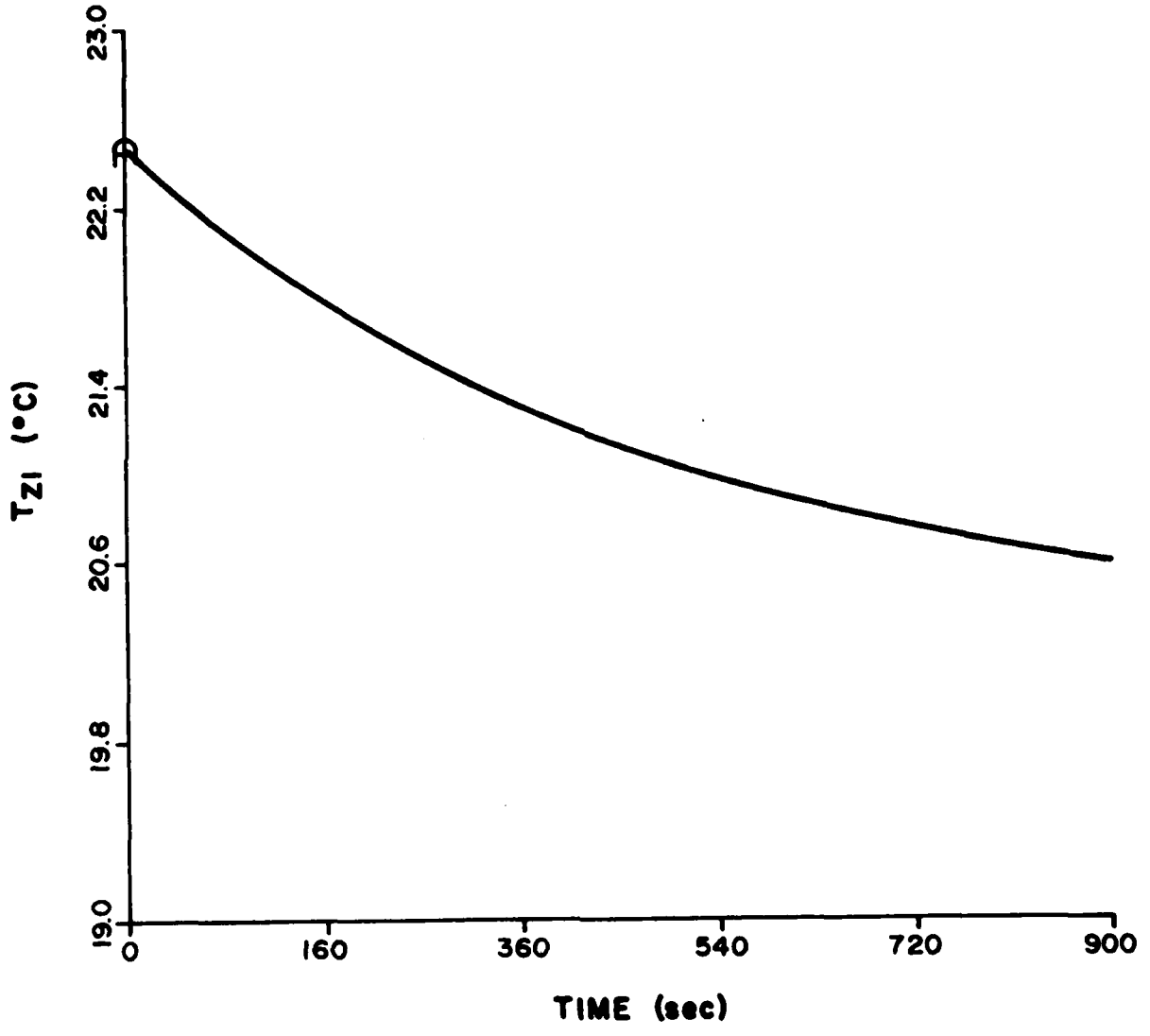

Figure 54. Zone (m10n00) load step change - primary subsystem response.

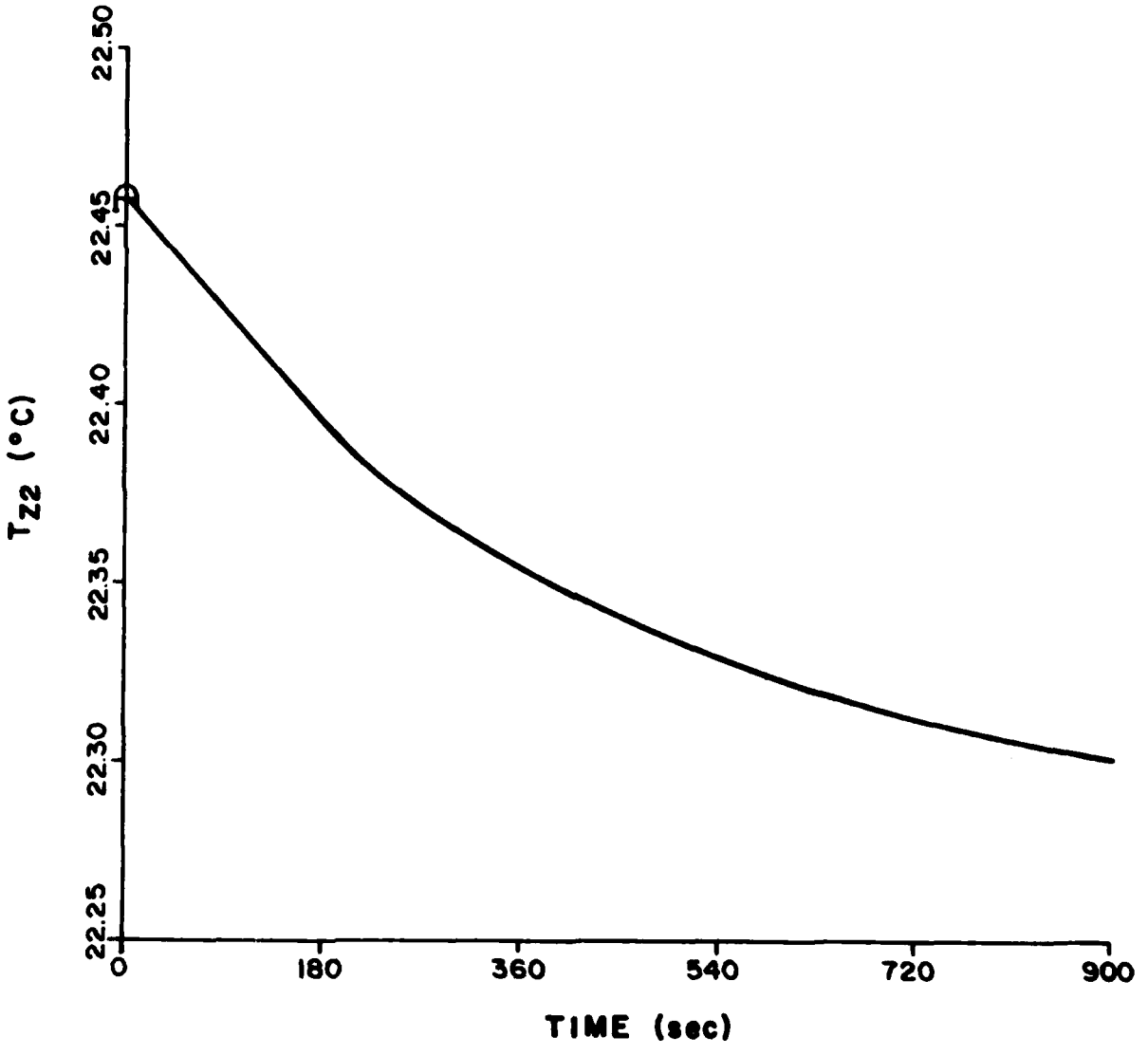

Figure 55. Zone (m10n00) load step change - secondary subsystem response - T_{z2}.

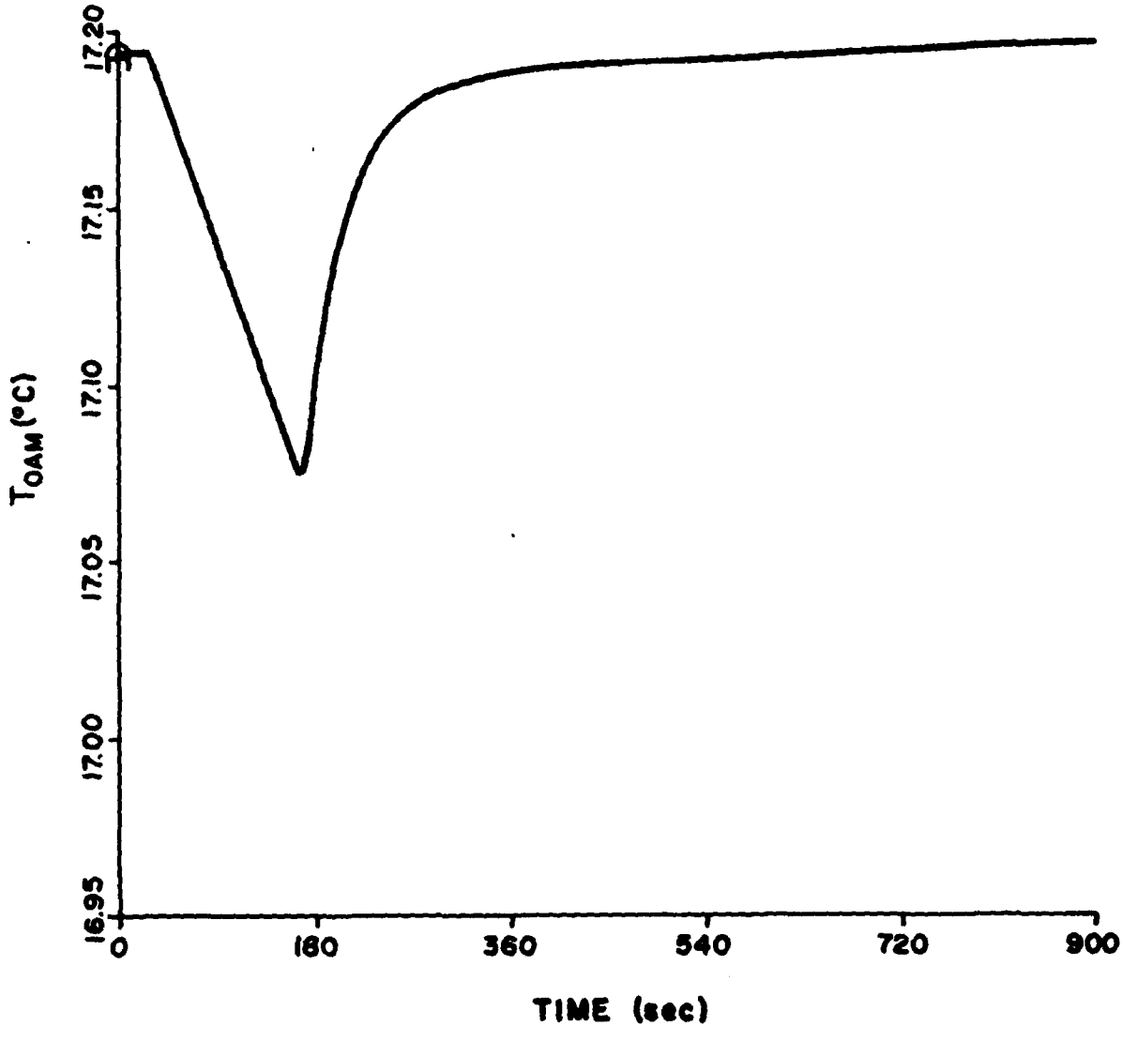

Figure 56. Zone (m10n00) load step change - secondary subsystem response - T_{oam}.

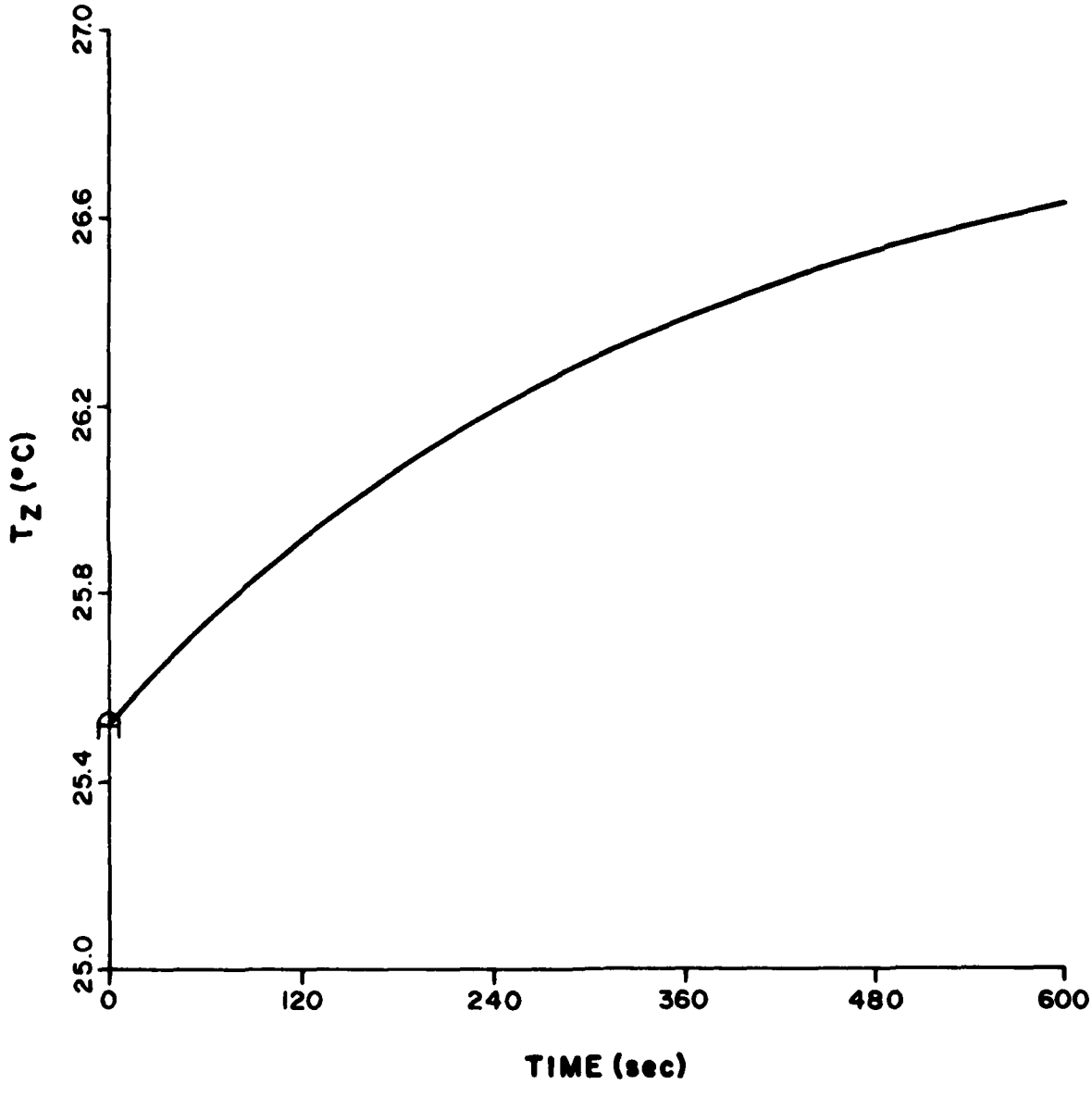

Figure 57. Zone (m40y04) load step change - isolated subsystem response.

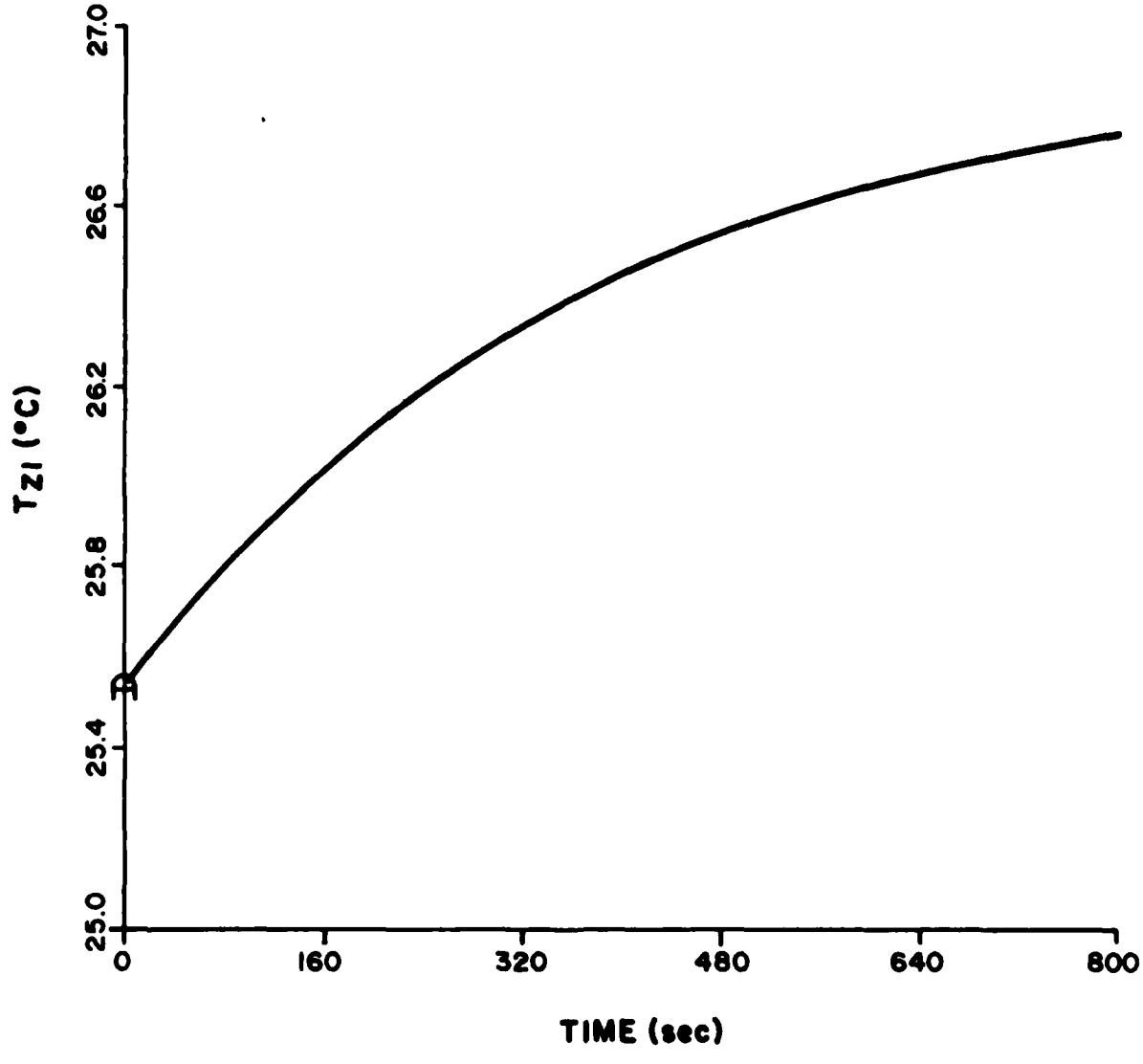

Figure 58. Zone (m40y04) load step change - primary subsystem response.

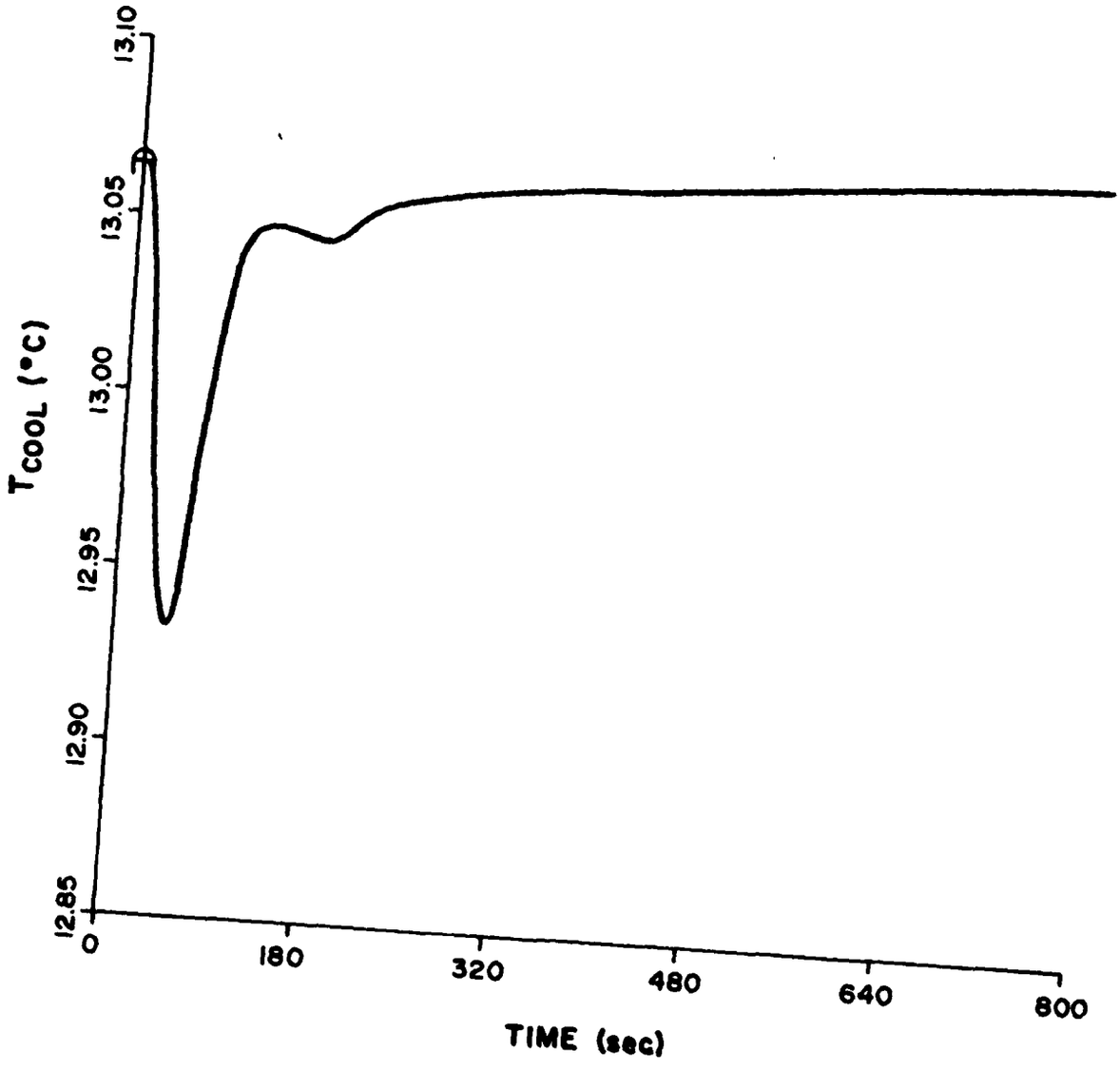

Figure 59. Zone (m40y04) load step change - secondary subsystem response - T_{cool}.

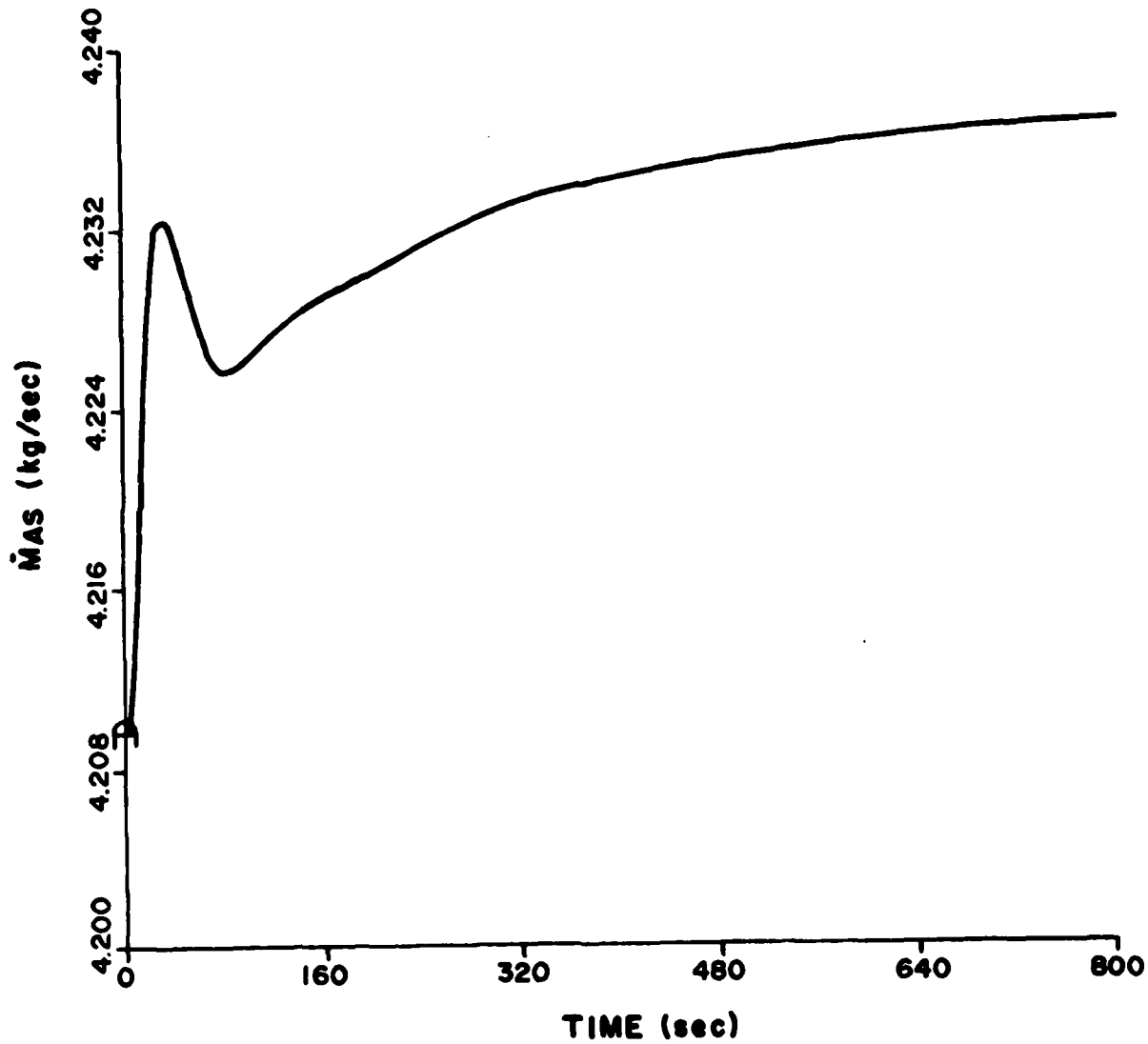

Figure 60. Zone (m40y04) load step change - secondary subsystem response - $\dot{m}_{as}$.

setpoint. The degradation of response does not seem to be a valid measure for the zone subsystem since its isolated response was not designed by selection of controller gain settings. Although the interconnections are designed to assist in maintaining constant zone temperatures, the comparison of isolated and primary zone subsystem final temperature values indicates that the interconnections do little to maintain the zone temperature when zone load changes occur.

In summary, this chapter has demonstrated, by computer simulation, that effects of interconnection of the isolated subsystem are of insignificant magnitude. There are degradations from the design responses, but these, at worst, increase the settling time, e.g., the cooling coil. There are variations in the secondary control variables, but all but one of these returned to the setpoint. So by these two measures, the SISO-designed MIMO control system is rather insensitive to the interconnections which were neglected during the design.

It seems important to mention here what was not seen. The interconnection of the subsystem results in a closed loop among these subsystems. By examining Figure 2, this loop can be seen; it includes the mixing box, the cooling coil (or just the supply air duct if the coil is off), the zones, and back to the mixing box. Now, when the return air fraction is large, there is a continuous loop of air among these subsystems further complicated by the transport lags of the ductwork. Problems can occur if the zone heat capacities are small, e.g., C_{zi} = 50 kJ/°C (the size of the USA-CERL HVAC test facility zones), rather than the size considered for this study, C_{zi} = 700 kJ/°C (the average size of a zone in which this HVAC system might be used). Then, this loop is capable of sustaining oscillations which do not decay. This was in fact observed in the earlier simulations until the zone size was changed from the smaller to the larger values indicated. As long as larger zones are used, this should not be a problem.

VIII. CONCLUSIONS

The conclusions to this report fall into three categories: modeling, comparison sensitivity, and simulation.

The results of Chapters III and IV indicate that modeling of an HVAC system can be accomplished. From experimental results, many of the responses can be described by single-pole transfer functions. The problem of hysteresis can be handled by the ACSL package. And finally, the system plant, in linearized form, can be described by a transfer function matrix.

The comparison sensitivity of the system could not be established by the singular value technique which was employed. This does not mean that the system does not satisfy the comparison sensitivity condition, but that, in this instance, the results of this test were inconclusive.

The simulations of the isolated subsystems and the entire system were useful in establishing two results. First, the Ziegler-Nichols technique for controller parameter value selection is useful for the PI controllers as used on the three subsystems. But, to achieve the desired 1/4-wave responses, the revised Z-N formulas must be used. Second, by comparing the isolated subsystem setpoint step change responses to the primary subsystem setpoint step change responses, and observing the associated secondary subsystem control variable changes, it was possible to establish that the sensitivity of the SISO design to the presence of the MIMO interconnections was insignificant, as measured by the degradation of the primary subsystem response and the variation of the secondary subsystem control variables.

IX. RECOMMENDATIONS

The recommendations of this study are of two types: 1) those pertaining to testing, based on the results of this study; and 2) those pertaining to the course of future study.

As to testing, based on the conclusions of this report, it is suggested that if this design is also considered desirable from energy considerations, it should be tested on a full-size facility. This should be done using the Z-N technique for controller parameter value selection, but with the modified formulas. Caution should be taken to assure that the zones are large enough to avoid the system loop oscillations mentioned at the end of Chapter VII. Finally, the system should of course be observed during all seasons before any conclusions are made.

For any future study utilizing the results of this report, two items should be mentioned. First, the model of the system might be improved by taking energy considerations into account when modeling the fan system, combining the E/P and actuator transfer functions, and finding a different description of the coils. Second, use the system plant transfer function matrix, P', to find feedback and feedforward compensators, G and H, which insure MIMO system criteria. This procedure could take the form of using the singular value test as a design criterion to insure comparison sensitivity of the system.

REFERENCES

1. J. G. Ziegler and N. B. Nichols, "Optimum Settings for Automatic Controllers," Trans. ASME, pp 759-768, November 1942.

2. J. R. Gartner and H. L. Harrison, "Frequency Response Transfer Functions for a Tube in Crossflow," ASHRAE Transactions, Vol. 69, pp 323-330.

3. I. Gondal, personal communication.

4. William Dolan, Validation Data for Mechanical System Algorithms Used in Building Energy Analysis Programs, Technical Report E-177/ADA115182 (USA-CERL, 1982), p 51.

5. Benjamin C. Kuo, Automatic Control Systems, 4th ed. (Englewood Cliffs, New Jersey, Prentice-Hall, 1982), p 95.

6. Jose B. Cruz, Jr., Feedback Systems (New York, McGraw-Hill, 1972), p 19.

7. J. B. Cruz, Jr., J. S. Freudenberg, and D. P. Looze, "A Relationship Between Sensitivity and Stability of Multivariable Feedback System," IEEE Trans. Automatic Control, Vol. AC-26, No. 1, pp 66-74, February 1981.

8. Ibid., p 70.

9. J. S. Freudenberg, D. P. Looze, and J. B. Cruz, Jr., "Robustness Analysis Using Singular Value Sensitivities," Inter. Journal Control 35 (January 1982), pp 95-6.

BIBLIOGRAPHY

Advanced Continuous Simulation Language (ACSL) User Guide/Reference Manual. Concord Mass.: Mitchell and Gauthier, 1981.

ASHRAE Handbook 1981 Fundamentals. Atlanta, GA.: American Society of Heating, Refrigerating and Air-Conditioning Engineers, Inc., 1982.

Brogan, W. L. Modern Control Theory. Englewood Cliffs, NJ: Prentice-Hall/Quantum, 1982.

Cruz, J. B., Jr., ed. Feedback Systems. New York: McGraw-Hill, 1972.

Cruz, J. B., Jr.; Freudenberg, J. S.; and Looze, D. P. "A Relationship Between Sensitivity and Stability of Multivariable Feedback Systems." IEEE Trans. on Automatic Control Vol. AC-26, No. 1, February 1981, pp 66-74.

Dolan, William. Validation Data for Mechanical System Algorithms Used in Building Energy Analysis Programs. Champaign, IL: U.S. Army Construction Engineering Research Laboratory, Technical Report E-177/ADA115182, February 1982.

Freudenberg, J. S.; Looze, D. P.; and Cruz, J. B., Jr. "Robustness Analysis Using Singular Value Sensitivities," Inter. Journal Control 35 (January 1982) pp 95-116.

Friedman, F. L., and Koffman, E. B. Problem Solving and Structured Programming in FORTRAN, 2nd ed. Philippines: Addison-Wesley, 1981.

Gartner, J. R., and Harrison, H. L. "Frequency Response Transfer Functions for a Tube in Crossflow," ASHRAE Transactions Vol. 69 (1963): pp. 323-330.

Kreyszig, Erwin. Advanced Engineering Mathematics, 5th ed. New York: John Wiley and Sons, 1983.

Kuo, B. C. Automatic Control Systems, 4th ed. Englewood Cliffs, NJ: Prentice-Hall, 1982.

Symon, K. R. Mechanics, 3rd ed. Philippines: Addison-Wesley, 1971.

Ziegler, J. G., and Nichols, N. B. "Optimum Settings for Automatic Controllers," Trans. of the ASME, November 1942, pp 759-768.

DISTRIBUTION

Chief of Engineers
ATTN: DAEN-ZCF-U

FESA, ATTN: Library 22060
ATTN: DET III 79906

U.S. Military Academy 10966
ATTN: Dept of Geography &
Computer Science

Fort Belvoir, VA 22070
ATTN: Canadian Liaison Office
ATTN: Engr Studies Center
ATTN: R&D Command

CRREL, ATTN: Library 03755

WES, ATTN: Library 39180

NAVFAC
ATTN: Naval Civil Engr Lab. (3)

NCEL ATTN: Library, Code L08A 93041

Defense Technical Info. Center 22314
ATTN: DDA (12)

Engr Societies Library, NY 10017

National Bureau of Standards 20760

END

FILMED

10-85

DTIC